ANTIOXIDANTS & REDOX SIGNALING
Volume 13, Number 6, 2010

DOI: 10.1089/ars.2009.2876

COMPREHENSIVE INVITED REVIEW

Superoxide Dismutase Mimics: Chemistry, Pharmacology, and Therapeutic Potential

Ines Batinić-Haberle,[1] Júlio S. Rebouças,[2] and Ivan Spasojević[3]

Abstract

Oxidative stress has become widely viewed as an underlying condition in a number of diseases, such as ischemia–reperfusion disorders, central nervous system disorders, cardiovascular conditions, cancer, and diabetes. Thus, natural and synthetic antioxidants have been actively sought. Superoxide dismutase is a first line of defense against oxidative stress under physiological and pathological conditions. Therefore, the development of therapeutics aimed at mimicking superoxide dismutase was a natural maneuver. Metalloporphyrins, as well as Mn cyclic polyamines, Mn salen derivatives and nitroxides were all originally developed as SOD mimics. The same thermodynamic and electrostatic properties that make them potent SOD mimics may allow them to reduce other reactive species such as peroxynitrite, peroxynitrite-derived $CO_3^{\bullet-}$, peroxyl radical, and less efficiently H_2O_2. By doing so SOD mimics can decrease both primary and secondary oxidative events, the latter arising from the inhibition of cellular transcriptional activity. To better judge the therapeutic potential and the advantage of one over the other type of compound, comparative studies of different classes of drugs in the same cellular and/or animal models are needed. We here provide a comprehensive overview of the chemical properties and some *in vivo* effects observed with various classes of compounds with a special emphasis on porphyrin-based compounds. *Antioxid. Redox Signal.* 13, 877–918.

Reviewing Editors: *Maria T. Carri, David Harrison, Carlos C. Lopes de Jesus, Ronald P. Mason, Juan J. Poderoso, and Naoyuki Taniguchi*

Departments of [1]Radiation Oncology and [3]Medicine, Duke University Medical School, Durham, North Carolina.
[2]Departamento de Química, CCEN, Universidade Federal da Paraíba, João Pessoa, Brazil.

I. Introduction

A. General

Redox imbalance between reactive species and endogenous antioxidants, which results in oxidative damage to biologic molecules and impairment in signaling pathways [(*i.e.*, in oxidative stress (145)], has been widely implicated in many ailments, including central nervous system pathologies (46, 51, 61, 122, 219, 330) [*e.g.*, amyotrophic lateral sclerosis, (46), Parkinson's disease (219), bipolar disorder (330), Alzheimer's disease (61)], cardiovascular conditions (61, 112), pulmonary conditions (65, 153), diabetes (111, 154), eye diseases (19, 235), aging (290, 323, 236), cancer (52, 70, 317), radiation injury (220), pain/chronic morphine tolerance (89), Fanconi anemia (229). Reactive species, such as nitric oxide ($^{\cdot}NO$), superoxide ($O_2^{\cdot-}$), hydrogen peroxide (H_2O_2), peroxynitrite ($ONOO^-$), and others have been widely recognized as signaling species that, by affecting redox-based cellular transcriptional activity, control inflammatory and immune responses and enhance secondary oxidative stress (27, 47, 96, 151, 188, 273, 276, 298, 335, 336). Mitochondria, the major producers of reactive species, are consistently found to play a critical role in oxidative stress (55, 155, 228, 312).

B. Antioxidants

The increased perception and understanding of the involvement of oxidative stress in many pathologic conditions has been accompanied by an increased search for synthetic antioxidants, as well as by further exploration of the antioxidant potential of several natural products. Recently, it also became evident that a number of drugs, such as antiinflammatory drugs, statins, and antibiotics, which supposedly aimed at different targets in unlike disorders, have the regulation of oxidative stress as a prominent mode of action, thus potentiating the widespread awareness of the role that oxidative stress plays in several diseases and injuries (3, 27, 47, 55, 64, 155, 175, 188, 209, 228, 312, 336). Superoxide dismutase is an endogenous and first-line-of-defense enzyme that eliminates superoxide by catalyzing its dismutation into O_2 and H_2O_2 (119, 120, 212, 240). Historically, most early synthetic antioxidant compounds were originally developed as SOD mimics, especially because the role of $ONOO^-$ and its decomposition products in biology were, at the time, neither accepted nor well defined (106). A greater understanding of the biologic activity of SOD mimics and redox-active compounds paralleled the increased insight into the nature and the role of ROS/RNS in oxidative-stress conditions. The redox properties that allow SOD mimics to eliminate $O_2^{\cdot-}$ make them also potentially efficient peroxynitrite scavengers, as well as scavengers of $CO_3^{\cdot-}$, $^{\cdot}NO_2$ radicals, and likely of peroxyl radicals and alkoxyl radicals (110, 151, 273). Therefore, most SOD mimics are not specific $O_2^{\cdot-}$ scavengers. Multiple strategies and controls must be used to assure which is the predominant species involved. Whatever mechanism is in action, antioxidants would also decrease the levels of oxidatively modified biologic molecules. Reactive species, such as $O_2^{\cdot-}$, H_2O_2, and $^{\cdot}NO$, and oxidatively modified biologic molecules (*e.g.*, nitrated lipids and nitrosated proteins) all appear to be involved in signaling events; their removal affects both primary oxidative damage and redox-based cellular transcriptional activity (27, 47, 55, 188, 273, 298, 312, 336). Therefore, antioxidants influence both inflammatory and immune pathways and also modulate secondary oxidative-stress processes.

Removal of reactive species is redox-based. Thus, it is only natural that the search for potent SOD mimics has been concentrated primarily on metal complexes that possess a redox-active metal site and rich coordination chemistry. Redox-based pathways play major role in supporting life. Nature has developed natural metalloporphyrins (*e.g.*, heme) as major prosthetic groups embedded in a variety of biomolecules, such as hemoglobin, myoglobin, nitric oxide synthase, cytochrome oxidase, prolyl hydroxylase, cyt P450 systems (including aromatase), and cyclooxygenase. Molecules such as heme have been found to play a critical role in nearly all living organisms (145). No wonder thus that the synthetic Fe and Mn porphyrins appeared as a natural choice for developing SOD mimics: (a) they are "body-friendly" molecules; (b) they are chemically accessible, (c) they are not antigenic, (d) there are nearly limitless possibilities of modifying the porphyrin core structure; (e) porphyrin complexes are extremely stable, assuring the integrity of the metal site under biologic conditions; and finally, (f) they are of low molecular weight and can penetrate the cellular and subcellular membranes, whereas superoxide dismutase enzymes cannot.

The pioneering work on metalloporphyrins as SOD mimics (most notably, MnTM-4-PyP^{5+} and FeTM-4-PyP^{5+}) was done by Pasternack, Halliwell, Weinberg, Faraggi, and others in the late 1970s and early 1980s (104, 157, 246–248, 252, 293, 332, 333). These early studies encompassed the rich chemistry of these metalloporphyrins toward radicals other than $O_2^{\cdot-}$ alone. The next milestone came from our group; we established a structure–activity relation between metal-site redox ability and catalytic rate constant for $O_2^{\cdot-}$ dismutation (30) that guided most of the work thereafter.

Reports on both toxic and protective effects of Fe porphyrins have been published (30, 231, 238, 313). Although the corresponding Fe and Mn porphyrins have very similar rate constants for $O_2^{\cdot-}$ dismutation, all Fe porphyrins studied by us thus far were toxic to *Escherichia coli*; no aerobic growth was detected in SOD-negative mutants with Fe porphyrins at levels at which analogous Mn porphyrins were fully protective (30). A loss of metal from the metal complexes during redox cycling could occur, whereby "free" Fe would give rise, through Fenton chemistry, to highly oxidizing $^{\cdot}OH$ species; Fenton chemistry presumably occurs even if reduced iron is still bound to the porphyrin ligand (338). Thus, we limited our studies to Mn porphyrins as SOD mimics (Fig. 1). Although Cu porphyrins possess SOD-like activity in a simple cyt *c* assay (33), the ability of "free" copper(II) to produce $^{\cdot}OH$ radical through Fenton chemistry (like Fe) disfavored exploiting Cu porphyrins for

biomedical applications. Whereas Fe porphyrins were the first compounds considered as SOD mimics (246, 247), Mn porphyrins remain the most stable and most active prospective SOD mimics. The activity of some Mn porphyrins approaches that of the SOD enzymes themselves (85). Further, closely related porphyrin compounds, such as phthalocyanines (193), porphyrazines (193), biliverdins (302), corroles (144, 275), and texaphyrins (282), have been explored as SOD mimics. Although it is not an SOD mimic, a texaphyrin MGd (282) is also addressed in this review, as it appeared efficacious as an anticancer agent and produced effects similar to those of Mn porphyrins in ameliorating amyotrophic lateral sclerosis (66).

Other types of Mn complexes have also been considered as SOD mimics (Fig. 1). Cyclic polyamine (aza crown ethers)-based SOD mimics were characterized in details *in vitro* and *in vivo* (295). Mn salen derivatives were investigated as well (88). Along with metal-based SOD mimics, some nonmetallic and, thus far less-efficient compounds, such as nitroxides (140) and fullerenes (181, 349), also have been explored. Further, covalently bound porphyrins and nitroxides were studied (160). The increased understanding of the critical role played by mitochondria in numerous pathologic conditions (55, 155, 227, 228, 308) gave rise to the design of mitochondrially targeted systems with antioxidant properties. Among the most successful ones are monocationic MitoQ compounds, developed by Michael Murphy *et al.* (227, 228). These compounds possess a positively charged moiety (triphenylphosphonium cation) that drives them into mitochondria and a lipophilic alkyl chain that facilitates their transfer across the lipid bilayer. At the end of the alkyl chain, different redox-active compounds have been attached, including nitroxides (18, 90, 227, 228, 305, 308). Mitochondrially targeted oligopeptides have been attached to Mn porphyrins as well (18). Driven by the mitochondrial membrane potential, potent pentacationic Mn porphyrins with no particular targeting moiety also were found to be directly taken up by mitochondria (305). An MnSOD knockout yeast study suggested that Mn salen can also enter mitochondria (at least those of yeast) (131). In addition to synthetic antioxidants that act catalytically, natural antioxidants have been used in numerous studies and clinical trials with partially satisfactory results (270, 291, 292, 311). The lack of full success is often ascribed to a poor design, quality of the study, external and internal validity, homogeneity of the sample, baseline status, dosing, timing, interaction among nutrients, gene polymorphism, and statistical power. Debate still exists, and a detailed study is ongoing to understand which component/s of tea, olive oil, wine, and so on, are beneficial, whether it be polyphenols or something else (146). Lately, the combined therapy of synthetic and natural antioxidants has been frequently employed.

The *in vivo* effects of different types of compounds are influenced primarily by (a) antioxidant ability; (b) bioavailability (*i.e.*, the ability to accumulate within a cell and its compartments); and (c) toxicity. Bioavailability is dependent on the size, charge, shape, (conformational flexibility and overall geometry), and lipophilicity and greatly affects the *in vivo* efficacy; data already indicate that whereas some drugs may be good in one model, they may fail or be less efficient in another one, as a consequence of differences in the extent of accumulation in subcellular compartments targeted (88, 131, 255). Detailed pharmacokinetic and toxicology data are still scarce. None of the SOD mimics thus far has been approved for clinical use. To better judge the therapeutic potential and the advantage of one over the other type of compound, comparative studies of different types of drugs in the same cellular or animal model or both are needed. Thus far, only limited data have been provided (77, 131, 225, 255). Further, few studies have shown that protective effects *in vivo* parallel the *in vitro* magnitude of the catalytic rate constant for $O_2^{\cdot-}$ dismutation or peroxynitrite reduction or both (241, 255). Such data justify further efforts to understand the role of structure–activity relationship in designing SOD mimics and peroxynitrite scavengers.

We here provide an overview of the chemical properties and some *in vivo* effects observed with different classes of compounds, with a special emphasis on porphyrin-based compounds. Of note, in many instances, clear activities toward particular reactive species (in the form of rate constants) are missing, and assumption has been often made about such action, or the lack thereof. Finally, financial interests involved in the pharmaceutical development of these compounds have often influenced the objectivity of some of the reviews published. Often, poor management of patenting and licensing rights has resulted in the "Valley of Death" status of SOD mimics, preventing them from reaching clinical trials and clinical use in a timely manner, if at all (118).

Most potent SOD mimics are metal complexes, which may eventually lose metal while redox cycling. Mn, in its own right, is able to catalyze $O_2^{\cdot-}$ dismutation at a fair rate, and thus is, in essence, an SOD mimic, too (14, 25). In some instances, Mn released from a complex, rather than the metal complex itself, could be responsible for the effects observed (262). Therefore, we addressed herein the SOD-like ability of "free" Mn^{2+} both in aqueous solutions and *in vivo*.

The purity of any SOD mimic should be established very carefully with extensive and multiple analyses. Even minute impurities, negligible for most chemistry-related research, might decrease/increase/modify the SOD-like activity of the material, affect its therapeutic and/or mechanistic evaluations, jeopardize the conclusions of many studies, and harm the health of the antioxidant field as a whole (31, 263–265).

As $ONOO^-$ is an adduct of $O_2^{\cdot-}$ and $^{\cdot}NO$, and some SOD mimics are potent $ONOO^-$ reduction catalysts, we found it important to address herein also the $ONOO^-$-scavenging abilities of the SOD mimics.

II. Manganese and Mn Complexes with Simple Ligands

A. SOD-like activity of manganese

All Mn-based SOD mimics, but particularly those of lower metal/ligand stability, may lose Mn (to some extent) when they are in low oxidation state (such as + 2), during the Mn^{3+} and Mn^{2+} cycling in the $O_2^{\cdot-}$ dismutation catalysis. Furthermore, some of the biologic chelators may dechelate Mn from SOD mimics of low metal/ligand stability, such as Mn cyclic polyamines, Mn salen derivatives, and Mn β-octabrominated porphyrins. Thus, it is important to verify whether "free" Mn^{2+} (*i.e.*, unbound from the corresponding ligand) can exert SOD-like activity *in vitro*/*vivo*. Control experiments with Mn^{2+} and nonmetallated ligands are, therefore, critical for mechanistic conclusions.

The SOD-like activity of Mn^{2+} is dependent on the type of the ligand, whether it is a hexaaqua-, carboxylato-, monohydroxo-, or oxo/hydroxo/acetato species. A few data on the

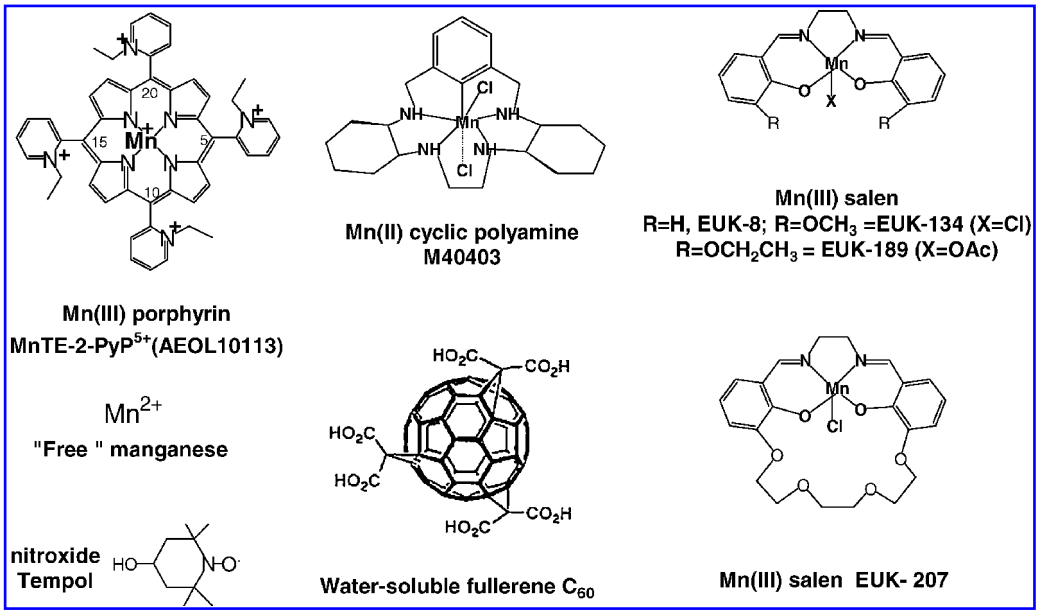

FIG. 1. SOD mimics. Mn(III) porphyrins, Mn(II) cyclic polyamines, Mn(III) salen derivatives, nitroxides, and fullerenes were shown to possess SOD-like activity. "Free" Mn (*i.e.*, low-molecular-weight Mn(II) species) such as aqua, oxo, hydroxo, and carboxylato species are able to dismute $O_2^{\cdot-}$ also. 5,10,15,20: *meso* positions of methine bridges between pyrrolic rings.

SOD-like activity of $MnCl_2$ in medium containing phosphate buffer are available. Our group has reported k_{cat}, determined by pulse radiolysis in 0.05 *M* potassium phosphate buffer, pH 7.8, 25°C, to be $k_{cat} = 1.3\times10^6$ $M^{-1}s^{-1}$ (302). Joan Valentine's group (25) reported a higher value, $k_{cat} = 8.9\times10^6$ $M^{-1}s^{-1}$, in essentially identical 0.05 *M* phosphate medium, pH 7 (25), with superoxide produced through ^{60}Co gamma irradiation; the formation of monoformazan in the reaction of XTT or MTS with $O_2^{\cdot-}$ was followed. Archibald and Fridovich (14) reported the SOD-like ability of different Mn complexes prepared *in situ*. The ligands investigated were phosphate, pyrophosphate, formate, lactate, citrate, succinate, acetate, cacodylate, and propionate. Mn lactate was the most potent SOD mimic; its activity expressed per milligram Mn was only 65-fold lower than that of the SOD enzyme. The other complexes were several-fold less potent; Mn phosphate being ~253-fold less potent than SOD enzyme ($k_{cat} \sim 4\times10^6$ $M^{-1}s^{-1}$) (14).

The Naughton group published SOD-like activities of different Mn complexes with ligands such as EDTA, EGTA, EHPG, EBAME, and salen by using nitrobluetetrazolium (NBT) assay (114, 115). The SOD-like activities of those complexes were expressed as IC_{50} (μM) values (114, 115), which, if converted to the corresponding rate constants by comparison with Cu,ZnSOD and the SOD mimic MnTE-2-PyP^{5+} data, resulted in too high k_{cat} values (up to 10^7 $M^{-1}s^{-1}$). The k_{cat} values for aquated Mn(II) (115) and Mn salen were reported by Naughton's group (114, 115) as 3.6×10^6 $M^{-1}s^{-1}$ and 8.7×10^6 $M^{-1}s^{-1}$, respectively, which are three- and 10-fold higher than the values determined by us (302). The NBT assay has substantial disadvantages over the cytochrome *c* assay, as NBT itself can mediate the formation of $O_2^{\cdot-}$ (195). From the experimental section in references 114 and 115, the nature of the aquated ion is not obvious (whether it is a phosphate salt). The presentation of the data in different styles in different publications prevents their direct comparisons with other compounds. Furthermore, these same reports (114, 115) show the k_{cat} for MnEDTA to be 6×10^5 $M^{-1}s^{-1}$, whereas we (302), Archibald and Fridovich (14), and Baudry *et al.* (40) were not able to detect any measurable SOD-like activity of MnEDTA.

We recently reported that nonporphyrin Mn species, tentatively formulated as Mn hydroxo/oxo/acetato species, appear as impurities in commercial $MnTBAP^{3-}$ preparations and, although unstable, are very effective in dismuting $O_2^{\cdot-}$. Consequently, the impure $MnTBAP^{3-}$ preparations exhibit SOD-like activity (31, 264). $MnTBAP^{3-}$ preparations from different commercial sources and different batches from the same source contained different levels of those trace Mn species and, thus, each sample showed different SOD-like activities. As these species occur in trace amounts and are not stable (SOD activity of the commercial samples decreased with the aging of the solution), they were not isolated, and their absolute SOD-like activity was, therefore, not quantified (264). It is worth noting that because such species appear in trace amounts, they must, consequently, possess high SOD activity to account for the effect observed.

In summary, the SOD-like activity of Mn^{2+} is highly dependent on the type of potential counteranion/ligand present in the medium and may be equal to, or higher than 10^6 $M^{-1}s^{-1}$.

B. *The effects of manganese* in vitro *and* in vivo

Archibald and Fridovich (15) showed that *Lactobacillus plantarum* compensates for the lack of SOD enzyme by accumulation of manganese to millimolar levels. SOD-deficient *E. coli,* lacking cytosolic SOD enzymes, does not grow aerobically, but it grows equally well as wild type if an SOD mimic is supplied in the medium to substitute for the lacking SOD enzymes (9, 15, 30, 85). Aerobic growth of SOD-deficient *E. coli* is an $O_2^{\cdot-}$-specific, *in vivo* system that usefully predicts which compounds may be prospective therapeutics for clinical development. Mn^{2+} protects SOD-deficient *E. coli* when growing aerobically, although not as efficiently as Mn porphyrins

(9, 225). The effects are related to the decrease in oxidative stress, protection of aconitase activity, and decreased mutations, which result in increased growth; all effects become obvious at $>0.5\,mM$ $MnCl_2$ (9). We also showed that $1\,\mu M$ Mn^{2+} offers some radioprotection to ataxia telangiectasia cells, but is significantly less efficient than $1\,\mu M$ of a more potent SOD mimic, Mn porphyrin MnTnHex-2-PyP^{5+} (255). Although Mn^{2+} seems of comparable efficacy to Mn salen and Mn cyclic polyamine (255), the latter complexes were used at higher (10 or $20\,\mu M$) concentrations, which precluded a full assessment of the extent of radioprotection by $MnCl_2$ in comparison to all other compounds in that particular model (255). In MnSOD-knockout *Cryptococcus neoformans*, whose growth is susceptible to oxidative stress at elevated temperatures, Mn salen and ascorbate, but not $MnCl_2$ and none of several different anionic and cationic Mn porphyrins, were protective (131). Because of the low metal/ligand stability of Mn salen, it is not clear whether Mn salen remains as such, or whether the compound acts as an Mn-carrier into the mitochondria, where released Mn could act in its own right. Our data with *E. coli* (262) have unambiguously shown that such Mn-transporting mechanism may be relevant for certain SOD mimics *in vivo*: the Mn octabrominated porphyrin, $MnBr_8$ $TSPP^{3-}$, which has low metal/ligand stability, can transport Mn^{2+} into the *E. coli* cell (262); metal-free octabrominated porphyrin ligand was spectroscopically detected within the cells (262). Exogenous Mn in millimolar concentrations rescued $O_2^{\cdot-}$-sensitive phenotypes of *S. cerevisiae* lacking Cu,ZnSOD (279). Similar findings, wherein non-SOD manganese is a backup for Cu,ZnSOD in *S. cerevisiae*, was later reported by Reddi *et al.* and Culotta *et al.* (72, 267). Enhancement of stress resistance and the effect of Mn^{2+} supplementation on the life span of *Caenorhabditis elegans* was reported (193). The role of Mn transporters also was addressed, and carboxylates rather than phosphates were suggested as possible ligand carriers for Mn^{2+} (267). Data by Reddi *et al.* (267) are in agreement with our study, in which Mn oxo/hydroxo/acetato complexes, present as a non-innocent impurity in ill-purified $MnTBAP^{3-}$ preparations, are responsible for the SOD-like activity (264). The issues with respect to Mn^{2+} remain mostly unresolved, particularly the true nature of the Mn^{2+} complexes responsible for $O_2^{\cdot-}$ scavenging ability of Mn^{2+} *in vivo*. A very recent and intriguing *E. coli* report by the Imlay group (13) suggested that Mn substitutes for Fe in Fe enzymes vulnerable to $O_2^{\cdot-}$ attack (which would have otherwise resulted in deleterious effects of Fenton chemistry) rather than act by $O_2^{\cdot-}/H_2O_2$ scavenging.

Because of the dismuting ability of Mn^{2+}, and particularly when mechanistic purposes are the goal of the study, it is important to have Mn-based antioxidants very pure and devoid of "free", residual Mn^{2+} in any form. Anionic porphyrins are the most difficult to purify with respect to residual manganese. For such purposes, we developed a very sensitive method for quantifying residual, nonporphyrin-bound Mn^{2+} species in Mn-based SOD mimic systems of high metal/ligand stability (263).

III. Porphyrin-Based SOD Mimics

A. Metalloporphyrins

The metalloporphyrins, and preferably water-soluble Mn but not Fe complexes, have been chosen as potential SOD mimics for the reasons cited in the introduction. Two scientists greatly influenced the design and use of metalloporphyrins as SOD mimics, Irwin Fridovich, the "father" of the free radical biology and medicine, and Peter Hambright, the "father" of water-soluble porphyrins, with both of whom we have had the honor to work and to learn from. The seminal report of Irwin Fridovich group on Mn porphyrin-based SOD mimics in the 1994 *J Biol Chem,* included also the MnTM-4-PyP^{5+} and $MnTBAP^{3-}$ ($MnTCPP^{3-}$) complexes (105). Although $MnTBAP^{3-}$ was not explicitly shown to be an SOD mimic in its own right in that publication, the fact that its structure and some incorrect data were reported there may have misled the biomedical audience; for example, the $E_{1/2}$ of $MnTBAP^{3-}$ was reported as $\sim +110$ mV *versus* NHE, which is 304 mV more positive than the correct value published thereafter [–194 mV *vs.* NHE (30)] and recently was confirmed in a pure $MnTBAP^{3-}$ sample (264). It is worth noting that were the initial value true, $MnTBAP^{3-}$ might have functioned as an SOD mimic. Another incorrect assignment of the $MnTBAP^{3-}$ SOD-like activity followed in the *J Pharmacol Exp Ther* 1995 by Day *et al.* (81). Soon afterward, we established the first structure–activity relationship that correlated the ability of Mn and Fe porphyrins to dismute $O_2^{\cdot-}$ (log k_{cat}) with their metal-centered reduction potentials, $E_{1/2}$ (for $Mn^{III}P/Mn^{II}P$ redox couple) (30). The most potent compound at that time, MnTE-2-PyP^{5+}, was identified and forwarded to *in vitro* and *in vivo* studies. In 1998, Rafael Radi (105–109) suggested, and he and his group successfully tested, the possibility that potent SOD mimics could also be powerful $ONOO^-$ scavengers. A few years later, another mechanistic aspect of the *in vivo* efficacy of this and other Mn porphyrins emerged as a consequence of the ongoing efforts to understand the role of ROS/RNS in signaling events in oxidative stress–related conditions, disorders, and diseases as diverse as inflammatory and immune responses, cancer, radiation injury, diabetes, aging, central nervous system disorders, and so on. It became obvious that the effects observed when using Mn porphyrins were not only the consequence of mere scavenging of ROS/RNS, but that MnPs were also able to modulate ROS/RNS-based signaling pathways. Several articles that followed provided evidence that a potent SOD mimic/$ONOO^-$ scavenger, such as MnTE-2-PyP^{5+}, can strongly inhibit excessive activation of redox-sensitive cellular transcriptional activity (39, 221, 222, 259, 288, 322, 350).

Thus, over the years, our views on Mn porphyrins evolved from SOD mimics, to $O_2^{\cdot-}/ONOO^-$ scavengers, and finally to redox modulators of cellular transcriptional activity. The same is also true for other groups of synthetic SOD mimics discussed later. At this point, we do not exclude other possible roles of Mn porphyrins. The Tauskela group (314, 315, 342) suggested the action of MnP on Ca^{2+} metabolism (which may again be ROS modulated), whereas the Kalyanaraman group (176) reported on the induction of heme oxygenase by MnP. Because of the biologically accessible metal-centered reduction potential and the ability to reach four oxidation states *in vivo* ($+2, +3, +4$, and $+5$), cationic Mn porphyrins can redox cycle with a number of biologic molecules, such as cellular reductants, flavoenzymes and cytochrome P450 reductase, and can mimic the cyt P450 family of enzymes (79, 108, 304); as a consequence of their rich chemistry and redox-cycling capabilities, these compounds may be easily involved in beneficial and in adverse pathways. The possibility that

electrostatic interactions of MnPs with biologic molecules contribute to their action/s *in vivo* is not excluded and will be further explored (39).

B. Design of porphyrin-based SOD mimics

1. Thermodynamics. The design of porphyrinic SOD mimics has been based on the simulation of both the thermodynamic and electrostatic properties of the enzyme itself. Self-dismutation of $O_2^{\cdot-}$ at pH 7.4 occurs with a rate constant, $k \sim 5\times10^5\ M^{-1}s^{-1}$, and is increased more than three orders of magnitude in the presence of SOD (145) (Fig. 2). All SOD enzymes, regardless of the type of metal (Mn, Fe, Cu, Zn, Ni), have metal-centered reduction potential around +300 mV *versus* NHE, which is midway between the potential for the reduction (+850 mV *vs.* NHE) and oxidation of $O_2^{\cdot-}$ (−160 mV *vs.* NHE). Thus, both processes are thermodynamically equally favored at ~ +300 mV *versus* NHE. In turn, both reduction and oxidation reactions in the dismutation process occur with the same rate constant of $2\times10^9\ M^{-1}s^{-1}$ (100, 174, 325). In addition to the suitable thermodynamics of the active site, the appropriate placement of positively charged amino acid residues along a tunnel leading to the metal site in the enzymes provides electrostatic guidance for the approach of $O_2^{\cdot-}$ to the active site (87, 128).

The $O_2^{\cdot-}$ dismutation mechanism catalyzed by Mn porphyrins involves two steps in which the Mn center cycles between Mn(III) and Mn(II). As most Mn porphyrins contain Mn in the +3 oxidation state, the first step, which coincides with the rate-limiting step, corresponds to the reduction of Mn(III) by $O_2^{\cdot-}$ to yield Mn(II) and O_2. The second step corresponds to the oxidation of Mn(II) by $O_2^{\cdot-}$ to yield H_2O_2 and reestablish the Mn(III) porphyrins. This catalytic cycle is evidently modulated by the redox potential of the metal site (Fig. 2).

Mn(III) *meso*-tetrakisphenylporphyrin ($MnTPP^+$) has $E_{1/2} = -280$ mV *versus* NHE and *para* Mn(III) *meso*-tetrakis (4-pyridylporphyrin) ($MnT\text{-}4\text{-}PyP^+$) has $E_{1/2} = -200$ mV *versus* NHE (299) (Table 1). Both reduction potentials are outside the window for $O_2^{\cdot-}$ reduction and oxidation (Fig. 3). Therefore, these Mn(III) porphyrins cannot be reduced by $O_2^{\cdot-}$ in the first step of the catalytic cycle and were not found to be SOD mimics (30, 299). Attaching electron-withdrawing groups to the porphyrin molecule as close to the metal site as possible has been a viable strategy to increase the metal-site electron deficiency, which makes Mn more prone to accept electrons. In turn, as the reduction potential increases, the first step of the catalytic cycle is favored. Indeed, the introduction of positive charges on pyridyl nitrogens of $MnT\text{-}4\text{-}PyP^+$ to yield $MnTM\text{-}4\text{-}PyP^{5+}$ increased $E_{1/2}$ dramatically by 260 mV, from −200 mV to +60 mV *versus* NHE, respectively. With $E_{1/2}$ of $MnTM\text{-}4\text{-}PyP^{5+}$ placed between the potential for the reduction and oxidation of $O_2^{\cdot-}$, the catalytic cycle of $O_2^{\cdot-}$ dismutation could be established on thermodynamic grounds, giving rise to a fair value for the catalytic rate constant, $k_{cat} = 3.8\times10^6\ M^{-1}s^{-1}$ (29); the rate-limiting step still remained the reduction of $Mn^{III}P$ to $Mn^{II}P$. A problem associated with compounds such as $MnTM\text{-}4\text{-}PyP^{5+}$, which limits their use as SOD mimics in cell/animal experiments, is their ability to adopt a near-planar structure, as pointed out by Pasternack (249, 250), and consequently to associate with and intercalate into nucleic acids (249, 250). Still, the bulkiness imposed by the water molecules axially bound to the Mn center limits the intercalation. $Mn^{III}TM\text{-}4\text{-}PyP^{5+}$, with the manganese in the oxidized Mn(III) form, is more electron deficient and binds axial waters more strongly than the electron-rich reduced Mn(II) site in $Mn^{II}TM\text{-}4\text{-}PyP^{4+}$. Thus, because of the steric hindrance, the bulkier $Mn^{III}TM\text{-}4\text{-}PyP^{5+}$ associates with nucleic acids much less than the $Mn^{II}TM\text{-}4\text{-}PyP^{4+}$ (249, 250). Yet, while redox cycling with $O_2^{\cdot-}$, the reduced $Mn^{II}TM\text{-}4\text{-}PyP^{4+}$ is formed, which associates with nucleic acids. We have reported that such associations with nucleic acids fully prevented MnP from dismuting $O_2^{\cdot-}$ (29). When nucleic acids of $MnTM\text{-}4\text{-}PyP^{5+}$-treated *E. coli* were removed from the cell extract [by precipitation with protamine sulfate (29, 249, 250)], the SOD-like activity of the cell extract was fully restored. Furthermore, associations with nucleic acids not only affected the *in vivo* SOD activity of the compound but also introduced toxicity.

To overcome such problems and further to enhance SOD-like activity, we placed the electron-withdrawing groups closer to the Mn site, into the *ortho* positions, to yield $MnTM\text{-}2\text{-}PyP^{5+}$ (AEOL10112). The $E_{1/2}$ value of $MnTM\text{-}2\text{-}PyP^{5+}$ was increased by 160 mV relative to $MnTM\text{-}4\text{-}PyP^+$, resulting in a potential of +220 mV *versus* NHE, which was very close to the $E_{1/2}$ of the enzyme itself. Further, because of the steric hindrance between the methyl groups in the *ortho* positions of the pyridyl rings and the protons at the *β*-pyrrolic carbons, the pyridyl moiety remains relatively perpendicular to the porphyrin plane, and $MnTM\text{-}2\text{-}PyP^{5+}$ (and related compounds)

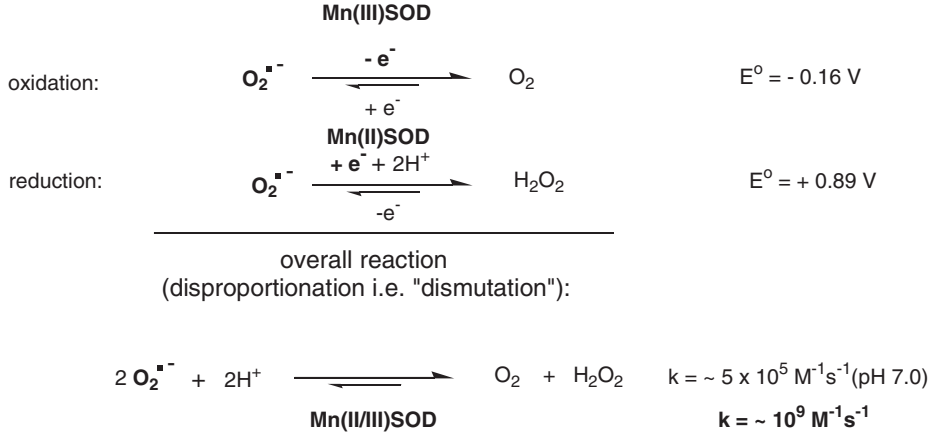

FIG. 2. The $O_2^{\cdot-}$ dismutation process.

Table 1. Selected Physicochemical Properties of Some SOD Mimics

Compound	$Mn^{III/II}$ potential, $E_{1/2}/mV$ vs. NHE[a]	SOD activity log $k_{cat}(O_2^{\bullet-})$[b]	PN red. activity log $k_{red}(ONOO^-)$[c]	Lipophilicity Rel. R_f[d]	Lipophilicity log P_{ow}	Ref.
Cationic porphyrins						
MnTM-2-PyP^{5+}	+220	7.79	7.28	0.5	−7.86	29, 179
MnTE-2-PyP^{5+}	+228	7.76 (cyt *c*) 7.73 (p.r.)	7.53	1	−6.89	30, 179, 302
MnTnPr-2-PyP^{5+}	+238	7.38	7.15	1.8	−5.93	37, 179
MnTnBu-2-PyP^{5+}	+254	7.25	7.11	3.2	−5.11	37, 179
MnTnHex-2-PyP^{5+}	+314	7.48	7.11	6.3	−2.76	37, 179
MnTnHep-2-PyP^{5+}	+342	7.65		7.7	−2.10	178, 179
MnTnOct-2-PyP^{5+}	+367	7.71	7.15	8.2	−1.24	179
MnTMOE-2-PyP^{5+}	+251	8.04 (p.r.)		1.2		38
MnTTEG-2-PyP^{5+}	+250	8.11		1.0		36
MnTrM-2-PyP^{4+}	+118	6.63		1.1		30, 265
MnBM-2-PyP^{3+}	+53	6.52		2.3		30, 265
MnTrE-2-PyP^{4+}				2.2		30, 265
MnBE-2-PyP^{3+}				4.4		30, 265
MnTDM-2-ImP^{5+}	+320	8.11		0.5		266
MnTDE-2-ImP^{5+}	+346	7.83 (p.r.)		2.3	−6.48	38
MnTDnPr-2-ImP^{5+}	+320	8.11				167
MnTM,MOE-2-ImP^{5+}	+356	7.98 (p.r.)		1.2		38
MnTDMOE-2-ImP^{5+}	+365	7.59 (p.r.)		1.6		38
MnTDTEG-2-ImP^{5+}	+412	8.55		2.0		36
MnTM-3-PyP^{5+}	+52	6.61	6.62	0.8	−6.96	29, 179
MnTE-3-PyP^{5+}	+54	6.65		1.7	−5.98	178, 179
MnTnPr-3-PyP^{5+}	+62	6.69		3.7	−5.00	178, 179
MnTnBu-3-PyP^{5+}	+64	6.69		6.7	−4.03	178, 179
MnTnHex-3-PyP^{5+}	+64	6.64		9.2	−2.06	178, 179
MnTM-4-PyP^{5+}	+60	6.58	6.63	0.5		29, 266
MnTE-4-PyP^{5+}	+70	6.86				299
MnTDM-4-PzP^{5+}	−4	5.83		0.6		266
MnT(TriMA)P^{5+}	−100	5.11		1.8		266
MnT(TFTriMA)P^{5+}	+58	6.02				30
$MnCl_1$TE-2-PyP^{5+}	+293	7.75		1.1		166
$MnCl_2$TE-2-PyP^{5+}	+343	8.11		1.2		166
$MnCl_3$TE-2-PyP^{5+}	+408	8.41		1.3		166
$MnCl_4$TE-2-PyP^{5+}	+448	8.60		1.3		165
$MnCl_5$TE-2-PyP^{5+}	+560	8.41				165
$MnBr_8$TM-3-PyP^{4+}	+468	≥8.85				85
$MnBr_8$TM-4-PyP^{4+}	+480	≥8.67				33, 85
CuTM-4-PyP^{4+}		<3.7				33
$CuBr_8$TM-4-PyP^{4+}		6.46				33
Neutral porphyrins						
MnT-2-PyP^+	−280	4.29		10.2		301
$MnBr_8$T-2-PyP^+	+219	5.63				261, 301
MnT-4-PyP^+	−200	4.53				299
$MnTPP^+$	−270	4.83				299
$MnTPFPP^+$	−120	5.00				299
$MnTBzP^+$	+88	5.20				182
Anionic porphyrins						
$MnTBAP^{3-}$ (pure form)	−194	3.16	5.02			264
$MnTSPP^{3-}$	−160	3.93	5.53			30
MnT(2,6-Cl_2-3-SO_3-P)P^{3-}	+88	6.00				30
MnT(2,6-F_2-3-SO_3-P)P^{3-}	+7	5.51				30
$MnBr_8TSPP^{3-}$	+209	5.56				262
$MnBr_8TCPP^{3-}$	+213	5.07				262
Salens						
$Mn(salen)^+$, EUK-8	−130	5.78[e]		12		255, 302
EUK-134		5.78				255
EUK-189		5.78				255
Cyclic polyamines						
M40403	+525 (ACN)	7.08, 6.55		13		204, 255, 269
M40404(2R,21R-Me_2-M40403)	+452 (ACN)	Inactive		12		204, 269, 255
2S,21S-Me_2-M40403	+464 (ACN)	8.37, 9.20				204, 26921

(*Continued*)

TABLE 1. (CONTINUED)

Compound	$Mn^{III/II}$ potential, $E_{1/2}/mV$ vs. NHE[a]	SOD activity log $k_{cat}(O_2^{\bullet-})$[b]	PN red. activity log $k_{red}(ONOO^-)$[c]	Lipophilicity Rel. R_f[d]	Lipophilicity log P_{ow}	Ref.
Fullerenes						
C_{60}-water-soluble fullerene (C_3)		6.30				8
Miscellaneous						
Mn^{2+}	+850[f]	6.11 (cyt *c*)6.28 (p.r.)6.95 (p.r.)		0		299, 255, 302, 25
Mn-EDTA		inactive (cyt *c*)				302, 14, 40
$[MnBV^{2-}]_2$	−300 (+460[g])	7.40 (cyt *c*)6.95 (p.r.)				302
$[MnBVDME]_2$	−230 (+450[g])	7.70 (cyt *c*)6.95 (p.r.)				302
$[MnMBVDME]_2$	−260 (+440[g])	7.36				299
$[MnBVDT^{2-}]_2$	−260 (+470[g])	7.40				299
4-carboxy-Tempo		7.54 (pH 5.4)				140
MnTrM-2-Corrole^{3+}	+910[g]	5.94				99
OsO_4		9.14[h]				135
CeO_2 (3-5 nm particles)		9.55				177
Honokiol		5.50				92
Mn texaphyrin		~4.48				289

Mn(III)/Mn(II) reduction potential ($E_{1/2}$); SOD activity ($O_2^{\bullet-}$ dismuting catalytic rate constant, log k_{cat}); peroxynitrite (PN) reducing activity ($ONOO^-$ reduction rate constant, log k_{red}); lipophilicity of $Mn^{III}P$ (chromatographic retention time, R_f; octanol-water partition coefficient, log P_{ow}).

[a]$E_{1/2}$ data measured either directly in 0.05 *M* phosphate buffer, pH 7.8, 0.1 *M* NaCl, or converted accordingly to this medium, unless noted otherwise.

[b]SOD activity measured by the cyt *c* assay in 0.05 *M* phosphate buffer, pH 7.8, 25 ± 1°C, unless noted otherwise.

[c]Measurements in 0.05 *M* phosphate buffer, pH 7.4, 37 ± 0.1°C.

[d]Data relative to the R_f value of MnTE-2-PyP^{5+} in plastic-backed silica-gel thin-layer chromatography plates eluted with 1:1:8 $KNO_{3(sat)}$:H_2O:MeCN.

[e]No SOD-like activity was observed in the presence of EDTA (283).

[f]Oxidation potential only, Mn^{III}/Mn^{II} redox couple is irreversible.

[g]$E_{1/2}$ data associated with the $Mn^{IV/III}$ reduction potential.

[h]pH 5.1–8.7.

p.r., pulse radiolysis.

can no longer adopt a near-planar conformation. The overall bulkiness diminishes the interactions with nucleic acids and toxicity. Retrospectively, moving the positive charges from distant *para* into closer *ortho* positions afforded also a large enhancement in the electrostatic facilitation for the approach of $O_2^{\bullet-}$ to the Mn site (266, 301) (see later).

Dramatic effects also were achieved by introducing electron-withdrawing bromines or chlorines onto *β*-pyrrolic positions of MnTM-4-PyP^{5+} or MnTE-2-PyP^{5+}. Such a maneuver shifted the reduction potential 420 mV and 220 mV more positively in octabrominated $MnBr_8$TM-4-PyP^{4+} ($E_{1/2}$ = + 480 mV *vs.* NHE), and tetrachlorinated $MnCl_4$TE-2-PyP^{5+}

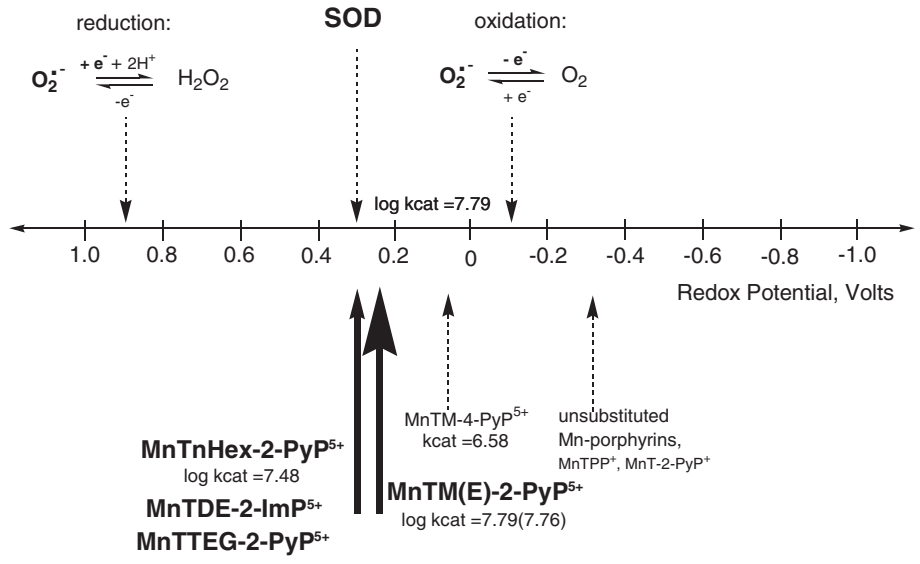

FIG. 3. Redox diagram for $O_2^{\bullet-}$ reduction and oxidation and the placement of Mn porphyrins on it.

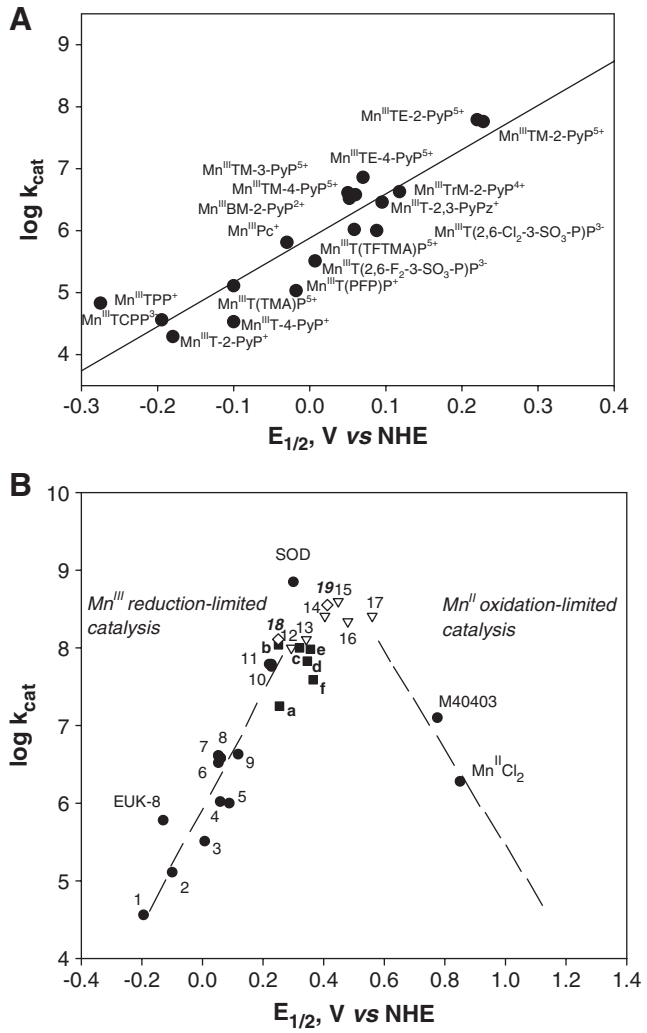

FIG. 4. Struture-activity relationships. (**A**) The very first structure–activity relationship between log k_{cat} ($O_2^{\cdot-}$) and $E_{1/2}$ ($Mn^{III}P/Mn^{II}P$) included porphyrins of different charge, different stericity, and different electrostatics for $O_2^{\cdot-}$ dismutation. (**B**) As the $E_{1/2}$ increases, the Mn^{+2} oxidation state gets stabilized, and eventually oxidation of porphyrin becomes the rate-limiting step, and k_{cat} starts to decrease again. Only water-soluble Mn(III) porphyrins are given in the left, linear section of the curve that obeys the Marcus equation, and data (*circles*) are from ref. 30: (1) $Mn^{III}TCPP^{3-}$, (2) $Mn^{III}T(TMAP)^{5+}$, (3) $Mn^{III}T(2,6\text{-}F_2\text{-}3\text{-}SO_3\text{-}P)P^{3-}$, (4) $Mn^{III}T(TFTMAP)P^{5+}$, (5) $Mn^{III}T(2,6\text{-}Cl_2\text{-}3\text{-}SO_3\text{-}P)P^{3-}$, (6) $Mn^{III}BM\text{-}2\text{-}PyP^{3+}$, (7) $Mn^{III}TM\text{-}3\text{-}PyP^{5+}$, (8) $Mn^{III}TM\text{-}4\text{-}PyP^{5+}$, (9) $Mn^{III}TrM\text{-}2\text{-}PyP^{4+}$, (10) $Mn^{III}TM\text{-}2\text{-}PyP^{5+}$, and (11) $Mn^{III}TE\text{-}2\text{-}PyP^{5+}$. Data for EUK-8 are from ref. 302, and for $MnCl_2$, from refs. 299 and 302; data for Mn(II) cyclic polyamine M40403 are from ref. 21. Data for SOD are from ref. 218. Data for $Mn^{III}Cl_{1\text{-}4}MnTE\text{-}2\text{-}PyP^{5+}$ (12–15) are from ref. 166, data for $Mn^{II}Br_8TM\text{-}4\text{-}PyP^{4+}$ (16) are from ref. 33, and for $Mn^{II}Cl_5TE\text{-}2\text{-}PyP^{4+}$ (#17), from ref. 165 (*triangles*). Data for $Mn^{III}TnBu\text{-}2\text{-}PyP^{5+}$ (a) are from ref. 37; $Mn^{III}TMOE\text{-}2\text{-}PyP^{5+}$ (b) from ref. 38; $Mn^{III}TD(M)E\text{-}2\text{-}ImP^{5+}$ (c, d) from refs. 38 and 167; $Mn^{III}TM,MOE\text{-}2\text{-}PyP^{5+}$ (e), and for $Mn^{III}TDMOE\text{-}2\text{-}ImP^{5+}$ (f) from ref. 38 (*squares*). Data points 18 and 19 (*diamonds*) belong to $MnTTEG\text{-}2\text{-}PyP^{5+}$ and $MnTDTEG\text{-}2\text{-}ImP^{5+}$ and are from ref. 36.

($E_{1/2} = +448$ mV *vs*. NHE) *versus* nonhalogenated analogues (Table 1) (33, 166). The $MnBr_8TM\text{-}4\text{-}PyP^{4+}$ has a very high k_{cat} of 2.2×10^8 $M^{-1}s^{-1}$. Yet, a huge shift in $E_{1/2}$ (*i.e*., a dramatic increase in electron-deficiency) stabilized Mn in its +2 oxidation state. (When cationic porphyrins bear 5^+ charge they have Mn in +3 oxidation state [$Mn^{III}P^{5+}$], and with 4^+ total charge, Mn is in +2 [$Mn^{II}P^{4+}$] or +4 oxidation states [$O=Mn^{IV}P^{4+}$].) Consequently, $MnBr_8TM\text{-}4\text{-}PyP^{4+}$ has a metal/ligand stability constant of only $10^{8.08}$ M (33), and loses Mn readily upon dilution at pH 7.8. Although its characterization was important for the design of Mn porphyrins, as a proof of concept, the compound itself was not of practical importance. With the availability of a wide spectrum of porphyrins (many provided by MidCentury Chemicals, Chicago, IL), their physicochemical and SOD-like activities were explored, and the very first structure–activity relationship was established for a variety of water-soluble Fe and Mn porphyrins possessing different charges and geometry (Fig. 4A) (30). We found that the higher the $E_{1/2}$, the more electron deficient the porphyrin is (as witnessed by the protonation of the pyrrolic nitrogens), and thus the higher the k_{cat}. The most potent SOD mimics are the cationic Mn(III) *N*-alkylpyridylporphyrins, in particular, the *ortho* isomers. Further increase in $E_{1/2}$ stabilizes Mn^{2+} so much that the Mn porphyrins exist predominantly in the reduced Mn(II) form; the $Mn^{II}P$ oxidation step then becomes rate limiting, and the SOD-like activity decreases (Fig. 4B) (37). It must be emphasized that the validity of k_{cat} data obtained with cytochrome *c* assay was confirmed by both pulse-radiolysis study (302) and stopped-flow technique (184, 185). The same agreement between these two methods was further confirmed by the Zeev Gross group (99).

Over the years, given the lipophilic nature of the major drugs, the biomedical community has been concerned that excessively charged, pentacationic Mn porphyrins would fail to accumulate within the cell at levels sufficient to provide therapeutic effects. To account for such reasonable objections, the $MnTalkyl\text{-}2\text{-}PyP^{5+}$ series was synthesized (alkyl moieties ranging from methyl to octyl) and their k_{cat} and $E_{1/2}$ determined (37). The lipophilicity described firstly by thin-layer chromatography retention factor, R_f and later by partition between *n*-octanol and water (P_{OW}) (179), increased from methyl to *n*-octyl in a linear fashion (Table 1). All of the analogues, bearing alkyl chains of different length, have high SOD activity. Small fluctuations observed were attributed to the interplay of the hydration and steric effects (37).

Based on the same thermodynamic and electrostatic premises, the imidazolyl derivatives, $MnTD\text{-}alkyl\text{-}2\text{-}ImP^{5+}$, were then synthesized, where alkyls were methyl, ethyl (AEOL10150), and propyl (38, 167). These porphyrins again bear five positive charges close to the metal site that allowed both thermodynamic and electrostatic facilitation; thus the compounds possessed SOD-like activity similar to that of their *ortho* pyridyl analogues. The synthesis of methoxyethyl derivatives, $MnTMOE\text{-}2\text{-}PyP^{5+}$ (38) and the *N*-triethyleneglycolated pyridylporphrin, $MnTTEG\text{-}2\text{-}PyP^{5+}$ (36) and the corresponding imidazolium derivative, $MnTDTEG\text{-}2\text{-}ImP^{5+}$ (36), followed; all three compounds showed as high or higher k_{cat} than the previous complexes of the pyridyl and imidazolyl series (Table 1). These structures are bulkier, particularly the imidazolium series, in which alkyl or triethyleneglycols are located on both sides of the porphyrin plane. The goal of

introducing triethyleneglycol moieties was to increase the blood-circulation lifetime (36, 313). Yet bulkiness may limit to some extent their access to cells and in turn their efficacy, as observed with protection of SOD-deficient *E. coli* (36, 38, 241).

With our ongoing goals to improve SOD-like activity *in vitro* and the efficacy *in vivo*, we recently synthesized and characterized the *β*-brominated *meta* isomer, $MnBr_8TM\text{-}3\text{-}PyP^{4+}$; with an $E_{1/2}$ of $+468$ mV *versus* NHE and log $k_{cat} > 8.85$, this complex has, thus far, the highest dismuting ability among metalloporphyrins (85), which approximates that of the enzyme itself (21, 26, 100, 136, 218, 269, 325). As observed for the *para* analogue, $MnBr_8TM\text{-}4\text{-}PyP^{4+}$, the *meta* isomer has Mn in its $+2$ oxidation state and, thus, has insufficient metal/ligand stability for *in vivo* studies.

2. Electrostatics. To quantify the electrostatic effects, we initially compared the related porphyrins, the monocationic $MnBr_8T\text{-}2\text{-}PyP^{+}$ and the pentacationic $MnTE\text{-}2\text{-}PyP^{5+}$ (301); of note, the former porphyrin is neutral on the periphery. Whereas the $E_{1/2}$ values for these Mn porphyrins were nearly identical (219 mV for $MnBr_8T\text{-}2\text{-}PyP^{+}$ and 228 mV *vs.* NHE for $MnTE\text{-}2\text{-}PyP^{5+}$), their k_{cat} values differed by almost two orders of magnitude (log $k_{cat} = 5.63$ for $MnBr_8T\text{-}2\text{-}PyP^{+}$; log $k_{cat} = 7.76$ for $MnTE\text{-}2\text{-}PyP^{5+}$) (Fig. 5A). The remarkable contribution of the electrostatics seen in these Mn porphyrins parallels the effect observed in the SOD enzyme catalysis and was confirmed by kinetic salt-effect measurements (301), and further substantiated in other studies.

A second study was designed to investigate the impact of spatial charge distribution on the SOD catalysis, which also included the imidazolium and pyrazolium porphyrins (Fig. 5B) (266). Both compounds have been viewed as having delocalized charges. Yet, as the imidazolium compound has charges closer to the Mn site than does the pyrazolium porphyrin, the former had a k_{cat} value more than two orders of magnitude higher than the latter. Whereas the charges in imidazolium, pyrazolium, and $MnTM\text{-}4\text{-}PyP^{5+}$ compounds are distributed in plane with the porphyrin ring, the charges of $MnTM\text{-}2\text{-}PyP^{5+}$ are either above or below the plane, which results in a more efficient channeling of the negatively charged superoxide toward the axial positions of the Mn porphyrin, as revealed by kinetic salt-effect measurements.

In a third study, we compared negatively and positively charged porphyrins of the same $E_{1/2}$, such as $MnBr_8TSPP^{3-}$ to $MnTE\text{-}2\text{-}PyP^{5+}$. The difference in k_{cat}, as expected, was much bigger than that when $MnBr_8T\text{-}2\text{-}PyP^{+}$ and $MnTE\text{-}2\text{-}PyP^{5+}$ were compared (Fig. 5A; Table 1). The overall negative charge of the anionic porphyrins hampered the approach of the negatively charged superoxide, as additionally supported by kinetic salt-effect measurements (262).

With such strong electrostatic effects, the original structure–activity relationship (30) was revised (262), and three separate relations were established to account for the electrostatics of Mn compounds derived from neutral, positively, or negatively charged porphyrins (Fig. 6) (262). With potentials close to the optimum, the pentacationic Mn porphyrins are more than two orders of magnitude more potent SOD mimics than the Mn complexes derived from anionic or neutral porphyrins (Fig. 6). The design of the potent SOD mimics based on anionic and neutral Mn porphyrins is, thus, severely limited by the lack of

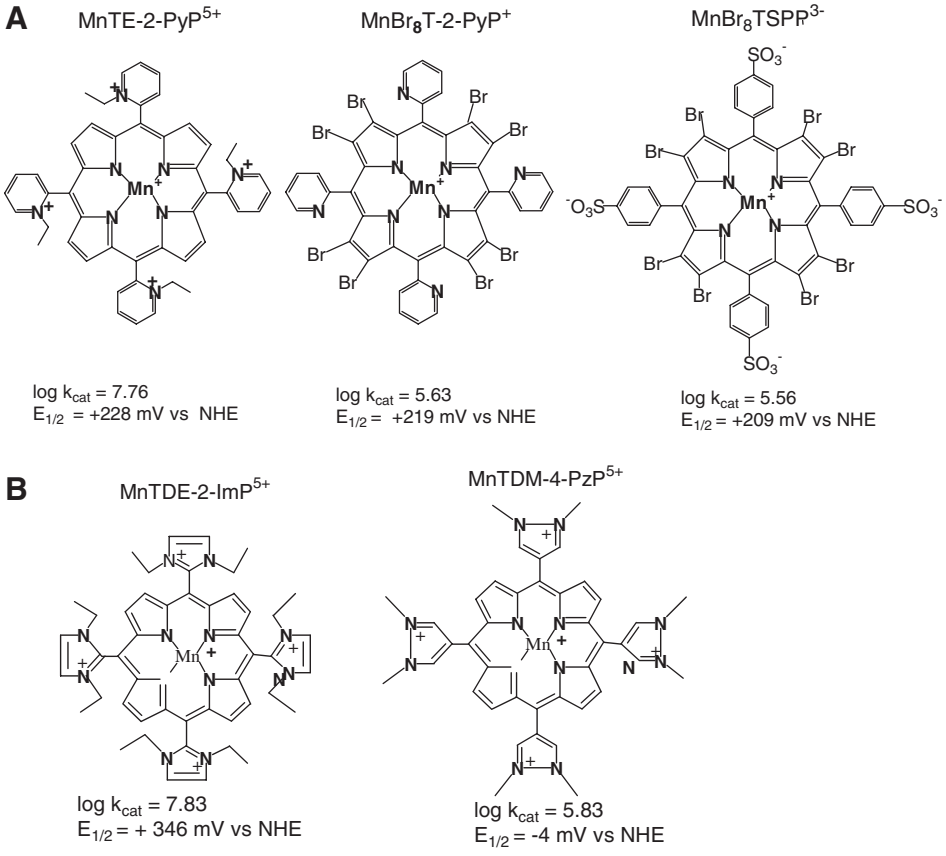

FIG. 5. The effect of charges on k_{cat} ($O_2^{\cdot -}$). Mono- *vs.* pentacationic porphyrins differ in k_{cat} for 2 log units, whereas cationic vs. anionic porphyrins differ in k_{cat} for more than two orders of magnitude (**A**), like imidazolium *vs.* pyrazoliumporphyrins (**B**).

appropriate electrostatic facilitation, even when the thermodynamics is suitably tuned (262).

3. Anionic porphyrins, $MnTBAP^{3-}$ ($MnTCPP^{3-}$), and $MnTSPP^{3-}$. These anionic porphyrins, which lack sufficiently strong electron-withdrawing groups, are stabilized in the Mn + 3 oxidation state, and with $E_{1/2} = -194$ and -160 mV *vs.* NHE cannot be reduced in aqueous systems with superoxide (Fig. 3; Table 1). Further, negative charges at the periphery repel $O_2^{\cdot-}$ (and $ONOO^-$) away from the Mn site. Thus, they possess neither thermodynamic nor electrostatic facilitation for $O_2^{\cdot-}$ dismutation; consequently, they are not SOD mimics (262, 264). As expected, $MnTBAP^{3-}$ lacks efficacy in the $O_2^{\cdot-}$-specific model of aerobic growth of SOD-deficient *E. coli* (31, 262). $MnTBAP^{3-}$ (most likely in some impure form) has been used in numerous studies (73, 76, 194, 206, 229, 251). Most of the reports assigned the effects observed *in vivo* to $MnTBAP^{3-}$ SOD-like activity. Only two "shy" reports claimed no effects with $MnTBAP^{3-}$ (172, 214). We have clearly shown that $MnTBAP^{3-}$ is not an SOD mimic, as it has negligible SOD-like activity (log $k_{cat} = 3.16$) (31, 264). Instead, $MnTBAP^{3-}$ prepared by a "conventional" (unsuitable) route (81) and commercial preparations contain different degrees of SOD-like impurities that were tentatively assigned as Mn oxo/hydroxo/acetato complexes (264) (see Mn^{2+} section). The presence of such impurities can lead to unreliable and nonreproducible data and incorrect mechanistic interpretations.

Pure $MnTBAP^{3-}$ is able to scavenge $ONOO^-$ with a k_{red} of 10^5 $M^{-1}s^{-1}$ and, most notably, the impurities in commercial $MnTBAP^{3-}$ preparations did not affect $ONOO^-$ decomposition significantly (31). Although it is more than two orders of magnitude less efficient than $MnTE\text{-}2\text{-}PyP^{5+}$ in scavenging $ONOO^-$, pure $MnTBAP^{3-}$ can still ameliorate $ONOO^-$-related oxidative-stress conditions if given at high enough doses. Further, in conjunction with $MnTE\text{-}2\text{-}PyP^{5+}$, and if pure, it can be used in mechanistic studies to distinguish whether $O_2^{\cdot-}$ or $ONOO^-$ is responsible for the effects seen *in vivo* (31).

When the electron-withdrawing groups, such as bromines or chlorines, are placed on a $MnTSPP^{3-}$ and $MnTCPP^{3-}$ ($MnTBAP^{3-}$) porphyrin core, the metal center becomes more electron-deficient/more reducible. In turn, the $E_{1/2}$ of such compounds, $MnBr_8TSPP^{3-}$ or $MnBr_8TCPP^{3-}$, becomes positive enough to allow them to catalyze $O_2^{\cdot-}$ dismutation (262). Yet, they still have fairly low efficacy, as they lack favorable electrostatic guidance (Fig. 5A; Fig. 6; Table 1).

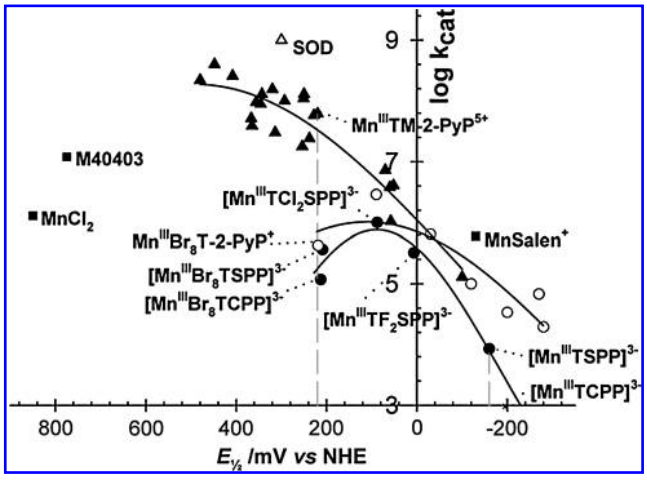

FIG. 6. Structure–activity relations between log k_{cat} ($O_2^{\cdot-}$) and $E_{1/2}$ ($Mn^{III}P/Mn^{II}P$) for porphyrins that have negative charges (*lower curve*), no charges (*middle curve*), and positive charges on the periphery (*upper curve*).

Interestingly, with $Mn^{III}Br_8TSPP^{3-}$, another possibility emerged. In contrast to our expectations based on k_{cat} values, it proved more efficacious than $MnTE\text{-}2\text{-}PyP^{5+}$ in protecting SOD-deficient *E. coli* when growing aerobically (262). This octabrominated Mn porphyrin is not very stable and would eventually release Mn upon reduction. The metal-free ligand was indeed found in *E. coli* cytosol. Thus, the unexpected efficacy was attributed to the Mn-transporting action of $Mn^{III}Br_8TSPP^{3-}$, which would favor the accumulation of Mn^{2+} intracellularly. Of note, $MnTE\text{-}2\text{-}PyP^{5+}$ and related compounds are found intact within cells and tissues, as revealed by UV-VIS spectroscopy and ESI-MS/MS spectrometry (180, 262, 303).

4. Neutral porphyrins. Based on incorrect interpretation of the *J Biol Chem* 1994 publication (105) and the *J Pharmacol Exp Ther* 1995 article (81), numerous studies on $MnTBAP^{3-}$ were conducted. Further $MnTBAP^{3-}$ neutral analogues and porphyrins that have alkylcarboxylates or alkylamides directly on the porphyrin *meso* positions were thus synthesized (125, 321). The critical data on the elemental analyses were provided in only a few instances. Such data, along with other analyses, are critical in describing the purity of the compounds essential for their *in vivo* actions. Neutral porphyrins bear one positive charge on the Mn site, but possess no charges on the periphery to guide $O_2^{\cdot-}$ toward the metal center. Thus, they are of small or no SOD-like activity (182). We clearly showed that even the esterification of $MnTBAP^{3-}$ to yield methyl ester derivatives (alkylcarboxylates) does not increase the electron deficiency of metal site enough to introduce any significant SOD-like activity (264). A variety of neutral Mn porphyrins that contain electron-withdrawing groups, such as CF_3 or benzoyl, were prepared in attempts to increase the electron deficiency of the metal site (125, 182, 321). With neutral porphyrins, the increase in bioavailability was targeted, as well as the synthesis of a smaller molecule that could cross the plasma membrane or the blood–brain barrier more easily. Yet, without electrostatic facilitation and with only low or no thermodynamic facilitation, none of the compounds are functional SOD mimics. Also, their mitochondrial and nuclear accumulation is likely hampered because of the lack of positive charges.

Another group of neutral porphyrins was reported recently by Rosenthal *et al.* (272). Yet, critical analytical data, such as elemental analyses, were again not provided. Further, based on structure–activity relationship (30, 262), no structural features of these compounds would predict them to be good SOD mimics. The SOD-like activity has been assayed by NBT assay to avoid the artifact problems with cyt *c* assay, which the authors incorrectly (272) claimed were previously (105) observed with $MnTBAP^{3-}$. Although the oral availability of those porphyrins was shown, the data on the oral efficacy were not provided.

C. Stability of metalloporphyrins

Because of the macrocyclic effect, all undistorted Mn porphyrins are extremely stable with respect to the metal loss,

even in concentrated acids. MnTnHex-2-PyP^{5+} undergoes no demetallation for 3 months in 36% HCl. Under such conditions, only 50% of MnTM-2-PyP^{5+} loses Mn within a month. As expected, EDTA is not able to demetallate Mn porphyrins under all concentration conditions (37).

D. Aerobic growth of SOD-deficient Escherichia coli

Since the early 1990s, the aerobic growth of the SOD-deficient *E. coli* strain provided by J. Imlay (JI132), was used as $O_2^{\cdot-}$ specific *in vivo* assay, and as a first step to identify prospective SOD mimics *in vivo*. Based on *E. coli* studies, *ortho* isomeric Mn(III) *N*-alkylpyridylporphyrins were forwarded to *in vivo* mammalian models. In all cases thus far studied, the *E. coli* model unambiguously and correctly identified compounds that proved efficacious in mammalian studies (241). In addition, the *E. coli* studies helped us to understand which factors, other than k_{cat}, contribute to the *in vivo* efficacy of MnPs. Thus, with the *E. coli* model, we recently started to comprehend fully the impact of lipophilicity, size, charges, bulkiness, and substituents on the *in vivo* cellular accumulation and efficacy of MnP (179).

E. Bioavailability of Mn porphyrins

Our growing insight into the *in vivo* action of SOD mimics taught us that both antioxidant capacity (as a result of thermodynamics and electrostatics of the metal site) and bioavailability of a compound determine its *in vivo* efficacy. *The lack of either of these properties will lead to the absence of efficacy.* Quantification of the lipophilicity of SOD mimics has been a challenge until recently. For years we used the thin-layer chromatography retention factor, R_f to assess porphyrin lipophilicity. We recorded very small, severalfold differences only between the R_f values of MnTE-2-PyP^{5+} and MnTnHex-2-PyP^{5+}, whereas the latter was up to 120-fold more potent *in vivo*, and the former, in some models, was ineffective (see later under the *in vivo* effects of Mn porphyrins). Recently, we were able to overcome the methodologic difficulties associated with the determination of the partition coefficient of MnPs between *n*-octanol and water, P_{OW} (179). Whereas R_f is linearly related to log P_{OW}, small differences in R_f translate into considerable differences in log P_{OW}. The P_{OW}, as opposed to R_f, is a common and practical indicator of drug lipophilicity that allows comparison of MnPs with other drugs (Table 1). By using P_{OW}, we showed that a ~10-fold gain in lipophilicity is achieved by either (a) moving the alkyl groups from *ortho* to *meta* positions of *meso* pyridyl substituents, or (b) by increasing the length of alkyl chains by one CH_2 group (Table 1). Because of a significant increase in the lipophilicity (~13,500-fold MnTnHex-2-PyP^{5+} *vs.* MnTE-2-PyP^{5+}, and ~450,000-fold MnTnOct-2-PyP^{5+} *vs.* MnTE-2-PyP^{5+}), an up to 3,000-fold increase in *in vivo* efficacy occurs, going from ethyl (MnTE-2-PyP^{5+}) to hexyl (MnTnHex-2-PyP^{5+}) to octyl porphyrin (MnTnOct-2-PyP^{5+}) in different models of oxidative stress (see later under *in vivo* effects).

F. The effect of the length of the N-alkylpyridyl chains on in vivo efficacy of ortho isomers

With aerobic growth of SOD-deficient *E. coli*, higher accumulation of lipophilic MnTnHex-2-PyP^{5+} within the cell paralleled high SOD-like activity of the cell extract, which in turn resulted in a 30-fold higher efficacy when compared with MnTE-2-PyP^{5+} (241). The second study, radioprotection of ataxia telangiectasia cells, showed that compounds that either lack appropriate bioavailability, or possess low or no antioxidant capacity, exert low or no efficacy (255). MnTnHex-2-PyP^{5+}, but not MnTE-2-PyP^{5+}, was effective; both compounds have nearly identical abilities to dismute $O_2^{\cdot-}$ and to reduce $ONOO^-$ in aqueous solutions. Lipophilic Mn salen compounds and Mn cyclic polyamine of fair antioxidant potency but without positive charges to attract $O_2^{\cdot-}$ or to drive their accumulation in mitochondria, or both, were not efficacious. In a rabbit cerebral palsy study (Tan *et al.*, unpublished data), MnTnHex-2-PyP^{5+}, but not MnTE-2-PyP^{5+}, was effective. Preliminary data on the efficacy of MnTnHex-2-PyP^{5+} in a rat stroke (MCAO) model are highly encouraging (305).

G. The effect of the location of pyridinium nitrogens with respect to porphyrin meso position: meta vs. ortho vs. para isomeric Mn(III) N-alkylpyridylporphyrins

The effect of the location of alkyl groups on the pyridyl rings with respect to the porphyrin core *meso* positions is schematically shown in Fig. 7. Although the first evidence of their *in vivo* effects was published in *J Biol Chem* 1998 (29), *meta* isomers have been overlooked for decade. They are 3.6- to 15-fold less-potent SOD mimics, but are 10-fold more lipophilic and accumulate more in *E. coli* than *ortho* analogues (Table 1) (178). Figure 7 depicts the most obvious case; *meta* MnTE-3-PyP^{5+} is an ~10-fold less potent SOD mimic but is ~10-fold more lipophilic than MnTE-2-PyP^{5+}. Because of higher lipophilicity and greater planarity plus conformational flexibility, the *meta* isomer crosses cell wall more easily, which leads to ~10-fold higher cytosolic accumulation (Fig. 7). Higher accumulation in cytosol overcomes its inferior thermodynamics for $O_2^{\cdot-}$ dismutation; in turn, both isomers exert identical ability to compensate for the lack of cytosolic SOD in SOD-deficient *E. coli* (18).

Para isomers appear more lipophilic than their *ortho* analogue (with the exception of methyl porphyrin). The *in vivo* studies with the shorter methyl analogue, MnTM-4-PyP^{5+}, were reported, presumably because of its commercial availability (191, 223, 224). With longer alkyl chains, bulkiness restrain toxic interactions with nucleic acids, whereas lipophilicity may compensate for the lower SOD-like activity. Such analogues may thus be prospective therapeutics.

H. Mitochondrial accumulation of Mn porphyrins

As the awareness of the importance of mitochondria grows, so grows the interest in compounds that may be both mechanistic tools to increase our insight into mitochondrial function and potential therapeutics in mitochondrially based disorders. Michael Murphy (227, 228) advanced the field by showing that redox-able compounds possessing both positive charge and appropriate lipophilicity would enter mitochondria driven by mitochondrial potential. Roberston and Hartley (271) reported a similar design to target mitochondria with a molecule in which cationic *N*-arylpyridyl (instead of triphenylphosphonium cation) is coupled with nitrone and with a lipophilic moiety. We and others using pentacationic Mn porphyrins wondered what is the intracellular site of accumulation of these excessively charged and thus very

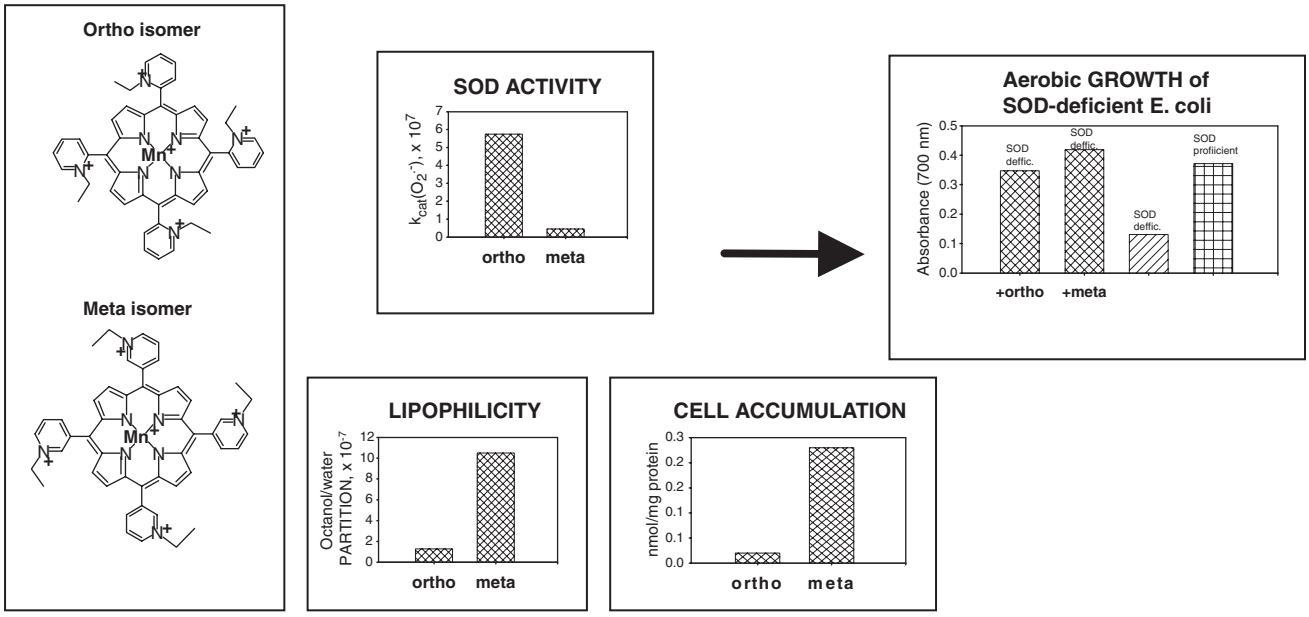

FIG. 7. Higher lipophilicity of *meta* Mn(III) *N*-alkylpyridylporphyrins drives their higher accumulation inside *E. coli* and compensates for lower antioxidant potency when compared with *ortho* analogues. Consequently, *meta* and *ortho* isomers are similarly efficacious in protecting SOD-deficient *E. coli* that lacks cytosolic SOD (178). Here, the most obvious case with *ortho* and *meta* *N*-ethylpyridylporpyrin is illustrated: *meta* isomer is ~10-fold less SOD-active than the *ortho* species, but is ~10-fold more lipophilic and accumulates ~10-fold more in *E. coli*. In turn, both compounds are equally efficient in substituting for cytosolic superoxide dismutases.

hydrophilic compounds. We first aimed to see whether they can enter mitochondria (305). The study was preceded by the Ferrer-Sueta work (108) in which it was shown that, if submitochondrial particles are exposed to $ONOO^-$ fluxes, the components of the mitochondrial electron-transport chain were protected with $>3\,\mu M$ MnTE-2-PyP^{5+}. Our subsequent study, in which C57BL/6 mice were injected with a single IP dose of 10 mg/kg of MnTE-2-PyP^{5+}, showed that heart mitochondria contained $5.1\,\mu M$ MnTE-2-PyP^{5+}; based on the Ferrer-Sueta study, such levels are high enough to protect mitochondria against peroxynitrite-mediated damage (305). Preliminary data from a collaborative study with Edith Gralla (UCLA) (Gralla *et al*, unpublished data) suggest that all *ortho* Mn(IIII) *N*-alkylpyridylporphyrins accumulate in yeast mitochondria at levels which are dependent upon the length of the alkyl chains.

I. Nuclear and cytosolic accumulation of Mn porphyrins

Macrophages and lipopolysaccharide (LPS)-stimulated macrophages were cultured with $34\,\mu M$ MnTE-2-PyP^{5+} for 1.25 h (39). Threefold higher levels of MnTE-2-PyP^{5+} were found in nucleus than in cytosol: 35 and 44 ng/mg of cytosolic protein and 99 and 156 ng/mg of nuclear protein when macrophages and LPS-stimulated macrophages were treated (39). It is obvious that positively charged porphyrin favors environments with the abundance of anionic polymers, such as nucleic acids.

J. Pharmacokinetics

1. Intraperitoneal administration. Driven by the interest in cellular and subcellular accumulation of SOD mimics, we developed methods for analyzing cationic porphyrins in plasma and tissues. Our first method was based on the reduction of the Mn(III) site with ascorbic acid, exchange of Mn(II) with excess Zn, and detection of Zn porphyrin fluorescence by using HPLC/fluorescence methods (303). When given IP to B6C3F1 mice at 10 mg/kg, MnTE-2-PyP^{5+} distributed into all organs studied (liver, kidney, spleen, lung, heart, and brain), and mostly in liver, kidney, and spleen. The plasma half-life is $\sim$1 h, and the organ half-life is $\sim$60–135 h. Whereas the levels in all organs continuously decreased after the initial buildup, accumulation in the brain continues beyond day 7. Recently, a more sensitive LCMS-MS method that directly detects MnPs was developed and successfully applied (180, 303).

2. Oral administration. Despite all odds, the highly charged MnTE-2-PyP^{5+} is $\sim$25% orally available; the PK parameter, AUC (area under curve), was calculated with respect to IP data (180). The t_{max} for IP and *per os* injections was identical. The IP and *per os* study on more-lipophilic MnTnHex-2-PyP^{5+} is in progress; preliminary data indicate its higher oral availability as compared with MnTE-2-PyP^{5+}.

K. Other modes of action

Still only limited knowledge exists about the action of synthetic antioxidants/redox modulators *in vivo*. Even if they possess high k_{cat} ($O_2^{\cdot -}$) *in vivo*, they likely exert more, rather than a single action because of their multiple redox states and varied axial coordination. Therefore, other possible "chemistries," which are likely dependent on the thermodynamics and electrostatics of the metal site discussed previously, are given here in brief.

1. Superoxide reductase–like action. Given the positive reduction potential of most potent MnPs, it is highly likely that *in vivo* they will be readily reduced by cellular reductants, flavoenzymes, NO etc, to Mn(II)P (35, 107, 108, 110), which will then in turn reduce $O_2^{\cdot -}$ to H_2O_2, acting as superoxide reductases rather than SOD, in a similar fashion as that proposed for rubredoxin oxidoreductase (desulfoferrodoxin) (102).

2. Peroxynitrite reducing ability. Peroxynitrite relates to the sum of $ONOO^-$ and ONOOH. Given its pK_a of 6.6 (103), peroxynitrite exists predominantly as $ONOO^-$ at pH 7.8. All synthetic SOD mimics can scavenge peroxynitrite or its degradation products (Table 1). It has been claimed that Mn(II) cyclic polyamine cannot do so (see later under Mn cyclic polyamines), but no experimental evidence or explanation was given to support such claims (230). $MnTBAP^{3-}$ is not an SOD mimic, but is an $ONOO^-$ scavenger and could thus be used for mechanistic studies, in combination with SOD mimic, MnTE-2-PyP^{5+}, to distinguish the role of those species *in vivo. Caution must be exercised, as the impact of different charges on differential localization of these porphyrins and thus on potential differences in their* in vivo *effects must be accounted for.* The $ONOO^-$ reducing ability of MnPs was investigated by us and others (69, 110, 184, 185, 310, 320). Lee *et al.* (185) reported the ability of *para*-MnTM-4-PyP^{5+} and its Fe analogue to reduce $ONOO^-$ with log $k_{red} \sim 6$–7 (25°C). The possibility that reduction of $ONOO^-$ may be coupled to the oxidation of $O_2^{\cdot -}$ was indicated by Lee *et al.* (185). We first undertook a comparative study of isomeric methyl species, MnTM-2(3 or 4)-PyP^{5+} (107). The *ortho* isomer was the most potent scavenger of $ONOO^-$ with a $k_{red} = 3.67 \times 10^7$ $M^{-1}s^{-1}$ (37°C) (107). A study of the series of *ortho* Mn(III) *N*-alkylpyridylporphyrins followed, alkyl being methyl to octyl. The dependences of the reactivity toward $ONOO^-$ and $O_2^{\cdot -}$ on the alkyl chain length paralleled each other (37, 110). The electron deficiency that provides thermodynamic facilitation for the $O_2^{\cdot -}$ dismutation favors the binding of $ONOO^-$ to the Mn site in the first step of $ONOO^-$ reduction. Mn porphyrins can reduce $ONOO^-$ uni- or divalently, giving rise either to the oxidizing radical, $^{\cdot}NO_2$, or to a benign nitrite, NO_2^-, respectively (109). Removal of $ONOO^-$ can happen in a catalytic manner if coupled with cellular reductants, ascorbate, glutathione, tetrahydrobiopterin, flavoenzymes, or uric acid (35, 108, 110, 320). The most likely scenario *in vivo* involves the facile reduction of $Mn^{III}P$ to $Mn^{II}P$ with cellular reductants, followed by binding of $ONOO^-$ (to Mn site) and its two-electron reduction to NO_2^- (109). The rate constant for two-electron reduction of $ONOO^-$ by MnPs was found to be greater than 10^7 $M^{-1}s^{-1}$. The $O=Mn^{IV}P$ species, formed in the process, would then be reduced back by cellular reductants, closing the catalytic cycle, and sparing biologic molecules from a strong oxidizing potential of $O=Mn^{IV}P$. In a study in which low-density lipoproteins (LDLs) were exposed to $ONOO^-$ in the presence of uric acid (cellular reductant) and MnP, a shift from an anti- to a prooxidant action of the Mn(III)porphyrin was observed only after uric acid was mostly consumed, supporting competition reactions between LDL targets and uric acid for $O=Mn^{IV}P$ (320). The data were consistent with the catalytic reduction of $ONOO^-$ (producing $^{\cdot}NO_2$) in a cycle that involves a one-electron oxidation of $Mn^{III}P$ to $O=Mn^{IV}P$ by $ONOO^-$, followed by the reduction of $O=Mn^{IV}P$ to $Mn^{III}P$ by uric acid. These antioxidant effects should predominate under *in vivo* conditions having plasma uric acid concentrations ranging between 150 and 500 μM.

3. Nitrosation. MnTE-2-PyP^{5+} undergoes rapid nitrosation with $^{\cdot}NO$ donor or gaseous $^{\cdot}NO$ in the presence of reductants and slow nitrosation in their absence, whereby Mn^{II}TE-2-$PyP(NO)^{4+}$ is formed. The nitrosated complex slowly loses $^{\cdot}NO$ under aerobic condition (300). With Angeli salt as HNO donor, however, Mn^{III}TE-2-PyP^{5+} reacts fast with $k_{on} = 1.2 \times 10^4$ $M^{-1}s^{-1}$ at pH 7 (205). The same product, Mn^{II}TE-2-$PyP(NO)^{4+}$, was formed, which oxidizes back to Mn^{III}TE-2-PyP^{5+} under aerobic conditions.

4. Reactivity toward HOCl. HOCl (p$K_a \sim 7.5$) is formed *in vivo* by the action of myeloperoxidase with H_2O_2 and Cl^- in neutrophils, monocytes, leukemic cell lines, and under certain conditions in macrophages (145). Carnieri *et al.* (54) found that Mn(III) porphyrins underwent one-electron oxidation with HOCl to Mn(IV)porphyrins in a first step, followed by another one-electron oxidation to Mn(V) porphyrins. The *para* cationic porphyrin MnTM-4-PyP^{5+} is significantly more reactive than anionic porphyrins (145, 196). It is likely that *ortho* isomers will be even more reactive toward HOCl in the manner similar to their reactivity toward $ONOO^-$ when compared with *para* isomers (107).

5. Reactivity toward H_2O_2. Although fully resistant to concentrated acids, Mn porphyrins undergo dose-dependent oxidative degradation in the presence of H_2O_2 (30). Thus, stoichiometric removal of H_2O_2 would occur at the expense of porphyrin degradation. MnTE-2-PyP^{5+} is 16-fold more prone to oxidative degradation than is $MnTBAP^{3-}$, but the Fe analogue $FeTBAP^{3-}$ is 30-fold more prone to oxidative degradation than is MnTE-2-PyP^{5+} (30 and Batinić-Haberle, unpublished data).

Cationic Mn porphyrins are not potent H_2O_2 scavengers (30, 83, 80). Day *et al.* (56, 83) discussed the catalase-like activity of neutral and anionic porphyrins. He reported that the Mn(III) porphyrin with two aldehyde groups and two methylbenzoates on *meso* positions (AEOL11209) has the highest reported catalase activity (34% of the activity of catalase) (56). For comparison, reported by the same authors (158), the cationic imidazolyl derivative, MnTDE-2-ImP^{5+} (AEOL10150) has 0.2% of the catalase activity (56). A pyridyl analogue, MnTE-2-PyP^{5+} (30), with all the antioxidant properties in aqueous solution similar to MnTDE-2-ImP^{5+} (38, 167), may thus have similar low catalase-like activity. Of note, the purification of neutral porphyrin from residual manganese again is important to assure that catalase-like activity can be unambiguously assigned to Mn(III) 5,15-bis(methylcarboxylato)-10,20-bis(trifluoromethyl)porphyrin (AEOL11207) and is not an artifact arising from residual manganese species (56, 192).

6. Prooxidative action of porphyrins. In a fashion similar to that of cyt P450 enzymes, Mn porphyrins, once reduced *in vivo* may bind oxygen and reduce it to superoxide and peroxide. Thus, we observed that in the presence of ascorbate in phosphate buffer at pH 7.8, Mn(III) *N*-alkylpyridylporphyrins undergo oxidative degradation; UV/VIS evidence suggests that degradation involves H_2O_2 formation (36–38). We also showed that both Fe and (less so) Mn

porphyrins can mimic the cyt P450–catalyzed cyclophosphamide hydroxylation under biologically relevant conditions, using O_2 as a final electron acceptor and ascorbate as a sacrificial reductant (304). In another study, the cytotoxic effects of MnTE-2-PyP^{5+}, MnTnHex-2-PyP^{5+}, and MnTnHex-3-PyP^{5+} in four cancer cell lines were studied in the presence and absence of ascorbate (346). Neither ascorbate alone ($\leq$3.3 m*M*), nor any of MnPs ($\leq$30 μM) was cytotoxic to cancer cells. A mechanism whereby H_2O_2 was produced suggested a prooxidative mode of anticancer action of MnPs in the presence of cellular reductants (346). A prooxidative mode of action has been proposed to explain the anticancer effects of the MnSOD enzyme itself by several groups (101,190). A prooxidative action of metalloporphyrins was also reported by others (161, 234, 253). Jaramillo *et al.* (161) reported that treatment with MnTE-2-PyP^{5+} can improve the outcome in hematologic malignancies treated with glucocorticoids, cyclophosphamide, and doxorubicin. In addition to accelerating dexamethasone-induced apoptosis in the mouse thymic lymphoma cells WEHI7.2 and primary follicular lymphoma FL cells, MnTE-2-PyP^{5+} potentiated cyclophosphamide toxicity while inhibiting lymphoma cell growth and attenuating doxorubicin toxicity in H9c2 cardiomyocytes (immortalized clonal cell line derived from BDIX rat embryonic heart tissue). Thus, reportedly, MnTE-2-PyP^{5+}, at least in part acting as an oxidant, could benefit lymphoma patients who receive combined therapy, which includes glucocorticoids, doxorubicin, and cyclophosphamide (161). A suggestion was made by Tse *et al.* (see under Diabetes) that MnTE-2-PyP^{5+} oxidizes cysteine SH groups of the p50 subunit of NF-κB within the nucleus (39, 107), which prevents p50 DNA binding (322). In an LDL study, the O = Mn^{IV} P acted as an oxidant when cellular reductant uric acid was depleted (320). Because of the rich redox chemistry at the Mn site and redox-based cellular pathways, more studies are needed to comprehend fully MnP action(s) *in vivo*.

7. Inhibition of redox-controlled cellular transcriptional activity. Mn(III) *N*-alkylpyridylporphyrins inhibit *in vitro* and *in vivo* activation of several redox-controlled transcription factors (TFs), HIF-1α, NF-κB, AP-1, and SP-1 (158, 221, 222, 288, 322, 350). Although not studied yet, such action may occur with other redox-controlled TFs. The identity of particular ROS/RNS involved is not fully resolved. In a Moeller *et al.* study (222), 10 μM H_2O_2 (or species originated from H_2O_2-derived oxidative stress, including $O_2^{\cdot-}$) and $^{\cdot}NO$ (as $^{\cdot}NO$ donor, 10 μM NOC-18, DETA NONO-ate) activated HIF-1α in 4T1 mouse breast tumor cells, and MnTE-2-PyP^{5+} brought that activation to control levels, suggesting H_2O_2, $^{\cdot}NO$, and $ONOO^-$ as possible direct or indirect actors. The effect of superoxide and $^{\cdot}OH$ (produced when cells are stressed with H_2O_2) on signaling pathways may not be excluded. In biologic systems, because of the high levels of reductants and easy reducibility of MnP, MnTE-2-PyP^{5+} would be reduced to MnTE-2-PyP^{4+}, which may then act as an $O_2^{\cdot-}$ reductase, producing 1 mol of H_2O_2 per 1 mol of $O_2^{\cdot-}$. In such a scenario, H_2O_2 levels would remain unchanged. In the Moeller *et al.* study (221, 222), equimolar concentrations of H_2O_2 and MnP were used, suggesting a possibility that MnTE-2-PyP^{5+} removed peroxide through a stoichiometric reaction at the expense of its own degradation. With NF-κB (301), $ONOO^-$ may be a likely actor oxidizing MnP to O = Mn^{IV}P, which in turn would oxidize cysteine SH groups of the p50 subunit. Still, in an NF-κB experiment performed with LPS-stimulated macrophages in which significant production of $O_2^{\cdot-}$ by NADPH oxidases occurs, the SOD-like antioxidant action of MnP should not be excluded. Of note, Mn(III) *N*-alkylpyridylporphyrins are still very efficacious scavengers of $O_2^{\cdot-}$, $ONOO^-$, and $ONOO^-$-derived radicals. The ability of MnP to prevent oxidative deactivation of $NADP^+$-dependent isocitrate dehydrogenase [the enzyme found mutated in a majority of several types of malignant gliomas (345)], whereby normalizing cellular redox status may contribute to the decreased oxidative stress and suppressed activation of redox active transcription factors. This enzyme is essential for providing electrons for $NADP^+$ and assuring regeneration of cellular antioxidant defense (28). Much is still needed to understand the roles of both ROS/RNS and MnPs in redox-controlled pathways.

L. The effects of Mn porphyrins in suppressing oxidative-stress injuries in vitro *and* in vivo

1. General considerations. More than 80 articles have been published on *ortho* isomer, MnTE-2-PyP^{5+}, and five articles have been published on the lipophilic analogues, MnTnHex-2-PyP^{5+} and MnTnOct-2-PyP^{5+} (34, 180, 241, 255, 337) (Table 2). Although the beneficial effects of the *para* isomer, MnTM-4-PyP^{5+}, were reported also (191, 224, 283), its lower antioxidant capacity and the propensity to associate with nucleic acids, which in turn suppresses its SOD-like activity and imposes toxicity, limits its utility (29).

More than 200 articles published on the *in vivo* effects of MnTBAP^{3-} used commercial sources that all have significant levels of impurities with SOD-like activity. Although the effects observed may be real, mechanistic explanations attributing them to an SOD-like activity of MnTBAP^{3-} are likely not real (73, 76, 194, 206, 229, 251). As already mentioned, either the effects are due to the SOD-like impurities or the MnTBAP^{3-} acts through $ONOO^-$-mediated pathways.

The purity and identity of the cationic MnTE-2-PyP^{5+}(and any compound that will be eventually used in an *in vivo* study) is an important issue also (263, 264). For a while, CalBiochem was selling MnTE-2-PyP^{5+}. Although originally of sufficient purity, the later batches were a mix of equal amounts of nonethylated, mono-, di-, tri-, and tetraethylated compounds. Such preparations thus possessed much lower SOD-like potency and altered bioavailability. Two studies showed lesser or no efficacy of commercial MnTE-2-PyP^{5+} (225, 255). In another report, the effects observed were explained by dubious mechanistic considerations (344). We published two reports warning the scientific community to consider the purity of SOD mimics seriously, if proper assignments of the effects are to be made (263, 265).

2. Central nervous system injuries

a. Stroke. The very first study on central nervous system injuries was done with MnTE-2-PyP^{5+} at Duke University in a rat stroke model (199). Rats were subjected to a 90-min focal ischemia (*via* middle cerebral artery occlusion, MCAO). They were given a single dose of MnTE-2-PyP^{5+} (150 or 300 ng or vehicle) intracerebroventricularly (ICV) 60 min before ischemia, or 5 min, 90 min, 6 h, or 12 h after reperfusion. Neurologic

scores and infarct size were measured at 7 days, and oxidative stress markers at 4 h after postischemic treatment. MnTE-2-PyP^{5+} reduced infarct size and improved neurologic function at all time points, except if given at 12 h after reperfusion. MnTE-2-PyP^{5+}, given at 60 min before ischemia, reduced total infarct size by 70%. MnTE-2-PyP^{5+}, given at 5 or 90 min after reperfusion, reduced infarct size by 70–77%. MnTE-2-PyP^{5+} treatment at 6 h after reperfusion reduced total infarct volume by 54%. Protection was observed in both cortex and caudoputamen. MnTE-2-PyP^{5+} had no effect on body temperature. MnTDE-2-ImP^{5+} also was efficacious in a stroke model (286). On a longer run, the effects faded off, as a single injection did not assure the levels of Mn porphyrin needed to suppress cellular transcriptional activity and thus also a secondary oxidative stress due to the sustained inflammation. When MnTDE-2-ImP^{5+} (ICV, 900 ng bolus dose + 56 ng/h for a week) was given to rats continuously for a week (starting at 90 min after 90-min MCAO), the effects were observed even at 8 weeks after stroke (288). The suppression of oxidative stress and of NF-κB activation was clearly seen and indicated the role of Mn porphyrin in modulating cellular signaling pathways. Encouraging preliminary data with the more lipophilic MnTnHex-2-PyP^{5+} have been obtained (305). That compound distributes 12-fold more in brain than MnTE-2-PyP^{5+}. At 30 min after intravenous (IV) injection, plasma-to-brain ratios were 8:1 for MnTnHex-2-PyP^{5+} and 100:1 for MnTE-2-PyP^{5+} (95). Thus, MnTnHex-2-PyP^{5+} was effective in an MCAO model at significantly lower doses of 0.45 mg/kg/day, delivered for a week. Based on the very first enthusiastic data in treating stroke with delayed IV injections of MnTnHex-2-PyP^{5+} (305), a comprehensive study is in progress.

b. Subarachnoid hemorrhage. A beneficial effect of commercial preparation of MnTBAP^{3-} in a rat double-hemorrhage model of experimental subarachnoid hemorrhage (SA) was reported (6). Pure MnTBAP^{3-} must be used to distinguish between the beneficial effects of residual Mn^{2+} (see under Mn^{2+}) and/or the $ONOO^-$ reducing ability of MnTBAP^{3-} in its own right (31, 264). Preliminary data indicate the potency of MnTnHex-2-PyP^{5+} in SA model (Sheng *et al*. unpublished).

c. Spinal cord injury. Because of the deteriorating effects of ROS/RNS continuously formed after spinal cord injury, MnTDE-2-ImP^{5+} was protective in a mouse spinal cord–injury model given intrathecally into the spinal cord at a single 2.5- and 5-μg dose at 60 min after the spinal cord compression (SCC) (287). The total damage score and the rotarod performance were improved at days 3, 7, 14, and 21 after SCC. The effects also were observed but did not reach statistical significance when MnTE-2-PyP^{5+} was given intravenously. As shown in a stroke model, continuous administration of the lipophilic MnP (given intrathecally or IV) could be more beneficial.

3. Amyotrophic lateral sclerosis. If given to G93A transgenic mice from the onset of ALS until death, the anionic porphyrin FeTBAP^{3-} and its methylester prolonged the survival after the onset, the ester being twice as efficacious. The effects may be ascribed to the $ONOO^-$- rather than $O_2^{\cdot -}$-scavenging ability discussed earlier (340). Also, the cationic MnTDE-2-ImP^{5+} and MnTnHex-2-PyP^{5+} were both tested and proved more efficacious than anionic compounds (in agreement with higher antioxidant potency and possibly higher accumulation within mitochondria due to cationic charges) (66–68). Because of around a four-orders of magnitude increase in lipophilicity (which would favor central nervous system accumulation) (38, 179), the hexyl porphyrin was efficacious at 5–10 times lower doses than MnTDE-2-ImP^{5+} (0.1–0.3 mg/kg/day) (67, 68). The Phase I clinical trials on ALS patients with MnTDE-2-ImP^{5+} (AEOL10150) showed no toxicity at doses well above the therapeutic dose (42, 244).

4. Alzheimer's disease. A homozygous mouse that incorporates the humanized AD mutation (APP$^{NLh/NLh\times PS\text{-}1\ P264L/P264l\ (APP/PS1)}$ and therefore simulates the natural progression of β-amyloid pathology observed in AD patients, was used to study the oxidative stress and MnSOD production during neural development. Overexpression of MnSOD or addition of MnTE-2-PyP^{5+} at 0.1 to 1 ng/ml protected developing neurons *in vitro* against β-amyloid–induced neural death and improved mitochondrial respiration (294).

5. Parkinson's disease. A review was recently published in this Journal addressing catalytic antioxidants in neurodegenerative disorders (133). Patel *et al.* successfully used Mn porphyrins for treating Parkinson-related disorders in animal models. Recently, the protection against 1-methyl-4-phenyl-1,2,3,6-tetrahydropyridine neurotoxicity (decreased dopamine depletion and dopaminergic neuronal death, decreased oxidative stress) *in vivo* by an orally available porphyrin analogue (AEOL11207, Mn(III) 5,15-bis(methylcarboxylato)-10,20-bis(trifluoromethyl)porphyrin) was reported (192). The compound has only two electron-withdrawing CF_3 groups that could slightly increase electron deficiency of the metal center, but lacks electrostatic facilitation (192, 321). Thus, it is not SOD active (56). Catalase-based activity of that porphyrin, referred to by Castello *et al.* (56), may not be sufficient to account for the effects observed in a mouse model of Parkinson's disease. The purity of the compound (*i.e*., the presence of the residual Mn) may account for the effects seen; the critical data on the elemental analysis of porphyrin and its Mn complex are missing (192, 321).

6. Cerebral palsy. In a rabbit cerebral palsy model, preliminary data show that only MnTnHex-2-PyP^{5+}, but not MnTE-2-PyP^{5+}, was effective when given twice IV to a pregnant rabbit dam, 30 min before and 30 min after 40-min uterus ischemia at only 0.1 mg/kg (1.0 mg total dose per rabbit dam) (348). Of eight pups in an MnTnHex-2-PyP^{5+} group, seven were born normal, and one, with mild symptoms, whereas in a control group, three were born normal, one had severe symptoms, and five were born dead. The efficacy has been ascribed to the improved ability of MnTnHex-2-PyP^{5+} to cross several lipid barriers before entering the fetal brain.

Although both MnTE-2-PyP^{5+} and MnTnHex-2-PyP^{5+} are promising for clinical development, the latter is advantageous for the central nervous system injuries because of its higher ability to cross the blood–brain barrier.

7. Radiation injury. The very first effects of MnTE-2-PyP^{5+} (6 mg/kg/day, IP) in a rat model of lung radioprotection were published in 2002 (328). The remarkable

Table 2. Selected *In vitro* and *In vivo* Studies of the Most Commonly Used SOD Mimics

Mimic	*Physiopathology*	*Model*	*Common dose*	*Ref.*
MnTE-2-PyP^{5+}	Superoxide toxicity	SOD-deficient *E. coli*	10–30 μM, s (10–20 h)	30, 31, 241
(AEOL 10113)	Stroke	Rat (MCAO model)	150–300 ng, s	199
	Alzheimer's disease	Primary mouse neuron (humanized AD mutation)	0.1–1 ng/ml, s (3 h)	294
	Radiation injuries	Rat	1–6 mg/kg/day, m	123, 124
	Cancer (MnP alone)	Mouse	15 mg/kg/day, m	259
	Cancer (MnP + radiation therapy)	Mouse	6 mg/kg/day, m	222
	Cancer (MnP + hyperthermia)	Mouse	10 mg/kg/day, m	159
	Pain therapy: prevention of chronic morphine tolerance	Mouse	3 mg/kg/day, m	34, 95
	Diabetes	Human islet cells;	34 μM s (>0.5 h);	48, 49
		allotransplants;	34 μM, s (up to 7 days)	48, 49
		rat	10 mg/kg, m;	254
			1 mg/kg/day, m	44
	Sickle-cell disease	Mouse aortic segment	50 μM, s (1 h)	20
	Lung injuries	Baboon	0.5 mg/kg/day, m	59
	Osteoarthritis	Porcine cartilage explants	25 μM, s (72 h)	57
MnTnHex-2-PyP^{5+}	Superoxide toxicity	SOD-deficient *E. coli*	0.3–1 μM, s (10–20 h)	241
	Stroke	Rat (MCAO model)	0.45 mg/kg/day, m	306
	Amyotrophic lateral sclerosis	G93A mouse	0.1–0.3 mg/kg/day, m	68, 67
	Radiation injuries	Rat	0.05–1 mg/kg/day, m	32, 123
	Pain therapy: prevention of chronic morphine tolerance	Mouse	0.1 mg/kg/day, m	34, 95
	Renal ischemia/reperfusion injuries	Mouse	50 μg/kg, s	274
	Ataxia telangiectasia	A-T human lymphoblastoid cells	1 μM, s (18 h)	255
MnTDE-2-ImP^{5+}	Superoxide toxicity	SOD-deficient *E. coli*	>30 μM, s (10–20 h)	241
(AEOL 10150)	Stroke	Rat (MCAO model)	900 ng bolus + 56 ng/h for a week, m	286, 288
	Spinal cord injury	Mouse	2.5–5 μM	287
	Radiation injuries	Rat	10–30 mg/kg/day, m	257
	Diabetes	Human islet cells; allotransplants	34 μM, s (7 d) 10 mg/kg, m	322 and refs therein

EUK-8	Stroke	Rat	1.9 mg/k, s	24
	Pressure-overload–induced heart failure	Harlequin mouse	25 mg/kg/day, m	324
	Multiple organ failure (endotoxic shock)	Rat	0.3–1 mg/kg/h, m	213
	ALS	G93A mouse	33 mg/kg/day, m	164
	Diabetes	Mouse	5–100 mg/kg/day, m	243
	Lung inflammation	Swine	1–10 mg/kg/h, m	141
	Ischemia/reperfusion	Rat	2×1 mg/kg, m	331
EUK-134	Stroke	Rat	0.25 mg/kg, s	24
	ALS	G93A mouse	33 mg/kg/day, m	164
	Superoxide-induced heart-reperfusion injury	Mouse	10 mg/kg, s	343
EUK-189	Prion disease	Mouse	30 mg/kg/day, m	51
	Whole-body radioprotection	Mouse	70 mg/kg, s	307
	Cognitive deficit	Mouse	15 μg/kg/day m	62
M40403	Radiation-induced mucositis	Hamster	6–60 mg/kg/day, m	226
	Septic shock	Rat	0.25 mg/kg, s	198
	Inflammatory pain	Rat	10 mg/kg, m	329
	Allergic asthma-like reaction	Guinea pig	1 mg/kg, s	207
	Colitis	Rat	5 mg/kg/day, m	74
	Chronic hypoxia-induced pulmonary hypertension	Piglet artery	3 μg/ml, s (0.3 h)	86
	Superoxide-induced heart-reperfusion injury	Mouse	4 mg/kg, s	343
Tempol	Hypertension	Rat	275 mg/kg, s	297 and refs therein
	Whole-body radiation injury	Mouse	275 mg/kg, s	296 and refs therein
	Radiation-related hair loss	Human	100 ml/day (of 70 mg/ml of 70% of ethanol, (topically), m	296 and refs therein
	Stroke	Mouse (MCAO model)	10 mg/kg, s	297 and refs therein

s, a single dose; m, multiple doses used. The time in parenthesis indicates the exposure of cells to a single dose.

radioprotective efficacy of methyl analogue, MnTM-2-PyP^{5+}, was subsequently indicated by the Park group (186, 187). When mice were treated 14 days before whole-body radiation with MnTM-2-PyP^{5+} at 5 mg/kg, ~80% survival was observed. The imidazolyl derivative, MnTDE-2-ImP^{5+}, also was radioprotective in two studies with single and fractionated radiation (257, 258). At 26 weeks after single-dose irradiation, and 16 weeks after the administration of Mn porphyrin ceased, rat pulmonary radioprotection was detected with respect to oxidative stress, lung histology, and collagen deposition. MnTDE-2-ImP^{5+} was administered for 10 weeks (10 and 30 mg/kg/day, subcutaneous osmotic pumps) starting at 24 h after 28-Gy right hemithorax radiation (257). Similar effects were observed with fractionated radiation, in which the injection of MnP started 15 min before radiation (258). Recently, we performed extended rat-lung radioprotective studies (28 Gy to right lung hemithorax) by using hydrophilic MnTE-2-PyP^{5+} (6 mg/kg/day for 14 days, via osmotic pumps or subcutaneously) in comparison to lipophilic MnTnHex-2-PyP^{5+} (0.05 mg/kg/day for 14 days, *via* osmotic pumps or subcutaneously) (123). Both drugs are similarly potent SOD mimics with respect to k_{cat}, yet MnTnHex-2-PyP^{5+} was effective *in vivo* at a 120-fold lower dose (123, 32). Importantly, protection was observed even when the administration started as late as 8 weeks (and lasted 2 weeks) after the lung irradiation (124). The decrease in the breathing-rate frequencies and tissue damage, and suppression of oxidative stress and signaling pathways, involving activated macrophages, HIF-1α, VEGF, and TGF-β were detected. With a wide therapeutic window, Mn porphyrins may be efficacious for treating a large population of injured individuals in the case of a nuclear event. Protection of eyes exposed to proton radiation has also been reported (203). One hour before radiation, 2.5 μg of MnTE-2-PyP^{5+} was administered into the vitreous humor of a rat eye. With combined radiation and MnP treatment, no morphologic changes were observed; both photoreceptors and retinal capillaries were protected from radiation damage, and apoptosis was significantly reduced. For radioprotection of ataxia telangiectasia and zebra fish embryos by MnP, see under the Comparative Studies section.

8. Cancer

a. Breast cancer. Because (a) MnSOD (the essential endogenous antioxidant) is reduced in many cancers; (b) increased expression of MnSOD inhibits cancer growth (152), and (c) SOD mimic, MnTE-2-PyP^{5+} enters mitochondria (306), it is only logical that we tested the possible anticancer activity of MnTE-2-PyP^{5+}. Three studies from our group were done within the last 8 years (with doses of MnTE-2-PyP^{5+} ranging from 6 to 15 mg/kg) with the goal to prove if and why a catalytic SOD mimic/peroxynitrite scavenger would exert anticancer effects [*i.e.*, to evaluate whether the attenuation of the oxidative stress by MnTE-2-PyP^{5+} could suppress tumor growth in a 4T1 mouse breast tumor model (222, 221, 259)]. In a most recent study (259), the effects were already observed with 2 mg/kg/day (subcutaneously), but reached significance at 15 mg/kg/day (SC, for the duration of the study). Oxidative stress was largely attenuated: levels of DNA damage, protein 3-nitrotyrosine, macrophage infiltration, and NADPH oxidase were decreased. Further, hypoxia was significantly decreased, as were the levels of HIF-1α and VEGF. Consequently, suppression of angiogenesis was observed; both the microvessel density and the endothelial cell proliferation were markedly decreased (259). Our studies indicate that MnTE-2-PyP^{5+} has anticancer activity in its own right, which occurs at the level of the tumor vasculature rather than with tumor cells *per se*. Another *in vitro* study provided additional evidence that high levels of different Mn(III) *N*-alkylpyridylporphyrins are not cytotoxic to CaCo-2, HeLa, 4T1, and HCT116 tumor cells (346). Thus, the anticancer activity by the HIF/VEGF pathways probably arises from the impact of the drug on cellular redox-based transcriptional activity, presumably through ROS/RNS scavenging. The possible prooxidative action of MnPs on transcription factors at nuclear level must be accounted for (39).

Finally, the Tome group (161) suggested that the anticancer action of MnTE-2-PyP^{5+} is at least in part prooxidative. Along with our *in vitro* data (346) on cytoxic effects of MnPs through H_2O_2 production when combined with ascorbate, several other groups reported that overexpression of MnSOD kills tumors through H_2O_2 production (101, 130, 152, 190). We hope that future studies will provide deeper insight into anti- *vs.* prooxidative actions of compounds (endogenous or exogenous) that are presently primarily considered antioxidants. See also under Prooxidative action of Mn porphyrins, Section K.6.

b. Skin cancer. In a TPA (12-*O*-tetradecanoylphorbol-13-acetate) skin cancerigenesis model, MnTE-2-PyP^{5+} was applied to skin of MnSOD heterozygous knockout mouse (*MnSOD*$^{+/-}$) at 5 ng daily, 4 days per week, for 14 weeks (350). Tumor was induced with 7,12-dimethylbenz (*a*)-anthracene. Timed administration of the drug, 12 h after cell apoptosis and before proliferation, afforded effects of greater magnitude than when MnSOD was overexpressed. With MnSOD overexpression, such timed manipulation was not possible, and thus both apoptosis and cell proliferation were suppressed. Scavenging ROS/RNS by MnTE-2-PyP^{5+} suppressed oxidative stress, AP-1 pathways, cell proliferation, and consequently, the incidence of the skin cancer. Only five papillomas *versus* 31 in control group were left.

c. Prostate cancer. In an RM-9 mouse prostate tumor radiation study, MnTE-2-PyP^{5+} did not significantly affect tumor growth in its own right (201), but enhanced radiation therapy. The group receiving only MnTE-2-PyP^{5+} had relatively high levels of T lymphocytes (helper, Th, and cytotoxic, Tc) and natural killer (NK) cells in the spleen, high B-cell counts in both blood and spleen, and high capacity to produce IL-2, which indicates that the drug has a potential to enhance the antitumor immune response.

Enhancement of the anticancer action may be achieved by optimizing the dosing regimen, using more bioavailable Mn porphyrins and combining MnP treatment with irradiation, hyperthermia, and chemotherapy.

d. MnTE-2-PyP^{5+} + chemotherapy. The enhancement of glucocorticoid-based and cyclophosphamide therapy with MnTE-2-PyP^{5+} along with inhibition of lymphoma cell growth and attenuation of doxorubicin toxicity was reported by Jaramillo *et al.* (see under Prooxidative action of Mn porphyrins) (161).

e. MnTE-2-PyP^{5+} + radiotherapy. A strong radiosensitizing effect was already observed in a breast cancer 4T1 window chamber mouse study (221). When MnTE-2-PyP^{5+} was administered IP at 6 mg/kg daily for 3 days immediately after three fractions of radiation (5 Gy each, 12 h apart), 78% decrease in vascular density and significant suppression of tumor growth was observed. Under same conditions, 100 mg/kg/day of amifostine had no effect on tumor vasculature (221). Radiation study with 4T1 mouse model suggested that cancer cells (but not normal surrounding cells) were not protected during tumor radiation, at least not at levels high enough to interfere with anticancer action (221). No radioprotection of RM-9 prostate tumor (C57Bl/6 mice) was seen with MnTE-2-PyP^{5+}, but radiation effectiveness was modestly increased (142); possible mechanisms include reduction of radiation-induced HIF-1α and altered cytokine profile (201), like the data we obtained with the 4T1 mouse study (259).

f. MnTE-2-PyP^{5+} + hyperthermia. The near-full tumor growth suppression was observed when MnTE-2-PyP^{5+} was used in combination with heat (159). Treatment of mice started at 10 days after tumor implantation (day 1). Heat was delivered at 41.5°C at days 1, 5, and 8. MnTE-2-PyP^{5+} was delivered at 5 mg/kg twice per day to C57/BL6 mice carrying the B16F10 melanoma cell line, starting on day 1 until mice were killed at day 9.

In summary, Mn porphyrins may be more advantageous in cancer therapy than other anticancer drugs, because of their ability to (a) exert anticancer effect; (b) radioprotect normal tissue; and (c) prevent chronic morphine tolerance, allowing efficacious pain therapy (see next).

9. Pain therapy: prevention of chronic morphine tolerance. Salvemini *et al*. (229) showed that chronic morphine tolerance is associated with oxidation of critical proteins involved in neurotransmission, such as glutamine synthase, glutamate transferase as well as oxidative inactivation of MnSOD (229). Peroxynitrite and/or $O_2^{\cdot-}$ and $^{\cdot}NO$ are likely the cause of such oxidative damage (229). Anionic MnTBAP^{3-}, and cationic Fe porphyrin, FeTM-4-PyP^{5+}, and Mn porphyrins, MnTE-2-PyP^{5+} and MnTnHex-2-PyP^{5+}, when given over the long term along with morphine, were able to prevent chronic morphine tolerance. Mn porphyrins were the most effective, particularly the lipophilic MnTnHex-2-PyP^{5+}, because of its ability to penetrate the blood–brain barrier, as already shown in a stroke model (34). The effect was seen at both spinal (34) and supraspinal levels (95).

10. Diabetes. Diabetes was studied by Piganelli *et al.* (48, 49, 254, 322), by using MnTE-2-PyP^{5+} and MnTDE-2-ImP^{5+}, and by Benov *et al.* (44) with MnTM-2-PyP^{5+}. Both MnTE-2-PyP^{5+} and MnTDE-2-ImP^{5+} preserved human islet cell functional mass intended for allotransplants at 34 μ*M*. MnTE-2-PyP^{5+} prevented adoptive transfer of autoimmune diabetes by a diabetogenic T-cell clone when given at 10 mg/kg every second day for 5 days, starting 1 day before the adoptive transfer (254). The effects observed are ascribed to the ability of Mn porphyrin to prevent NF-κB activation; more specifically, the DNA binding of the p50 subunit within nucleus. The authors argued that the effect is a consequence of MnP-driven oxidation of cysteine SH groups of p50. Alternatively, Mn porphyrin could "prevent" AEP1/Ref-1 or thioredoxin (enzymes that have been reported to control the redox state of cysteine 62) or both to secure the reduction of cysteine 62 and to facilitate p50 DNA binding (132, 322). Although no direct proof for such prooxidative action of MnP *in vivo* has yet been provided, the oxidation of glutathione by MnTE-2-PyP^{5+} in aqueous solution was detected (39, 107) (see also under Prooxidative action of porphyrins). The impact of electrostatics and thermodynamics on p50 DNA binding in the nucleus was recently detailed by Batinic-Haberle *et al.* (39).

In another study, MnTM-2-PyP^{5+} suppressed oxidative stress and extended the life span of the streptozotocin-diabetic rat delivered SC at 1 mg/kg/day for 4 days per week for 4 weeks, followed by 1 drug-free week (in total, 12 months of treatment) (44).

11. Sickle-cell disease. In patients with sickle-cell disease, the excessive $O_2^{\cdot-}$ production results from increased xanthine oxidase release into the circulation, as a consequence of local intrahepatic hypoxia/reoxygenation. Aslan *et al.* (20) showed that MnTE-2-PyP^{5+} was able to scavenge excessive $O_2^{\cdot-}$, preventing the $O_2^{\cdot-}$-mediated decrease in $^{\cdot}NO$ bioavailability, thus restoring acetylcholine-dependent relaxation.

12. Cardiac injury. MnTE-2-PyP^{5+} prevented the cytokine-induced decline in cardiac work in both wild-type and iNOS$^{-/-}$ hearts. The decline in iNOS$^{-/-}$ hearts was lower than that with wild-type hearts, indicating the involvement of both $^{\cdot}NO$ and $O_2^{\cdot-}$ in heart damage (71).

13. Other ischemia–reperfusion injuries (renal, hepatic). Saba *et al* (274) observed significant renal protection with a single dose of only 50 μg/kg of MnTnHex-2-PyP^{5+} given IV at 24 h before ischemia; MnP protected against ATP depletion, MnSOD inactivation, nitrotyrosine formation, and renal dysfunction. MnP also was able to restore levels of complex V (ATP synthase), which seemed to coincide with increased ATP levels (274). Mn porphyrins have also been reported to ameliorate hepatic ischemia–reperfusion injuries (223, 341).

14. Lung injuries. Inhibition of airway inflammation and an effect on the alveolar structural remodeling in bronchopulmonary dysplasia by MnTE-2-PyP^{5+} was reported (58, 59). The use of SOD mimics in lung fibrosis was reviewed by Day (82).

15. Osteoarthritis. MnTE-2-PyP^{5+} decreased oxidative damage in a porcine osteoarthritis model, as seen by the suppression of IL-1 expression and nitrotyrosine formation (57). At physiologically relevant low 1% O_2, Mn porphyrin also significantly inhibited IL-1α–induced proteoglycan degradation; a similar trend was observed at ambient oxygen tension.

16. Toxicity. We reported the toxicity dose, $TD_{50} = 91.1$ mg/kg for MnTE-2-PyP^{5+}, and $TD_{50} = 12.5$ mg/kg for MnTnHex-2-PyP^{5+} when MnPs were given subcutaneously (255). Toxicity was observed as hypotonia with shaking at higher doses. MnTnHex-2-PyP^{5+} was more toxic if given by an IP route. Blood pressure drop was observed in rats, particularly if MnPs were given IV; the longer the alkyl chain

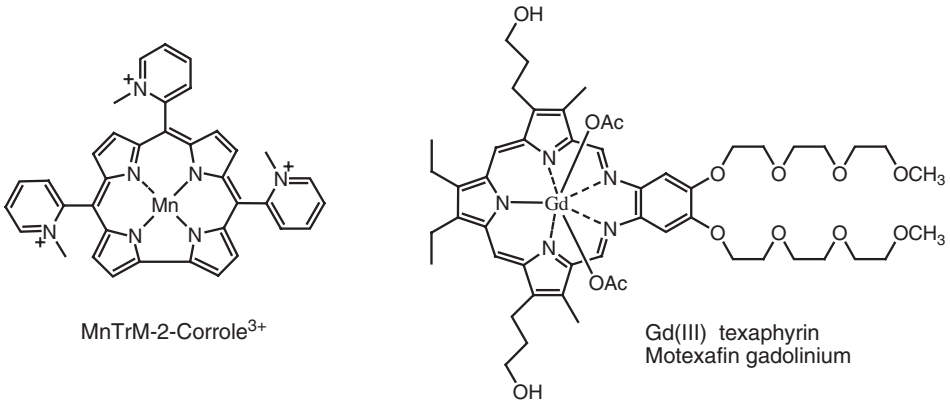

FIG. 8. Mn(III) 5,10,15 *tris*(*N*-methylpyridinium-2-yl)corrole and Gd(III) texaphyrin.

the lesser the effect due to the sterically hindered positive charges.

M. Fe porphyrins

We and several other groups worked extensively on *in vitro* and *in vivo* studies of Fe porphyrins as SOD mimics and $ONOO^{\cdot-}$ scavengers (17, 30, 45, 76, 91, 126, 169, 170, 184, 185, 197, 211, 229, 231, 232, 238, 239, 309, 310, 313). The k_{cat} for $O_2^{\cdot-}$ dismutation, as well as for $ONOO^-$ reduction, is very similar for Fe and Mn analogues (184, 185, 310) (Table 1). Beneficial effects *in vivo* and their impact on transcriptional pathways were reported (17, 91, 169, 170, 309), yet toxic effects also were published (234, 239). When in a reduced state, both Mn and Fe porphyrins could release metals; with H_2O_2 present, Fe, but not Mn, would produce highly damaging $^{\cdot}OH$ radicals (234). Also, like cyt P450 enzymes, metalloporphyrins in their own right, when metal site is reduced, can bind oxygen and reduce it to superoxide and hydrogen peroxide, leading eventually to the oxidation of other biomolecules. Fe porphyrins are more successful than Mn analogues in doing so, as we reported with hydroxylation of cyclophosphamide (304). Further, a suggestion was made by Ohse *et al.* (239) that, like "free" iron, the Fe(II) site of FeTM-4-PyP^{5+} reacts with H_2O_2 (formed through $O_2^{\cdot-}$ dismutation), giving rise to $^{\cdot}OH$ radicals. Finally, richer coordination chemistry of Fe than of Mn porphyrins (50, 53) may make difficult the mechanistic studies on FePs.

1. Ortho isomers of Fe(III) substituted pyridylporphyrins. Groves *et al.* (45, 126, 197, 211, 231, 232, 238, 313) synthesized and used in different animal models Fe analogues of *ortho* quaternized *N*-pyridylporphyrins as $ONOO^-$ scavengers. Two of those have frequently been studied: the triethyleneglycolated FP-15 and the WW-85 that bears pyridyl benzoate substituents ($-CH_2-C_6H_4COO^-$). Although data are lacking on $O_2^{\cdot-}$ dismutation, given the presence of positive charges in the vicinity of the metal site (and thus favorable thermodynamics and electrostatics), those compounds are likely potent SOD mimics *in vitro*. WW-85 is less so, as it bears negative charges on the periphery that can impose repulsion toward superoxide. Both molecules are very bulky; the FP-15 is, in addition, very hydrophilic. We used the Mn analogue of FP-15 (MnTTEG-2-PyP^{5+}) in our simple, but $O_2^{\cdot-}$-specific model of SOD-deficient *E. coli* (241). Despite its high k_{cat} ($O_2^{\cdot-}$) (36), its big size, bulkiness, and excessive hydrophilicity decrease its *in vivo* efficacy when compared with MnTE-2-PyP^{5+} or MnTnHex-2-PyP^{5+}. In radioprotection of ataxia/telangiectasia cells, the MnTTEG-2-PyP^{5+} was ineffective (255).

N. Cu porphyrins

Copper complexes have not been extensively studied. We have shown that $CuBr_8$TM-4-PyP^{4+} has a significant SOD-like activity, $\log k_{cat} = 6.46$ (33). Moreover, when compared with the Mn(II) analogue, $Mn^{II}Br_8$TM-4-PyP^{4+}, Cu porphyrin is significantly more stable and undergoes demetallation only in concentrated sulfuric acid. Whereas SOD activity was achieved by choosing highly electron-deficient porphyrins, such as the β-octabrominated derivatives, simpler Cu porphyrins, such as CuTM-4-PyP^{4+}, are not SOD mimics ($\log k_{cat} < 3.7$) (33). Possible Fenton chemistry on Cu(II) site within porphyrin has not been explored.

O. Co and Ni porphyrins

Co porphyrin is not a strong SOD mimic. Pasternack and Skowronek (247) reported the rate constants for the reduction of $O^{\cdot}{}_2^-$ of $3\times10^7\ M^{-1}s^{-1}$ for FeTM-4-PyP^{5+} and $1\times10^5\ M^{-1}s^{-1}$ for CoTM-4-PyP^+ in 0.05 *M* carbonate buffer, pH 10.1 (*via* NBT /XO/X assay) (247). Because NiSOD exists in nature, we were tempted to synthesize the Ni analogue of MnTE-2-PyP^{5+}, but to our disappointment and despite favorable electrostatics and electron-deficiency of porphyrin ligand, the $\log k_{cat}$ for NiTE-2-PyP^{4+} is only 5.43; it is more than two orders of magnitude less active than MnTE-2-PyP^{5+}. Its k_{cat} is around the rate constant for $O_2^{\cdot-}$ self-dismutation (5×10^5 M/s, pH 7.0). Contrary to the porphyrin ligand, the ligand field around Ni in NiSOD enzyme allows it to cycle easily between +2 and +3 oxidation state with $O_2^{\cdot-}$.

IV. Porphyrin-Related Compounds: Biliverdins, Texaphyrins, and Corroles

A. Mn(III) biliverdin and its analogues

We also studied Mn(III) biliverdin $[MnBV^{2-}]_2$ and its analogues with respect to $O_2^{\cdot-}$ dismutation (299, 302). They are dimmers, with each trivalent Mn bound to four pyrrolic nitrogens of one biliverdin molecule and to the enolic oxygen of another molecule. They are also the first compounds shown to dismute $O_2^{\cdot-}$ by using the Mn(IV)/Mn(III) redox couple,

which has the $E_{1/2} = +450$ mV *versus* NHE. This potential is similar to the potential of the Mn(III)/Mn(II) couple of Mn(III) *N*-alkylpyridylporphyrins and of the SOD enzyme (302). The complexes exhibit a high $k_{cat} \sim 5\times10^7$ $M^{-1}s^{-1}$ (302) (Table 1). The most recent data indicate that corroles, which may be considered modified porphyrins, dismute superoxide efficiently by using also the Mn(IV)/Mn(III) redox couple (99) (see under Corroles). The usefulness of Mn biliverdins is hampered by their water insolubility.

B. Texaphyrins

Texaphyrins and their lanthanide complexes (Fig. 8) are porphyrin-like compounds (282). Motexafin gadolinium (MGd^3, $Xcytrin^R$) has been used as a cancer chemotherapeutic in Phase III clinical trials. A prooxidative mechanism of tumor killing, through increased ROS production, was proposed. At the expense of NADPH or ascorbate, thioredoxin reductase TrxR would reduce MGd ($E_{1/2} \sim -40$ mV *vs.* NHE in *N*, *N*′-dimethylformamide), which would in turn transfer electrons to oxygen, producing superoxide and eventually H_2O_2 (148). The noncompetitive inhibition of thioredoxin reductase and ribonucleotide reductase, resulting in increased levels of ROS, may also play a role. Only modest peroxynitrite scavenging ability has been evaluated with an Mn analogue (289). The rate constant for Mn(II)/Mn(III) oxidation by $ONOO^-$ is estimated at 3×10^4 $M^{-1}s^{-1}$, whereby $^{\cdot}NO_2$ is formed. It has been proposed that the Mn(III) compound is reduced back to Mn(II) texaphyrin either by nitrite or by ascorbate *in vivo.* With fairly negative $E_{1/2}$ (though obtained in dimethylformamide, and thus not readily projected onto aqueous systems), and no electrostatic facilitation for $O_2^{\cdot-}$ dismutation, a significant SOD-like activity in aqueous systems is unlikely.

In addition to anticancer activity, MGd also was proposed to enhance tumor-radiation therapy by enhancing the anaerobic production of $^{\cdot}OH$ and aerobic formation of $O_2^{\cdot-}$. In clinical trials, it did not have sufficient anticancer effect as a single agent (10). It has been tested in combination with radiotherapy in brain metastases and primary brain tumors with varying success. Although promising results were obtained in some clinical trials in combination with radiation [non–small cell lung cancer with brain metastasis (215)], most recently, no effect on overall survival was reported with whole-brain radiotherapy of metastases from solid tumors (326).

Both MGd and $MnTnHex\text{-}2\text{-}PyP^{5+}$ (68) have been tested in an ALS model and exerted similar efficacy; the data still need explanation, given that production of ROS/RNS is reportedly a major pathway for MGd, and the opposite still holds true for $MnTnHex\text{-}2\text{-}PyP^{5+}$ (see also Prooxidative action of metalloporphyrins).

The lutetium analogue (Lu-Tex) is a photosensitizer developed for photodynamic tumor therapy (282). It is retained selectively in tumors, presumably because of the association with low-density lipoproteins. As it localizes in plaques, it has been tested for photoangioplastic treatment of atherosclerotic plaques in peripheral arteries. The efficacy has been demonstrated in various models (282).

C. Corroles

As compared with porphyrins, corroles contain one less *meso* bridge and therefore have only up to three *meso* substituents (Fig. 8). They are also tri-anionic compared with di-anionic porphyrin ligands (with respect to pyrrolic nitrogen deprotonation) (285). Thus, they tend to form high-oxidation-state air-stable Mn(IV) complexes (23). The synthesis of water-soluble derivatives led to their increased development for biomedicinal purposes (23). The first step in Mn(III) reduction is thermodynamically very unfavorable, as it occurs at very negative potentials (<-1 V *vs.* NHE in different solvents) (285). The oxidation of Mn(III) to Mn(IV) corroles is fairly facile and has been first examined in conjunction with the much stronger oxidant, $ONOO^-$. The potency of metal corroles (Mn, Fe, and Ga), as well as the ability to attenuate atherosclerosis (144), has thus far been ascribed to peroxynitrite or H_2O_2 scavenging; catalytic action was provided by the reduction of Mn(IV) corrole to Mn(III) corrole with either nitrite or ascorbate. The k_{cat} ranged from $\sim4\times10^4$ (negatively charged corrole with three pentafluorophenyl *meso* groups and two sulfonated pyrrolic positions) to 4×10^5 $M^{-1}s^{-1}$ (positively charged corrole with pentafluorophenyl group on one *meso* bridge and two *para* methylpyridyl groups on two opposing *meso* bridges) (127). The values for Fe corroles are much higher: $\leq 2\times10^6$ $M^{-1}s^{-1}$ for a positively charged corrole (200). Most recently, the synthesis of *ortho* isomeric *N*-methylpyridylcorrole, $MnTrM\text{-}2\text{-}corrole^{3+}$ and analogue of a potent SOD mimic and $ONOO^-$ scavenger, $MnTM(or\ E)\text{-}2\text{-}PyP^{5+}$, was reported (Fig. 8) (275). The SOD-like activity of this corrole and of other Fe and Mn anionic and cationic corroles, along with Mn(IV)/Mn(III) reduction potentials, has just been reported (99). The first step in a dismutation process, the oxidation of a metal center from +3 to +4 oxidation state is rate limiting, as opposed to most of the porphyrins, other than biliverdins. As a result of the thermodynamic and electrostatic effects, the log k_{cat} varies from 5.68 to 6.34. The $E_{1/2}$ for the Mn(IV)/Mn(III) redox couple varies between +760 and +910 mV *versus* NHE. In agreement with a bell-shaped curve that we have established for porphyrins (37, 38, 262, 266), as the reduction potential increases, the oxidation of porphyrins (and in this case, a corrole) eventually becomes a rate-limiting step, and the further enhancement of k_{cat} may be achieved only by decreasing the $E_{1/2}$ (introducing the electron-donating groups), which would in turn favor the oxidation of metal corrole (reduction of $O_2^{\cdot-}$). $MnTrM\text{-}2\text{-}corrole^{3+}$ bears 2 less charges than analogous porphyrin, $MnTE\text{-}2\text{-}PyP^{5+}$, and is thus more lipophilic. Enhanced lipophilicity may *in vivo* compensate for lower k_{cat}. Of note, whereas structural characteristics of new corroles were reported, no elemental analysis data were provided (22, 143, 275).

The antitumor effects of a 5,10,15-*tris*[2,3,5,6-tetrafluoro-4-(*N*-methyl-2-pyridinium)]corrole was reported by Aviezer *et al.* (22, 143) *in vitro* and *in vivo.* At 1–10 μg/ml, corrole inhibited binding of FGF2 to the FGF receptor. When Lewis lung carcinoma D122 cells (200,000 cells/mouse) were injected into foot pads of the 10-week-old C57 black mouse, mice were allowed to develop primary tumors for 4 weeks. Tumors were then amputated, and metastases were allowed to develop for 4 weeks before mice were killed. Mice were treated with corrole at 5 mg/kg twice per week. A significant suppression of tumor metastasis was observed. Peroxynitrite-based protection of rat β cells with cationic corroles also was reported (242).

The significant tumor growth suppression and tumor-imaging properties of the fluorescent, negatively charged gallium sulfonated corrole noncovalently associated with

breast cancer–targeted cell-penetration protein (HerOBK10), which accumulates in $HER2^+$ tumors, was recently reported; the complex retains integrity in human serum and accumulates in tumor (4, 5, 43). Nude mice bearing $HER2^+$ received daily IV injections of 0.008 mg/kg of HerGa complex for 7 days, starting at the time tumors reach 250–300 mm^3 volume; tumor size was measured until 25 days of growth. Sulfonated gallium corrole has a modest effect on tumor growth in its own right. The mechanism of action is not fully understood (4, 5).

V. Mn Salen Compounds

A. SOD-like activity of Mn salens

Mn salen compounds are complexes of Mn with *N*,*N*′-bis(salicylidene)ethylenediamine (Fig. 1). Although salen compounds have been of interest in catalysis since the beginning of the last century, the possible role of their Mn complexes in decreasing oxidative-stress injuries arose quite recently and parallels studies on another two groups of metal complexes, Mn cyclic polyamines and Mn porphyrins (40, 93). EUK-8, the Mn salen (Mn(III) complex with prototypical *N*,*N*′-bis(salicylidene)ethylenediamine) (Fig. 1), has a fairly negative reduction potential for the Mn(III)/Mn(II) redox couple, being −130 mV *versus* NHE, which is insufficient to provide high efficacy in catalyzing $O_2^{\cdot-}$ dismutation (302). Moreover, with only one positive charge on the Mn site, electrostatic guidance of $O_2^{\cdot-}$ to the Mn site is missing. The SOD-like activity of a EUK-8 (Fig. 1) is close to the activity of $MnCl_2$ in 0.05 *M* phosphate buffer, $k_{cat} = 6.0 \times 10^5$ $M^{-1}s^{-1}$ (302), which is further similar to 1.3×10^6 $M^{-1}s^{-1}$ determined by nitrobluetetrazolium assay by Baudry *et al.* (40), and represents only ∼0.1% of the k_{cat} of the SOD enzymes (24, 171). Because of the lack of the macrocyclic effect, both we and Baudry *et al.* (40) reported the loss of SOD-like activity of EUK-8 in the presence of EDTA due to the formation of the SOD-inactive, Mn complex with EDTA (14, 302). This may hold true for EUK-134 and EUK-189. Therefore, such derivatives are likely to lose Mn *in vivo* in the presence of other carboxylate- and phosphate-based cellular chelators. In EUK-207 (Fig. 1), the structural modifications have been made to enhance the stability by cyclizing the ligand with an eight-membered crown ether moiety, thus introducing the macrocyclic effects similar to the porphyrin (94). The catalase-like activity and the cytoprotective effects *in vivo* have been preserved in comparison with the EUK-8, EUK-134, and EUK-189 series. The *in vivo* effects of the latter three compounds have been continuously reported. Our data on *C. neoformans* (see later) suggest that EUK-8 may possess sufficient stability to reach, in an intact form, the targeted subcellular compartment and release Mn there (131). Doctrow *et al.* (94) reported that 220 μM Mn salens [EUK-113 (similar to EUK-134 but with axial acetate instead of chloride); EUK-189; EUK-178 (similar to EUK-113 but with an upper aromatic bridge); EUK-207] (Fig. 1) are stable for hours with 25 m*M* EDTA at room temperature and at pH 7.4. The most stable EUK-207 was found largely intact even after 70 h under same conditions (94). The EUK-134 (Fig. 1) analogue possesses two methoxy groups on phenyl rings instead of hydrogens; when compared with EUK-8; it has only slightly enhanced SOD-like activity, but alkoxy groups appear to enhance catalase-like activity (1, 130, 245).

B. Catalase-like activity of Mn salens

Mn salen derivatives reportedly possess significant catalase- and peroxidase-like activity. It has been reported that EUK-8 and EUK-134 have 0.6 and 0.5 U/mg (171), whereas the enzyme has ∼5,000 U/mg. If calculated per milligram basis, the EUK-8 would have 0.01% of catalase activity. If one does the calculation per molar basis, assuming the MW of the enzyme to be 250,000, and considering its tetramer structure (MW = 62,500), and the MW = 357 for EUK-8, EUK-8 has 7×10^{-5}% of catalase activity (171). In agreement with these calculations, Sharpe *et al.* (284) considered Mn salens to be poor catalysts of H_2O_2 breakdown (284). Although SOD-like activity is reportedly not dependent on the structure, the structure–activity relationship has been established for catalase-like activity (93, 94). Alkoxy groups in position 3 (EUK-134, EUK-189) enhanced, whereas in position 5, decreased the catalase activity when compared with EUK-8 compound. Although less stable (EUK-178 decomposes in aqueous solution within days), compounds containing six-membered aromatic bridge possess up to sevenfold higher catalase-like activity when compared with unsubstituted EUK-8 (93).

C. Reactivity toward other ROS/RNS

Besides $O_2^{\cdot-}$- and H_2O_2-related activity, Sharpe *et al.* (284) reported the reactivity of EUK-8 and EUK-134 toward OCl^- and $ONOO^-$, in which Mn(V) oxo species were formed by a two-electron process, thus giving rise to the benign species, H_2O, O_2, and $NO_2^{\cdot-}$. The Mn(V) oxo species can react with $^{\cdot}NO$, giving rise to $^{\cdot}NO_2$, which will combine with $^{\cdot}NO$, giving rise to N_2O_3, which, with water, will produce HNO_2. PEG-ylated compounds were also prepared (245). We provided data that although PEG-ylated porphyrins possess higher SOD-like activity than the non–PEG-ylated analogues (36), their cellular localization is hampered by their increased size (36). Thus, PEG-ylated salen compounds, although two- to threefold more potent than EUK-134, may also be of excessive size to enter the cell or mitochondria at sufficient levels (245).

D. Mn salens in suppressing oxidative-stress injuries in vivo

The *in vivo* effects of EUK compounds, as already noted, reflect their ability to scavenge different reactive species and not specifically superoxide or peroxide. Further, like porphyrins, such activities result in modulating cellular transcriptional activity, affecting NF-κB and MAPK pathways (260, 339). EUK-134 was first reported by Melov *et al.* (216) to increase life span of the nematode *Caenorhabditis elegans* by 50% (216), which was later contradicted by Keaney *et al.* (171) [*i.e.*, the effect was seen only if superoxide generators (paraquat and plumbagin) were used]. The data were further complicated with the effect on the decreasing life span of domestic fly, *Musca domestica*, under hypoxic conditions (41). EUK-8, EUK-134, and EUK-189 were shown to affect activation of microglia with the 42-amino-acid form of β-amyloid peptide (A β 42) when insulted with H_2O_2 or $ONOO^-$ (11). A modest but significant effect was observed in extending the survival in a mouse model of prion disease with IP injections of 30 mg/kg of EUK-189, 7 days per week,

starting at day 7 after the inoculation of the diseased brain homogenate (51). EUK-134 was able to decrease infarct size in a rat stroke model when given in a single dose of 2.5 mg/kg IV at 3 h after MCAO, and assessed at 21 h after MCAO (24). We showed with MnTDE-2-ImP^{5+} that such protective action in single treatment, on the level of primary oxidative stress as a direct consequence of ischemia–reperfusion, fades away later as a result of excessive upregulation of cellular transcriptional activity/inflammation (288). Prolonged treatment with an antioxidant that would modulate secondary oxidative stress is thus necessary; in turn, both delayed-treatment and long-term effects must be evaluated to address the clinical utility of any antioxidant for stroke treatment. In apoptosis inducing factor–deficient (harlequin) mouse, EUK-8 reduces oxidative stress after 4 weeks of pressure-overload–induced heart failure if given IP at 25 mg/kg/day, 3 times per week, for the duration of the study (324). Along with Mn cyclic polyamine M40403, EUK-134 protected mouse heart from superoxide-induced reperfusion injury (343). EUK-8 diminished the consequences of multiple organ failure in endotoxic shock caused by *E. coli* lipopolysaccharide (6 mg/kg) if given continuously IV at 0.3 and 1 mg/kg/h for 6 h (213). Along with Mn porphyrins, Mn salen derivatives attenuated lung inflammation in a porcine model of LPS-induced acute respiratory syndrome (260), supposedly through decreasing oxidative stress, which in turn suppresses NF-κB activation and pro-inflammatory gene expression (260). A mild effect on the survival of the G93A mouse in an amyotrophic lateral sclerosis model (eight low copies model) was observed with EUK-134 and EUK-8 (33 mg/kg, 3 times per week for the duration of the study), the former being more effective (164). The effect of Mn salens in neurodegenerative disorders was summarized in a review by Patel (133). The effect on the inhibition of MAPK signaling pathways and decrease in p53 accumulation in ultraviolet B–exposed primary human keratinocytes, leading to increased cell survival, was reported with EUK-134 (84). A rather unexpected effect of EUK-8 as well as of the NADPH oxidase inhibitor, diphenyleneiodonium, on promoting the induction of TGF-β, was observed (339). EUK-8 prolonged the survival of islet allografts (from BALB/c mice) in newly diabetic female NOD mice after treatment with 100 mg/kg for 50 days (starting at 6 weeks of age), and prevented the spontaneous type 1 diabetes with NOD mice for up to 1 year, if given at 100 mg/kg every other day for only 35 weeks (243). At 5 mg/kg/day for 50 days, EUK-8 prevented adoptive transfer of type 1 diabetes. EUK-189, given as a single SC injection of 70 mg/kg, 24 h before the whole-body radiation, exerted radioprotection of two mouse strains (C3H/HeN and CD2F1) (307). ^{60}Cobalt gamma irradiation was applied (midline tissue dose was 1–10 Gy) (307). Protection also was seen if the drug was given at 6 h after radiation but with one strain only (C3H/HeN). The $LD_{50/30}$ values were 7.96 and 9.13 Gy for saline- and EUK-189–treated groups. A study is in progress to fully evaluate EUK compounds as potential mitigators. Doctrow *et al.* (94) reported an increased survival of MnSOD$^{-/-}$ mice, improved neurologic deficits, and protected mitochondrial aconitase and complexes I–IV with EUK-207 and EUK-189. MnTBAP^{3-} was less effective, which the authors attribute to its lower ability to cross an intact blood–brain barrier and protect brain mitochondria (94). M40403 also was inefficient, presumably because of the inability to cross the blood–brain barrier or to enter mitochondria or both. In MnSOD-knockout yeast, *C. neoformans,* Mn salen (EUK-8) and ascorbate were able to offer protection, but not $MnCl_2$, or Tempol, or any of the five Mn porphyrins (cationic and anionic) (133). In aerobic growth of SOD-deficient *E. coli* and radioprotection of ataxia telangiectasia, Mn salen was, however, of inferior efficacy, as compared with Mn porphyrin, MnTnHex-2-PyP^{5+} (225, 241, 255). A limited effect of Mn salen was observed in a later study, and none, in the former. As in other redox-able metal complexes, Matthijssens *et al.* (210) reported that EUK-8 has prooxidant activity also, increasing the levels of ROS in *E. coli*; no protection of the SOD-deficient *E. coli* strain, when growing aerobically, was detected (210). When Mn salen and MnTM-2-PyP^{5+} were compared in a small bowel ischemia–reperfusion injury (given to rats into the portal vein before and after ischemia at 1 mg/kg), similar abilities to scavenge reactive species were observed (331). Prevention of cognitive deficits and brain oxidative stress was reported with EUK-189 and EUK-207 when C57/BL6 mice were injected with Mn salens *via* osmotic pumps for 6 months, starting at 17 months of age (62).

With EUK compounds, control experiments involving Mn^{2+} may be beneficial primarily for mechanistic purposes, to distinguish whether the effects observed originate from Mn ligated in Mn salen complex, or from Mn^{2+} in its own right; in other words, is Mn salen transporting Mn into the cell?

VI. Mn Cyclic Polyamines

A. SOD-like activity

Riley *et al.* (21, 204, 269, 277) developed Mn complexes with cyclic polyamines/tetraaza crown ethers as catalysts for $O_2^{\cdot-}$ dismutation (Fig. 9). Structural modifications led to compounds of increased activity; complexes with k_{cat} as high as 10^9 Ms have been reported (21). The detailed kinetic study published by Maroz *et al.* (204) found that the reaction of a transient adduct (formed with the first $O_2^{\cdot-}$ molecule) with the second molecule of $O_2^{\cdot-}$ is particularly dependent on the structure of the polyamine.

Thus, among three compounds studied, the so-called M40403 (SODm1), which is the 2S,21S nonmethylated analogue, has a k_{cat} of 3.55×10^6 $M^{-1}s^{-1}$ (Fig. 9). Its 2S,21S

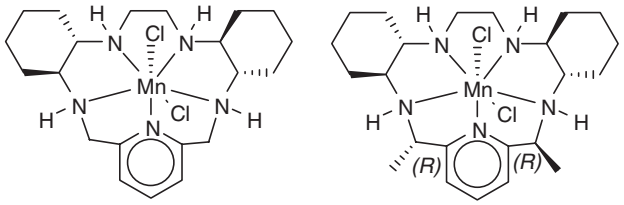

M40403 M40404

FIG. 9. Mn(II) cyclic polyamines: the SOD-active M40403 (2S,21S nonmethylated analogue) and SOD inactive M40404 (2R,21R dimethyl derivative).

dimethyl derivative (SODm2) is 100-fold more active, $k_{cat} = 2.35 \times 10^8\ M^{-1}s^{-1}$ at pH 7.4, whereas its 2R,21R dimethyl derivative (M40404, SODm3) is inactive. A sevenfold higher rate constant for the 2S,21S dimethyl derivative was reported by Aston *et al*. (21) ($k_{cat} = 1.6 \times 10^9$ M/s at pH 7.4). The $E_{1/2}$ values for all three complexes are fairly similar at +525 (SODm1), +464 (SODm2), and +452 mV *versus* NHE (SOD m3) in acetonitrile (204, 269) (Table 1), and cannot justify the total lack of activity of the 2R,21R derivative. Such values suggest that other effects, particularly conformational flexibility of pseudooctahedral geometry of oxidized species (as determined by X-ray data and may not necessarily describe the geometry in aqueous solution) presumably govern the differences in the SOD-like activity of those three compounds. The catalysis involves a fast oxidation of $[Mn^{II}(L)]^{2+}$ with $O_2^{\cdot -}$ to $[Mn^{III}(L)O_2]^{+}$, followed by the second rate-determining reduction of $[Mn^{III}(L)O_2]^{+}$ to $Mn^{II}(L)O_2]$, which rapidly equilibrates with $[Mn^{II}(L)]^{2+}$. Temperature studies revealed major differences in the thermodynamics of the catalytic cycles involving SODm2 or SODm1. In the case of SODm2, the observed high entropic contribution to the activation energy is indicative of ligand conformational changes during the catalytic cycle (21). The k_{cat} also may be increased if the charge distribution and substituents are changed. The most active compound (SODm2) has not been used in any *in vivo* studies. These complexes contain Mn in a +2 oxidation state and are thus of limited metal/ligand stability, with log K = 13.6 for the mostly *in vivo* studied polyamine 2S,21S-nonmethyl analogue, M40403 (269). Riley *et al.* (230) found the intact complex down to pH 6.1 only, which may be insufficient to account for the *in vivo* efficacy. Based on the reported *in vivo* efficacy, Mn cyclic polyamines may act as Mn transporters. Once Mn is lost from the complex, the ligand, which is in essence an aza crown ether with high affinity toward metals (particularly mono and divalent), may bind other biologic cations, therefore exerting toxicity. The specificity of Mn cyclic polyamines toward $O_2^{\cdot -}$ was claimed (277); activities toward $ONOO^-$, $^{\cdot}NO$ and H_2O_2 were assumed absent. Such specificity may be desirable for mechanistic studies, but not for therapeutic purposes.

B. Mn(II) cyclic polyamines in suppressing oxidative stress in vivo *and* in vitro

M40403 is thus far the most studied cyclic polyamine *in vivo*. It suppressed inflammation in a variety of models: carrageenan-induced pleurisy mouse model (75), rat model of septic shock (198), *E. coli* lipopolysaccharide serotype 0111:B4 (LPS)-induced cytokine production by cultured rat alveolar macrophages (233), inflammatory pain in a carrageenan model of paw edema (230, 277, 329), guinea-pig model of allergic asthma-like reactions (207), rodent model of colitis (74), myocardial ischemia–reperfusion injury (208, 343), chronic hypoxia-induced pulmonary hypertension (86), and so on. M40403 also was reported to provide protection against radiation-induced mucositis in the Syrian golden hamsters. The optimal regiment was 30 mg/kg, given IP twice daily for 3 days, starting at 30 min before 40-Gy focus radiation (226). The radiation was given at 40 Gy to a cheek pouch (226). The action on NF-κB signaling pathways has been indicated in the carrageenan-induced mouse pleurisy model (316). The strong enhancement of the antitumor effect of interleukin-2 (IL-2) by M40403, ascribed to the ROS-scavenging ability of the SOD mimic, has been reported (278). In addition, M40403 prevented IL-2 from causing dose-limiting hypotension. Since ActivBiotics, Inc., acquired the rights to M40403 (previously *Metaphore*) a few years ago, only a single report has been published. Recently, the protective effects of tetraaza polyamine (derivatized with carboxylates) with activated macrophages at nanomolar levels and in an animal acute and chronic inflammation model (5–15 mg/kg, single injection) were reported. The metal/ligand stability (log K = 14.73), and the k_{cat} ($O_2^{\cdot -}$) = $1.1 \times 10^6\ M^{-1}\ s^{-1}$ were given (103).

VII. Nonmetal-Based SOD Mimics

A. Fullerenes

1. SOD-like activity. The use of fullerenes for biologic applications progressed as soon as the water-soluble derivatives emerged (162, 280). Early studies suggested that direct reactions between hydroxyl, alkoxyl, alkylperoxyl, and benzyl radicals and the highly conjugated double-bond system of C_{60} fullerenes were responsible for their antioxidant actions; however, the mechanism is not quite understood (8). SOD-like catalytic action was reported for a water-soluble derivative (C_3) that bears three malonyl residues on its surface (8). The k_{cat} of 2×10^6 M/s at pH 7.4 increases 10-fold per each pH unit decrease, as a protonation of the carboxylate moieties becomes favorable. When deprotonated, the carboxylates constitute the electrostatic barrier to the incoming $O_2^{\cdot -}$.

2. The protective effects of fullerenes *in vivo*. The SOD-like activity was responsible for significantly increasing the *in utero* survival of clonogenic DBA2J $MnSOD^{-/-}$ mice when dams were given 100 mg/kg/day of C_3 in a drinking water (of which 10% was absorbed); a 300% increase in postnatal survival was reported when C_3 was given SC to pups at 10 mg/kg (8). Data indicate that C_3 localizes in mitochondria, where it replaces MnSOD. A carboxyfullerene protected the liver against carbon tetrachloride intoxication in rats (129). In an osteoarthritis model, a carboxylated C_{60} prevented catabolic-stress–induced production of matrix metalloproteinases 1, 3, and 13, downregulation of matrix production, apoptosis, and premature senescence of human chondrocytes (treated with interleukin-1β) *in vitro*, and degeneration of articular cartilage *in vivo*, in rabbit knees (349). By using EPR measurements, Yin *et al.* demonstrated the ROS (singlet oxygen, superoxide, and hydroxyl radical)-scavenging abilities of three water-soluble fullerenes, Gd-fullerenol, fullerenol, and carboxyfullerene (with two malonyl groups). They reported the ability of these compounds to inhibit lipid peroxidation (with EPR oximetry) in H_2O_2-induced cytotoxicity in human lung adenocarcinoma A549 and rat brain capillary endothelial cells (347). The effects are dependent on the structural characteristics; the polyhydroxy fullerenes are the most potent scavengers. Protective effects in neurodegenerative diseases were reported in a mouse model of familial amyotrophic lateral sclerosis and in Parkinson's disease (97). Robust neuropro-

tection by C_3 fullerene against excitotoxic, apoptotic, and metabolic insult was observed in cortical cell cultures (97, 98). A C_3 fullerene, given orally at 10 mg/kg/day, starting at 12 months of age until death reportedly extended both the life span and cognition of mice; the authors also reported the mitochondrial localization of C_3 and its ability to cross the blood–brain barrier (256, 137). Radioprotective effects *in vitro* and 15% survival rate of mice at 30 days after whole-body irradiation (7 Gy) was observed if 1 mg/kg of hydrated C_{60} fullerene was given 1 h before radiation (12). In a zebrafish embryo radiation study, 100 μM fullerene increased overall survival by $\sim$87 % relative to 55.6% of the absolute survival rate of the untreated, but radiated group (77).

B. Nitroxides

1. SOD-like activity of nitroxides. SOD-like activity of nitroxides was determined in early 1990s. Their chemistry was described by Sara Goldstein and co-workers (16, 137, 139, 140, 183) and more recently by Wilcox and Pearlman (334). Nitroxide ($RNO^{\cdot}$) cycles between the oxidized oxoammonium cation (RNO^+) and the reduced hydroxylamine (RNOH). For 4-$N(CH_3)_3$-tempo (CAT-1), the $E_{1/2}^{oxid}$ for $RNO^+/RNO^{\cdot}$ is +942 mV *versus* NHE, and the $E_{1/2}^{red}$ for $RNO^{\cdot}/RNOH$ is +360 mV *versus* NHE in 0.1 M phosphate buffer (140). Most nitroxides react with $O_2^{\cdot -}$ very slowly and are inefficient SOD mimics at

$$RNO^{\cdot} + HO_2 \rightarrow RNO^+ + HO_2^{\cdot -} \quad [1]$$

$$RNO^+ + O_2^{\cdot -} \rightarrow RNO^{\cdot} + O_2 \quad [2]$$

physiologic pH (Eq. [2], $k < 10^3\ M^{-1}s^{-1}$). Protonated superoxide, $HO_2^{\cdot}$ ($pK_a = 4.8$), however, reacts rapidly with nitroxides (Eq. [1]). The rate constant for the reaction of 2,2,6,6,-tetramethylpiperidine-1-oxyl (Tempo) with $HO_2^{\cdot}$ to form RNO^+ is $1.2\times10^8\ M^{-1}s^{-1}$ (137). However, $O_2^{\cdot -}$ reacts at a diffusion-limited rate ($k > 10^9\ M^{-1}s^{-1}$) with oxoammonium cation, giving rise to nitroxide (Eq. [2]). In the absence of a reducing agent, the oxoammonium cation forms readily and oxidizes various organic compounds, including DNA (16). Under reducing conditions *in vivo*, the oxoammonium cation can be reduced to hydroxylamine, whose antioxidant activity, as suggested by Trnka *et al.* (318), occurs presumably through hydrogen atom donation and may account for the *in vivo* protective effects of nitroxides (318). Also, the oxoammonium cation is susceptible to two-electron reduction to hydroxylamine by alcohols, thiols, and reduced nicotinamide nucleotides (319).

2. Reactivity toward other ROS/RNS. In addition to $O_2^{\cdot -}$, oxoammonium cation (but not nitroxide) reacts rapidly with $ONOO^-$ (and much more slowly with $^{\cdot}NO$), $k = 6\times10^6\ M^{-1}s^{-1}$ for Tempo (RNO^+) at pH 5 (139). The reactivity is dependent on the reduction potential (ranging between +770 and +1000 mV *vs.* NHE for the $RNO^+/RNO^{\cdot}$ couple), ring size, ring substituents, and charge (140). Nitroxides are very efficient scavengers of the products of peroxynitrite reactions with CO_2: $CO_3^{\cdot -}$ and $^{\cdot}NO_2$ radicals, for which the rate constants are in excess of $10^8\ M^{-1}s^{-1}$ at physiologic pH (139, 140). The authors suggest that, by scavenging $^{\cdot}NO_2$, they can effectively prevent 3-nitrotyrosine formation ($TyrO^{\cdot} + {}^{\cdot}NO_2$). No direct reaction of nitroxides with $^{\cdot}NO$ was reported (140); NO reacts with Tempo oxoammonium cation with $k = 9.8\times10^3\ M^{-1}s^{-1}$ (140). Recently, nitroxides were shown to be effective in scavenging protein-derived radicals (tyrosine-derived phenoxyl and semiquinone species, and tryptophan-derived carbon-centered and peroxyl radicals) in nearly stoichiometric fashion (183), thiyl radicals (at pH 5–7, $k = 5\text{–}7\times10^8\ M^{-1}s^{-1}$) (138), and peroxyl radicals (for Tempo, depending on the type of the peroxyl radical, k ranges from 2×10^7 to $10^8\ M^{-1}s^{-1}$) (134). The reactivity of 4-NH_3-Tempo toward myeloperoxidase (MPO) was recently reported to lead to MPO inhibition (IC_{50} $\sim$ 1–6 μM) and consequent suppression of HOCl production (268).

As with all other compounds that are redox active within biologically compatible limits, nitroxides also exerted prooxidative action (16).

3. The protective effects of nitroxides *in vitro* and *in vivo*. A detailed review of the protective effects of nitroxides was published by Soule *et al.* (296, 297) and is briefly summarized here. Nitroxides were shown to be radioprotective when given IP to mice before radiation. The significant blood pressure decrease associated with Tempol administration was overcome by using the reduced Tempol form, a hydroxylamine, which is rapidly oxidized *in vivo*, offering radioprotection. However, it was used to treat hypertensive rats at 72 μmol/kg, given IV (297). The radiation $LD_{50/30}$ (radiation that caused 50% lethality in C3H mice in 30 days) was 7.84 Gy without and 9.97 with Tempol in a study in which mice were exposed to whole-body radiation. Tempol was injected at 275 mg/kg, 5–10 min before radiation exposure (147, 296). *In vitro*, reduced Tempol (hydroxylamine) was not efficient in protecting Chinese hamster cells against radiation, whereas Tempol was most effective at 50 mM levels (297). Further experiments with animals bearing radiation-induced fibrosarcoma RIF-1 tumor cells, in which Tempol was injected 10 min before radiation, indicated that, fortunately, it does not protect tumor cells. The data suggest that, in the hypoxic tumor environment, Tempol is reduced and is thus inactive, whereas it is oxidized in surrounding normal tissue (297). Tempol also decreased radiation-related hair loss and increased hair recovery in guinea pigs and in 12 patients. Patients with metastatic cancer were treated with 100 ml of Tempol (70 mg/ml of 70% ethanol) applied uniformly to the patient's scalp 15 min before each fraction of radiation (10 fractions in total) (217). Tempol was washed off after the completion of the daily radiation fraction. Tempol remained on the scalp for $\sim$30–45 min each day and was well tolerated (296). Tempol also decreased radiation-induced salivary hypofunction with C3H mice (297). A few anticancer studies indicate that nitroxides can affect tumor redox status and thus affect apoptotic and proliferative pathways.

With ataxia telangiectasia (*Atm*-deficient cancer prone mice), tumorigenicity was ameliorated (281, 297); the results were attributed, at least in part, to the modulation of redox-sensitive signaling pathways. Increased apoptosis and decreased neovascularization were observed in a Chinese hamster ovary model, MCF-7 breast cancer, p53-negative

leukemia cells, and a murine xenograft glioma model, rendering Tempol a prospective anticancer drug (297). Based on its ROS-scavenging ability Tempol was effective in ischemia–reperfusion models, where it decreased myocardial infarct size and stroke infarct size in a rat MCAO model if given at 10 mg/kg IV 20 min after reperfusion and assessed at 4 h after reperfusion. It also lessened the renal damage in a study in which rats underwent bilateral renal pedicle clamping for 45 min, followed by reperfusion for 6 h (297). Tempol (30 mg/kg/h), desferrioxamine (DEF, 40 mg/kg/h), or a combination of Tempol (30 mg/kg/h) and DEF (40 mg/kg/h) was administered before and throughout reperfusion (297). Tempol was protective in toxic shock induced by the bacterial antigen lipopolysaccharide, and in hemorrhagic shock against multiorgan failure. It was further protective in several other inflammatory conditions, such as pancreatitis, pleurisy, arthritis, colitis, and uveoretinitis (297). Tempol also was studied in neurodegenerative diseases. It protected mice at 200 mg/kg from developing Parkinsonian symptoms induced by the administration of 6-hydroxydopamine (297). A topical application of reduced Tempol decreased the formation of cataracts in both rats and rhesus monkeys (297). A role in treating obesity and diabetes has been suggested (297).

Dhanasekaran *et al*. (318, 319), by using Michael Murphy strategy to target mitochondria, showed that mito-carboxy proxyl, but not untagged nitroxide, effectively inhibited mitochondrial oxidative damage (90). The activity is presumably due to the nitroxide being reduced by ubiquinol within respiring mitochondria (90, 318, 319). Jiang *et al.* (163) proposed peptidyl nitroxide conjugates for targeting mitochondria. With anticipated higher efficacy, smaller amounts of nitroxide would be required. Efficacy of peptidyl conjugates (particularly those using the five-residue segment of gramicidin D), was shown to decrease superoxide production, apoptosis, and cyt *c* release from mitochondria in actinomycin D–induced cardiolipin oxidation. Yet, another report from Dessolin *et al.* (297) indicated that mitochondrially targeted Tempol and Mn(III) salen EUK-134 were not better than untargeted analogues in an apoptosis model in which HeLa cells were cultured with staurosporine or sodium selenite. The results indicated that mitochondria may not always be the sites of injury. No pharmacokinetics or toxicology of nitroxides are available.

The spin traps, nitrones, have shown potential for the prevention and treatment of age-related diseases, likely through scavenging reactive species and affecting signal-transduction pathways (117). Floyd *et al.* (116) published a review on the potential of nitrones as therapeutics, primarily as anticancer drugs, particularly addressing the preventive action of a phenyl-*tert*-butylnitrone (PBN) in rat liver cancer (116). With carbon- and oxygen-centered radicals, nitrones will form nitroxides. Nitrones bearing cationic *N*-pyridyl and a lipophilic moiety were reported aiming at mitochondria (271). The design of such molecules is essentially the same as the one in Murphy's compounds in which, instead of cationic pyridyl, a triphenylphosphonium ion functions as a cationic moiety (see earlier). Such compounds are also similar to cationic Mn porphyrins that bear longer lipophilic side chains.

In addition to their use as spin probes in EPR detection, identification of free radicals, and the study of tumor hypoxia (296, 297), magnetic resonance imaging with nitroxides, as cell-permeable redox-sensitive contrast agents, has been used for noninvasive monitoring of tissue redox status in animal models (156, 160). The imaging technique uses differential reduction of nitroxides in hypoxic and normal oxygenated tissue.

VIII. Other Compounds

A number of other different types of compounds with $k_{cat} \sim 10^6\ M^{-1}s^{-1}$, have been synthesized and tested on SOD-like activity; only few are listed here. Such is Mn dipyridoxyl diphosphate (no k_{cat} provided) (270), and natural antioxidants such as the polyphenol types of compounds (7, 146), honokiol ($k_{cat} = 3.2\times10^5\ M^{-1}s^{-1}$) (92, 121), and curcumin (113, 202, 311). The effect of curcumin on NF-κB pathways, similar to the effect of other antioxidants on transcriptional activity (113), as well as a suppression of a prostate cancer through inhibition of NF-κB activation by a dietary flavonoid, apigenin, was reported (291).

Copper complexes lacking macrocyclic ligands may have insufficient metal/ligand stability to be of practical importance (189, 237). As with iron, loss of copper, a Fenton chemistry $^{\cdot}OH$ radical producer, may account for their *in vivo* toxicity.

Cerium oxide (CeO_2) nanoparticles also have been investigated as SOD mimics. Seal, Self, and co-workers (149, 177) have shown that the SOD activity of the nanoparticles is dependent on the size of the nanoparticles and the Ce^{4+}/Ce^{3+} ratio in these materials. Although a polycrystalline nanoparticle preparation with 3- to 5-nm crystals was as effective as Cu,ZnSOD in dismuting superoxide (k_{cat} for this preparation was $3.6\times10^9\ M^{-1}s^{-1}$), preparations composed of hard, agglomerated, relatively larger particles (5–8 nm) were far less efficient (177). Addition of EDTA (up to 5 m*M*) did not affect the SOD activity of these preparations (177). The SOD activity has been measured by using the cyt *c* assay, and, in light of the xanthine oxide inhibitory activity of the trace Mn cluster impurities of $MnTBAP^{3-}$ (264), it would have been valuable to know whether these cerium oxide nanoparticles truly inhibit cyt *c* reduction by scavenging superoxide and not by having inhibitory effects on the xanthine oxidase system, which is the superoxide generator in the cyt *c* assay. A decrease of the size of the particles is accompanied by a decrease in the Ce^{4+}/Ce^{3+} ratio, which correlates with higher oxygen and electron vacancy in the solid (149, 177). The increase in Ce^{3+} concentration at the particle surface has been directly related to the ability of the nanoparticle to scavenge superoxide (149). The mechanism of dismutation has been speculated (177) to involve the Ce^{4+}/Ce^{3+} redox pair through two consecutive one-electron transfers, similarly to that in the Mn^{3+}/Mn^{2+} porphyrins.

The involvement of simple cerium salts, such as cerium chloride, in Fenton-like reactions, has been demonstrated; electron paramagnetic resonance experiments revealed that hydroxyl and superoxide radicals can be generated by hydrogen peroxide in the presence of Ce^{3+} (150).

Some studies on the *in vitro* and *in vivo* effects of cerium oxide nanoparticles have been reported. These materials prevented retinal degeneration induced by intracellular

peroxide; cerium oxide nanoparticles (1–20 n*M*) prevented the increase of H_2O_2 in primary cell cultures of rat retina (60). In *in vivo* rat studies, the nanoparticles (0.1–1 μM) were injected into the vitreous humor of both eyes and shown to prevent loss of vision due to the light-induced degeneration of photoreceptor cells (60). Cerium oxide nanoparticle (at nanomolar levels) proved beneficial in an *in vitro* cell model of adult rat spinal cord neuroprotection (78). These nanoparticles (3–5 nm) can also protect normal tissue against radiation-induced damage; CeO_2 nanoparticles prevented the onset of radiation-induced pneumonitis when delivered (IP or IV) to athymic nude mice exposed to high doses of radiation in a study using amifostine as a positive control (63). Cerium oxide nanoparticles can bind to transferrin, and the resulting conjugate has been used to modulate CeO_2 cellular uptake, as demonstrated in human lung cancer cells (A549) and normal embryo lung cells (WI-38) (327). Toxicity data for cerium oxide nanoparticles of 3–5 nm administered *via* IP injections were obtained in athymic nude mice and shown to be nontoxic up to 33.75 mg/kg/daily for 4 days (63). It is noted in the study that CeO_2 nanoparticles, produced by different synthetic protocols that are of different size and shape, are expected to show different degrees of toxicity (63).

Goldstein *et al*. (135) showed that osmium tetraoxide (OsO_4), which is used in the treatment of arthritic joints, is about 60-fold more active (per mass unit) than Cu,ZnSOD. The dismutation catalysis takes place by making use of the Os^{VIII}/Os^{VII} redox couple: Os^{VIII} is reduced by superoxide with a bimolecular rate constant of $k = 2.6 \times 10^9\ M^{-1}s^{-1}$, and the resulting Os^{VII} is oxidized back to Os^{VIII} by superoxide, with a bimolecular rate constant of $1.0 \times 10^9\ M^{-1}s^{-1}$. Finally, the potential of Pt nanoparticles as SOD mimics has been reported in extending the life span of *Caenorhabditis elegans* (168, 173). The effect at 0.5 m*M* only, but lack of it at 0.1 and 1 m*M* concentrations, raises concerns.

IX. Comparative Studies

In deciding which drug or drugs may be useful in one or the other pathologic condition, comparative studies are needed. Only a few comparative studies with several different types of antioxidants have been reported. The most comprehensive ones were performed by our (131), the Valentine (225), the Gatti (255), and the Dicker (77) groups. With radioprotection of zebrafish embryos (77), M40403 was protective at 100 mg/kg, as was fullerene and amifostine, whereas Mn porphyrin assured the same degree of survival of radiated zebrafish embryos at a 50-fold lower dose of 2.5 mg/kg (174). With radioprotection of ataxia telangiectasia cells (255), M40403 was of no efficacy, whereas Mn salen compounds were slightly protective. Only a lipophilic porphyrin, MnTnHex-2-PyP^{5+} (but not hydrophilic analogue MnTE-2-PyP^{5+} and none of the other Mn porphyrins used) was of appreciable efficacy. With aerobic growth of SOD-deficient *E. coli* and *S. cerevisiae* lacking cytosolic SOD (225) besides mM Mn, only Mn porphyrins, MnTE-2-PyP^{5+} and MnTM-2-PyP^{5+} (and not Mn salen EUK-8 and Mn cyclic polyamine M40403 at the μM concentrations studied) were efficacious. With MnSOD knockout yeast *C. neoformans* (131), only the Mn salen, EUK-8, was protective, but neither of several Mn porphyrins (cationic and anionic), nor Tempol and $MnCl_2$; the data suggest that Mn salen transports Mn into mitochondria (131). Doctrow *et al.* (94) compared anionic porphyrin $MnTBAP^{3-}$ with EUK compounds, M40403, and a combination of acetyl-L-carnitine + lipoic acid in the survival of $MnSOD^{-/-}$ mice; only EUK-207 and EUK-189 were efficacious. (94).

The data clearly indicate that much is still to be understood; comparative studies are highly desirable, as is the use of $MnCl_2$ as a control for Mn-based SOD mimics. Only a few studies compared Mn with Fe porphyrins (316). The detailed comparative study of Fe *versus* Mn *versus* Cu porphyrins in mammalian models of oxidative-stress injuries have never been conducted and may be insightful to fully appreciate the impact of metalloporphyrins on $^{\cdot}OH$ radical production. Still, whenever possible, particularly for therapeutic purposes, the use of Mn porphyrins is a safer approach.

X. Conclusions

A number of different types of synthetic antioxidants with different degrees of SOD-like activities have been explored as therapeutics. Although still unusual in clinical settings, metal complexes bring promising perspectives that have not been fully explored in animal and human trials. Among metal complexes, metalloporphyrins may be advantageous over other types of compounds because of their high stability (which assures the integrity of the redoxable metal active site), extreme potency, unlimited possibilities of structural modifications to modulate *by design* their *in vivo* efficacy, bioavailability, toxicity, and unlimited shelf-life. Needless to say, nature uses metalloporphyrins as life-building blocks. Because of the lack of Fenton-related chemistry, Mn may be a preferred metal in porphyrin complexes. Comparative studies on the several classes of antioxidants in various *in vitro* and *in vivo* models are still very much limited; such studies are, however, highly desirable to allow a full comprehension of the potential of one compound over another in any given model of injury or disease. Finally, a thorough chemical characterization of the compounds, which is essential for the evaluation of their identity and purity, is unfortunately often missing; the purity of the SOD mimics, regardless of their source, should always be confirmed by several methods, as it is critically important for the assessment of their *in vivo* efficacy and the "healthy" development of the overall antioxidant and free radical chemistry, biology, and medicine fields. The combination of synthetic antioxidants with natural antioxidants for enhanced therapy has already been used and deserves further attention.

The nonspecificity of SOD mimics (which may also scavenge peroxynitrite and other ROS/RNS species) may be to their advantage in clinics when inflammatory and immune responses would lead to the production of diverse reactive species. The disadvantage is that mechanistic studies may be complicated, and different controls or the appropriate choice of models/experimental designs would be essential to allow unambiguous conclusions.

The overall in *vitro*/*in vivo* efficacy of any SOD mimic represents a balance between the intrinsic $O_2^{\cdot -}$ diproportionation ability (as given by the k_{cat} values) and all factors

affecting the compound bioavailability, such as lipophilicity, tissue/cell uptake, subcellular distribution, and pharmacokinetics. A great deal of effort has been exerted to understand such balance in a systematic manner, at least within the class of porphyrin-based mimics. The chemical integrity of the mimic under biologic concentrations and conditions is also of utmost relevance for the mechanistic studies, as the *in vivo* effect of the so-called mimic may arise from a facilitated Mn transport and its release into the cell instead. Such effects have been well characterized within the porphyrin system (and is dependent upon the porphyrin ligand design); the situation remains less clear with the other systems.

It is worth noting that most of the so-called antioxidant therapeutics (*e.g.*, porphyrins, salens, nitroxides, vitamins) can also function as prooxidants just as can most of the endogenous antioxidants themselves, given their ability to easily donate and accept electrons in biologic systems. Under certain circumstances, this prooxidant mechanism may be therapeutically favorable by leading to the oxidation of relevant biologic molecules/targets. The anticancer effect of Mn porphyrin and MnSOD overexpression through H_2O_2 production has been reported. Also, the suppression of NF-κB activation was suggested to occur through oxidation of p50 cysteine in the nucleus. Such reports add to the complexity of *in vivo* systems, and makes future research on redoxable compounds, either endogenous or exogenous ones, challenging and motivating.

Acknowledgments

We thank Irwin Fridovich for all the knowledge we obtained in free radical biology and medicine and for all the help and guidance in developing potent SOD mimics. We are in debt to Peter Hambright for a motivating and enlightening decade-long collaboration. His expertise in water-soluble porphyrins was invaluable to us in early 1990s when we were still newcomers. We are also grateful to Ludmil Benov for his contribution with *E. coli* studies to the development of SOD mimics. We thank Rafael Radi and Gerardo Ferrer-Sueta, who pointed out to us in 1998 that the so-called "specific" SOD mimics may reduce peroxynitrite *in vivo*; the enthusiastic and motivating collaboration that followed helped us to attain the objectivity in understanding the complexity of the *in vivo* effects of MnP. We also are grateful to all the researchers who performed *in vivo* experiments and whose exciting data keep us going and improving the development of porphyrins. A few individuals with their scientific integrity contributed to our research in a very special way; a prominent place is held by Daret St. Clair. The continuous support from our colleagues at Duke University, Mark Dewhirst, Zeljko Vujaskovic, David Warner, Huaxin Sheng, and Christopher Lascola is greatly appreciated. We also acknowledge fruitful collaboration with Daniela Salvemini, Jon Piganelli, Hubert Tse, and Sidhartha Tan. We are thankful to the contribution of past and present postdoctoral fellows, Ivan Kos, Artak Tovmasyan, and Zrinka Rajić.

In writing this review, we acknowledge the financial help from the National Institutes for Allergy and Infectious Diseases [U19AI067798], Wallace H. Coulter Translational Partners Grant Program; Duke University's CTSA grant 1 UL 1 RR024128-01 from NCRR/NIH and NIH R01 DA024074. I.S. thanks NIH/NCI Duke Comprehensive Cancer Center Core Grant [5-P30-CA14236-29]. J.S.R. appreciates financial help from Universidade Federal da Paraíba.

References

1. Abashkin YG and Burt SK. (Salen)Mn^{III} compounds as nonpeptidyl mimics of catalase. Mechanism-based tuning of catalase activity: a theoretical study. *Inorg Chem* 44: 1425–1432, 2005.
2. Abidi P, Leers-Sucheta S, Cortez Y, Han J, and Azhar S. Evidence that age-related changes in p38 MAP kinase contribute the decreased steroid production by adrenocortical cells from old rats. *Aging Cell* 7: 168–178, 2008.
3. Adam O and Laufs U. Antioxidant effects of statins. *Arch Toxicol* 82: 885–892, 2008.
4. Agadjanian H, Ma J, Rentsendorj A, Vallupiralli V, Hwang JY, Mahammed A, Farkas DL, Gray HB, Gross Z, and Medina-Kauwe LK. Tumor detection and elimination by a targeted gallium corrole. *Proc Natl Acad Sci USA* 106: 6105–6110, 2009.
5. Agadjanian H, Weaver JJ, Mahammed A, Rentsendorj A, Bass S, Kim J, Dmochowski IJ, Margalit R, Gray HB, Gross Z, and Medina-Kauwe LK, Specific delivery of corroles to cells via noncovalent conjugates with viral proteins. *Pharm Res* 23: 367–377, 2006.
6. Aladag MA, Turkoz Y, Sahna E, Parlakpinar H, and Gul M. The attenuation of vasospasm by using a SOD mimetic after experimental subarachnoidal haemorrhage in rats. *Acta Neurochir* (Wien) 145: 673–676, 2003.
7. Alexandre J, Nicco C, Chereau C, Laurent A, Weill B, Goldwasser F, and Batteux F. Improvement of the therapeutic index of anticancer drugs by the superoxide dismutase mimic, mangafodipir. *J Natl Cancer Inst* 98: 236–244, 2006.
8. Ali SS, Hardt JI, Quick KL, Kim-Han JS, Erlanger BF, Huang T-T, Epstein CJ, and Dugan LL. A biologically effective fullerene (C_{60}) derivative with superoxide dismutase mimetic properties. *Free Radic Biol Med* 37: 1191–1202, 2004.
9. Al-Maghrebi M, Fridovich I, and Benov L. Manganese supplementation relieves the phenotypic deficits seen in superoxide-dismutase-null *Escherichia coli*. *Arch Biochem Biophys* 402: 104–109, 2002.
10. Amato RJ, Jac J, and Hernandez-McClain J. Motexafin gadolinium for the treatment of metastatic renal cell carcinoma: phase II study results. *Clin Genitourin Cancer* 6: 73–78, 2008.
11. Anderson I, Adinolfi C, Doctrow S, Huffman K, Joy KA, Malfroy B, Soden P, Rupniak HT, and Barnes JC. Oxidative signaling and inflammatory pathways in Alzheimer's disease. *Biochem Soc Symp* 141–149, 2001.
12. Andrievsky GV, Bruskov VI, Tykhomyrov AA, and Gudkov SV. Peculiarities of the antioxidant and radioprotective effects of hydrated C_{60} fullerene nanostuctures *in vitro* and *in vivo*. *Free Radic Biol Med* 47: 786–793, 2009.
13. Anjem A, Varghese S, and Imlay JA. Manganese import is a key element of the OxyR response to hydrogen peroxide in *Escherichia coli*. *Mol Microbiol* 72: 844–858, 2009.
14. Archibald FS and Fridovich I, The scavenging of superoxide radical by manganous complexes: In vitro. *Arch Biochem Biophys* 214: 452–463, 1982.
15. Archibald FS and Fridovich I. Manganese, superoxide dismutase, and oxygen tolerance in some lactic acid bacteria. *J Bacteriol* 145: 422–451, 1981.

16. Aronovitch Y, Godinger D, Israeli A, Krishna MC, Samuni A, and Goldstein S. Dual activity of nitroxides as pro- and antioxidants: catalysis of copper-mediated DNA breakage and H_2O_2 dismutation. *Free Radic Biol Med* 42: 1317–1325, 2007.
17. Arora M, Kumar A, Kaundal RK, and Sharma SS. Amelioration of neurological and biochemical deficits by peroxynitrite decomposition catalysts in experimental diabetic neuropathy. *Eur J Pharmacol* 596: 77–83, 2008.
18. Asayama S, Kawamura E, Nagaoka S, and Kawakami H. Design of manganese porphyrin modified with mitochondrial signal peptide for a new antioxidant. *Mol Pharm* 3: 468–470, 2006.
19. Aslan M, Cort A, and Yucel I. Oxidative and nitrative stress markers in glaucoma. *Free Radic Biol Med* 45: 367–376, 2008.
20. Aslan M, Ryan TM, Adler B, Townes TM, Parks DA, Thompson JA, Tousson A, Gladwin MT, Tarpey MM, Patel RP, Batinić-Haberle I, White CR, and Freeman BA, Oxygen radical inhibition of nitric-oxide dependent vascular function in sickle cell disease. *Proc Natl Acad Sci U S A* 98: 15215–15220, 2001.
21. Aston K, Rath N, Naik A, Slomczynska U, Schall OF, and Riley DP. Computer-aided design (CAD) of Mn(II) complexes: superoxide dismutase mimetics with catalytic activity exceeding the native enzyme. *Inorg Chem* 40: 1779–1789, 2001.
22. Aviezer D, Cotton S, David M, Segev A, Khaselev N, Galili N, Gross Z, and Yayon A. Porphyrin analogues as novel antagonists of fibroblast growth factor and vascular endothelial growth factor receptor binding that inhibit endothelial cell proliferation, tumor progression, and metastasis. *Cancer Res* 60: 2973–2980, 2000.
23. Aviv I and Gross Z. Corrole-based applications. *Chem Commun* 1987–1999, 2007.
24. Baker K, Bucay Marcus C, Huffman K, Malfroy B, and Doctrow S. Synthetic combined superoxide dismutase/catalase mimetics are protective as a delayed treatment in a rat stroke model: a key role for reactive oxygen species in ischemic brain injury. *J Pharmacol Exp Ther* 284: 215–221, 1998.
25. Barnese K, Gralla EB, Cabelli DE, and Valentine JS, Manganous phosphate acts as a superoxide dismutase. *J Am Chem Soc* 130: 4604–4606, 2008.
26. Barrette WC Jr, Sawyer DT, Free JA, and Asada K. Potentiometric titrations and oxidation-reduction potentials of several iron superoxide dismutases. *Biochemistry* 22: 624–627, 1983.
27. Bartesaghi S, Ferrer-Sueta G, Peluffo G, Valez V, Zhang H, Kalyanaraman B, and Radi R. Protein tyrosine nitration in hydrophilic and hydrophobic environments. *Amino Acids* 32: 501–515, 2007.
28. Batinić-Haberle I and Benov LT. An SOD mimic protects $NADP^+$-dependent isocitrate dehydrogenase against oxidative inactivation. *Free Radic Res* 42: 618–624, 2008.
29. Batinić-Haberle I, Benov L, Spasojević I, and Fridovich I. The *ortho* effect makes manganese (III) *meso*-tetrakis (*N*-methylpyridinium-2-yl)porphyrin (MnTM-2-PyP) a powerful and potentially useful superoxide dismutase mimic. *J Biol Chem* 273: 24521–24528, 1998.
30. Batinić-Haberle I, Spasojević I, Hambright P, Benov L, Crumbliss AL, and Fridovich I. The relationship between redox potentials, proton dissociation constants of pyrrolic nitrogens, and *in vitro* and *in vivo* superoxide dismutase activities of manganese(III) and iron(III) cationic and anionic porphyrins. *Inorg Chem* 38: 4011–4022, 1999.
31. Batinić-Haberle I, Cuzzocrea S, Rebouças JS, Ferrer-Sueta G, Emanuela Mazzon E, Di Paola R, Radi R, Spasojević I, Benov L, and Salvemini D. Pure MnTBAP selectively scavenges peroxynitrite over superoxide: comparison of pure and commercial MnTBAP samples to MnTE-2-PyP in two different models of oxidative stress injuries, SOD-specific *E. coli* model and carrageenan-induced pleurisy. *Free Radic Biol Med* 46: 192–201, 2009.
32. Batinic-Haberle I, Gauter-Fleckenstein B, Kos I, Fleckenstein K, Spasojevic I, and Vujaskovic Z. MnTnHex-2-PyP^{5+} structural characteristics, lipophilicity and bioavailability contribute to its high potency in pulmonary radioprotection. 55th Radiation Research Society Meeting, Savannah 2009, PS6.40 (Book of abstracts), page 143.
33. Batinić-Haberle I, Liochev S, Spasojević I, and Fridovich I. A potent superoxide dismutase mimic: *β*-octabromo-*meso*-tetrakis-(*N*-methylpyridinium-4-yl) porphyrin. *Arch Biochem Biophys* 343: 225–233, 1997.
34. Batinić-Haberle I, Ndengele MM, Cuzzocrea S, Rebouças JS, Masini E, Spasojević I, and Salvemini D. Lipophilicity is a critical parameter that dominates the efficacy of metalloporphyrins in blocking morphine tolerance through peroxynitrite-mediated pathways. *Free Radic Biol Med* 46: 212–219, 2009.
35. Batinić-Haberle I, Spasojević I, and Fridovich I. Tetrahydrobiopterin rapidly reduces the SOD mimic Mn(III) ortho-tetrakis(*N*-ethylpyridinium-2-yl)porphyrin. *Free Radic Biol Med* 37: 367–374, 2004.
36. Batinić-Haberle I, Spasojević I, Stevens RD, Bondurant B, Okado-Matsumoto A, Fridovich I, Vujasković Z, and Dewhirst MW. New PEG-ylated Mn(III) porphyrins approaching catalytic activity of SOD enzyme. *Dalton Trans* 617–624, 2006.
37. Batinić-Haberle I, Spasojević I, Stevens RD, Hambright P, and Fridovich I. Manganese(III) *meso* tetrakis *ortho N*-alkylpyridylporphyrins: synthesis, characterization and catalysis of $O_2^{\cdot-}$ dismutation. *J Chem Soc Dalton Trans* 2689–2696, 2002.
38. Batinić-Haberle I, Spasojević I, Stevens RD, Hambright P, Neta P, Okado-Matsumoto A, and Fridovich I. New class of potent catalysts of $O_2^{\cdot-}$ dismutation. Mn(III) methoxyethylpyridyl- and methoxyethylimidazolylporphyrins. *J Chem Soc Dalton Trans* 1696–1702, 2004.
39. Batinic-Haberle I, Spasojevic I, Tse HM, Tovmasyan A, St. Clair DK, Vujaskovic Z, Dewhirst MW, and Piganelli JD. Design of Mn porphyrins for treating oxidative stress injuries and their redox-based regulation of cellular transcriptional activities. *Amino Acids* 2010 (in press).
40. Baudry M, Etinne S, Bruce A, Palucki M, Jacobsen E, and Malfroy B. Salen-maganese complexes are superoxide dismutase mimics. *Biochem Biophys Chem Commun* 192: 964–988, 1993.
41. Bayne AC and Sohal RS. Effects of superoxide dismutase/catalase mimetics on life span and oxidative stress resistance in the housefly, *Musca domestica*. *Free Radic Biol Med* 32: 1229–1234, 2002.
42. Benatar M. Lost in translation: treatment trials in the SOD1 mouse and in human ALS. *Neurobiol Dis* 26: 1–13, 2007.
43. Bendix J, Dmochowski IJ, Gray HB, Mahammed A, Simkhovich L, and Gross Z. Structural electrochemical and

photophysical properties of gallium(III) 5,10,15-tris(pentafluorophenyl)corrole. *Angew Chem Int Ed* 39: 4048–4051, 2000.
44. Benov L and Batinić-Haberle I. A manganese porphyrin SOD mimic suppresses oxidative stress and extends the life span of streptozotocin-diabetic rats. *Free Radic Res* 38: 81–88, 2005.
45. Bianchi C, Wakiyama H, Faro R, Khan T, McCully JD, Levitsky S, Szabó C, and Sellke FW. A novel peroxynitrite decomposer catalyst (FP-15) reduces myocardial infarct size in an in vivo peroxynitrite decomposer and acute ischemia-reperfusion in pigs. *Ann Thorac Surg* 74: 1201–1207, 2002.
46. Boillee S, Velde VC, and Cleveland DW. ALS: a disease of motor neurons and their nonneuronal neighbors. *Neuron* 52: 39–59, 2006.
47. Bonello S, Zahringer C, BelAiba RS, Djordjevic T, Hesss J, Michiels C, Kietzmann T, and Gorlach A. Reactive oxygen species activate the HIF-1a promoter via a functional NFκB site. *Arterioscl Thromb Vasc Biol* 27: 755–761, 2007.
48. Bottino R, Balamurugan AN, Bertera S, Pietropaolo M, Trucco M, and Piganelli JD. Preservation of human islet cell functional mass by anti-oxidative action of a novel SOD mimic compound. *Diabetes* 51: 2561–1567, 2002.
49. Bottino R, Balamurugan AN, Tse H, Thirunavukkarasu C, Ge X, Profozich J, Milton M, Ziegenfuss A, Trucco M, and Piganelli JD. Response of human islets to isolation stress and the effect of antioxidant treatment. *Diabetes* 53: 2559–2568, 2004.
50. Boucher LJ. Manganese Schiff's base complexes-II: synthesis and spectroscopy of chloro-complexes of some derivatives of (salicylaldehydeethylenediimato) manganese(III). *J Inorg Nucl Chem* 36: 531–536, 1974.
51. Brazier MW, Doctrow SR, Masters CL, and Collins SJ. A manganese-superoxide dismutase/catalase mimetic extends survival in a mouse model of human prion disease. *Free Radic Biol Med* 45: 184–192, 2008.
52. Brown NS and Bicknell R. Hypoxia and oxidative stress in breast cancer: oxidative stress: its effects on the growth, metastatic potential and response to therapy of breast cancer. *Breast Cancer Res* 3: 323–327, 2001.
53. Buchler JW, Kokisch W, Smith PD. Cis, trans, and metal effects in transition metal porphyrins. *Struct Bond* 34: 79–134, 1978.
54. Carnieri N, Harriman A, and Porter G. Photochemistry of manganese porphyrins, part 6: oxidation-reduction equilibria of manganese(III) porphyrins in aqueous solution. *J Chem Soc Dalton Trans* 931–938, 1982.
55. Carreras MC and Poderoso JJ. Mitochondrial nitric oxide in the signaling of cell integrated responses. *Am J Physiol Cell Physiol* 292: C1569–C1580, 2006.
56. Castello PR, Drechsel DA, Day BJ, and Patel M. Inhibition of mitochondrial hydrogen peroxide production by lipophilic metalloporphyrins. *J Pharmacol Exp Ther* 324: 970–976, 2008.
57. Cernanec JM, Weinberg BJ, Batinić-Haberle I, Guilak F, and Fermor B. Influence of oxygen tension on interleukin-1-induced peroxynitrite formation and matrix turnover in articular cartilage. *J Rheumatol* 34: 401–407, 2007.
58. Chang LY and Crapo JD. Inhibition of airway inflammation and hyperreactivity by an antioxidant mimetic. *Free Radic Biol Med* 33: 379–386, 2002.
59. Chang LY, Subramanian M, Yoder BA, Day BJ, Ellison MC, Sunday ME, and Crapo JD. A catalytic antioxidant attenuates alveolar structural remodeling in bronchopulmonary dysplasia. *Am J Respir Crit Care Med* 167: 57–64, 2003.
60. Chen J, Patil S, Seal S, and McGinnis JF. Rare earth nanoparticles prevent retinal degeneration induced by intracellular peroxides. *Nat Nanotechnol* 1: 142–150, 2006.
61. Christen Y. Oxidative stress and Alzheimer disease. *Am J Clin Nutr* 71: 621S–629S, 2000.
62. Clausen A, Doctrow S, and Baudry M. Prevention of cognitive deficits and brain oxidative stress with superoxide dismutase/catalase mimetics in aged mice. *Neurobiol Aging* 31: 425–433, 2010.
63. Colon J, Herrera L, Smith J, Patil S, Komanski C, Kupelian P, Seal S, Jenkins DW, and Baker CH. Protection from radiation-induced pneumonitis using cerium oxide nanoparticles. *Nanomedicine* 5: 225–231, 2009.
64. Cremades N, Velazquez-Campoy A, Martínez-Júlvez M, Neira JL, Perez-Dorado I, Hermoso Dominguez JA, Jimenez P, Lanas A, Hoffman PS, and Sancho J. Discovery of specific flavodoxin inhibitors as potential therapeutic agents against *Helicobacter pylori* infection. *ACS Chem Biol* 4: 928–938, 2009.
65. Crimi E, Ignarro LJ, and Napoli C. Microcirculation and oxidative stress. *Free Radic Res* 41: 1364–1375, 2007.
66. Crow J. Catalytic antioxidants to treat amyotrophic lateral sclerosis, *Expert Opin Invest Drugs* 15: 1383–1392, 2006.
67. Crow JP, Calinasan NY, Chen J, Hill JL, and Beal MF. Manganese porphyrin given at symptom onset markedly extends survival of ALS mice. *Ann Neurol* 58: 258–265, 2005.
68. Crow JP. Administration of Mn porphyrin and Mn texaphyrin at symptom onset extends survival of ALS mice. In: *Medicinal Inorganic Chemistry*, edited by Sessler JS, Doctrow SR, McMurray TJ, Lippard SJ. Washington, DC: American Chemical Society, 2005, pp. 295–318.
69. Crow JP. Peroxynitrite scavenging by metalloporphyrins and thiolates. *Free Radic Biol Med* 28: 1487–1494, 2000.
70. Csiszar A, Wang M, Lakatta EG, and Ungvari ZI. Inflammation and endothelial dysfunction during aging: role of NF-κB. *J Appl Physiol* 105: 1333–1341, 2008.
71. Csont T, Viappiani S, Sawicka J, Slee S, Altarejos JY, Batinić-Haberle I, and Schulz R. The involvement of superoxide and iNOS-derived NO in cardiac dysfunction induced by pro-inflammatory cytokines. *J Mol Cell Cardiol* 39: 833–840, 2005.
72. Culotta VC, Yang M, and Hall MD. Manganese transport and trafficking: lessons learned from *Saccharomyces cerevisiae*. *Eukaryot Cell* 4: 1159–1165, 2005.
73. Cuzzocrea S, Costantino G, Mazzon E, Zingarelli B, De Sarro A, and Caputi AP. Protective effects of Mn(III)tetrakis (4-benzoic acid) porphyrin (MnTBAP), a superoxide dismutase mimetic, in paw oedema induced by carrageenan in the rat. *Biochem Pharmacol* 58: 171–176, 1999.
74. Cuzzocrea S, Mazzon D, Dugo L, Caputi AP, Riley DP, and Salvemini D. Protective effects of M40403, a superoxide dismutase mimetic in a rodent model of colitis. *Eur J Pharmacol* 432: 79–89, 2001.
75. Cuzzocrea S, Pisano B, Dugo L, Ianaro A, Ndengele M, and Salvemini D. Superoxide-related signaling cascade mediates nuclear factor-κB activation in acute inflammation. *Antioxid Redox Signal* 6: 699–704, 2004.
76. Cuzzocrea S, Zingarelli B, Constantino G, and Caputi AP. Beneficial effects of Mn(III) tetrakis (4-benzoic acid) porphyrin (MnTBAP), a superoxide dismutase mimetic, in a

carrageenan-induced pleurisy. *Free Radic Biol Med* 26: 25–33, 1999.
77. Daroczi B, Kari G, Zengin AY, Chinnaiyan P, Batinić-Haberle I, Rodeck U, and Dicker AP. Radioprotective effects of two superoxide dismutase (SOD) mimetics and the nanoparticle DF-1 in a vertebrate zebrafish model (abstract). 48th ASTRO, Annual Meeting of the American Society for Radiation Oncology, 2006.
78. Das M, Patil S, Bhargava N, Kang JF, Reidel LM, Seal S, and Hickman JJ. Auto-catalytic ceria nanoparticles offer protection to adult rat spinal cord neurons. *Biomaterials* 28: 1918–1925, 2007.
79. Day BJ and Kariya C. A novel class of cytochrome P450 reductase redox cycling: cationic manganoporphyrins. *Toxicol Sci* 85: 713–719, 2005.
80. Day BJ, Batinić-Haberle I, and Crapo JD. Metalloporphyrins are potent inhibitors of lipid peroxidation. *Free Radic Biol Med* 26: 730–736, 1999.
81. Day BJ, Shawen S, Liochev SI, and Crapo JD. A metalloporphyrin superoxide dismutase mimetic protects against paraquat-induced endothelial cell injury, in vitro. *J Pharmacol Exp Ther* 275: 1227–1232, 1995.
82. Day BJ. Antioxidants as potential therapeutics for lung fibrosis. *Antioxid Redox Signal* 10: 355–370, 2008.
83. Day BJ. Catalase and glutathione peroxidase mimics. *Biochem Pharmacol* 77: 285–296, 2009.
84. Decraene D, Smaers K, Gan D, Mammone T, Matsui M, Maes D, Declercq L, and Garmyn M. A synthetic superoxide dismutase/catalase mimetic (EUK-134) inhibits membrane-damage-induced activation of mitogen-activated protein kinase pathways and reduces p53 accumulation in ultraviolet B-exposed primary human keratinocytes. *J Invest Dermatol* 122: 484–491, 2004.
85. DeFreitas-Silva G, Rebouças JS, Spasojević I, Benov L, Idemori YM, and Batinić-Haberle I. SOD-like activity of Mn(II) β-octabromo-meso-tetrakis(*N*-methylpyridinium-3-yl)porphyrin equals that of the enzyme itself. *Arch Biochem Biophys* 477: 105–112, 2008.
86. Dennis KE, Aschner JL, Milatovic D, Schmidt JW, Aschner M, Kaplowitz MR, Zhang Y, and Fike CD. NADPH oxidases and reactive oxygen species at different stages of chronic hypoxia-induced pulmonary hypertension in newborn piglets. *Am J Physiol Lung Cell Mol Physiol* 297: L596–L607, 2009.
87. Desideri A, Falconi M, Parisi V, Morante S, and Rotilio G. Is the activity-linked electrostatic gradient of bovine Cu, Zn superoxide dismutases conserved in homologous enzymes irrespective of the number and distribution of charges? *Free Radic Biol Med* 5: 313–317, 1988.
88. Dessolin J, Schuler M, Quinart A, De Giorgi F, Ghosez L, and Ichas F. Selective targeting of synthetic antioxidants to mitochondria; towards a mitochondrial medicine for neurodegenerative diseases? *Eur J Pharmacol* 447: 155–161, 2002.
89. Dewhirst M, Cao Y, and Moeller B. Cycling hypoxia and free radicals regulate angiogenesis and radiotherapy response. *Nat Rev Cancer* 8: 425–437, 2008.
90. Dhanasekaran A, Kotamraju S, Karunakaran C, Kalivendi SV, Thomas S, Joseph J, and Kalyanaraman B. Mitochondria superoxide dismutase mimetic inhibits peroxide-induced oxidative damage and apoptosis: role of mitochondrial superoxide. *Free Radic Biol Med* 39: 567–583, 2005.
91. Dhar A, Kaundal RK, and Sharma SS. Neuroprotective effects of FeTMPyP: a peroxynitrite decomposition catalyst in global cerebral ischemia model in gerbils. *Pharmacol Res* 54: 311–316, 2006.
92. Dikalov S, Losik T, and Arbisr JL. Honokiol is a potent scavenger of superoxide and peroxyl radicals. *Biochem Pharm* 76: 589–596, 2008.
93. Doctrow S, Huffman K, Bucay-Marcus C, Tocco G, Malfroy E, Adinolfi CA, Kruk H, Baker K, Lazarowych N, Mascarenhas J, and Malfroy B. Salen-manganese complexes as catalytic scavengers of hydrogen peroxide and cytoprotective agents: structure-activity relationship. *J Med Chem* 45: 4549–4558, 2002.
94. Doctrow SR, Baudry M, Huffman K, Malfroy B, and Melov S. Salen-manganese complexes: multifunctional catalytic antioxidants protective in models for neurodegenerative diseases of aging in *Medicinal Inorganic Chemistry*. In: *American Chemical Society Symposium Series* 903, edited by Sessler JS, Doctrow SR, McMurray TJ, Lippard SJ. ACS and Oxford University Press, 2005, pp. 319–347.
95. Doyle T, Bryant L, Batinić-Haberle I, Little J, Cuzzocrea S, Masini E, Spasojević I, and Salvemini D. Supraspinal inactivation of mitochondrial superoxide dismutase is a source of peroxynitrite in the development of morphine antinociceptive tolerance. *Neuroscience* 164: 702–710, 2009.
96. Du W, Adam Z, Rani R, Zhang X, and Pang Q. Oxidative stress in Fanconi anemia hematopoiesis and disease progression. *Antioxid Redox Signal* 10: 1909–1921, 2008.
97. Dugan LL, Lovett EG, Quick KL, Lotharius J, Lin TT, and O'Malley KL. Fullerene-based antioxidants and neurodegenerative disorders. *Parkinson Relat Disord* 7: 243–246, 2001.
98. Dugan LL, Turetsky TM, Du C, Lobner D, Wheeler M, Almli CR, Shen CK, Luh TY, Choi DW, Lin TS, and Choi DW. Carboxyfullerenes as neuroprotective agents. *Proc Natl Acad Sci U S A* 94: 9434–9439, 1997.
99. Eckshtain M, Zilbermann I, Mahammed A, Saltsman A, Okun Z, Maimon E, Cohen H, Meyerstein D, and Gross Z. Superoxide dismutase activity of corrole metal complexes. *Dalton Trans* 7879–7882, 2009.
100. Ellerby RM, Cabelli DE, Graden JA, and Valentine JS. Copper-zinc superoxide dismutase: why not pH-dependent? *J Am Chem Soc* 118: 6556–6561, 1996.
101. Epperly MW, Melendez JA, Zhang X, Nie S, Pearce L, Peterson J, Franicola D, Dixon T, Greenberger BA, Komanduri P, Wang H, and Greenberger JS. Mitochondrial targeting of a catalase transgene product by plasmid liposomes increases radioresistance in vitro and in vivo. *Radiat Res* 171: 588–595, 2009.
102. Eric D, Coulter ED, Emerson JP, Kurtz DM Jr, and Cabelli DE. Superoxide reactivity of rubredoxin oxidoreductase (desulfoferrodoxin) from *Desulfovibrio vulgaris*: a pulse radiolysis study. *J Am Chem Soc* 122: 11555–11556, 2000.
103. Failli P, Bani D, Bencini A, Cantore M, Di Cesare Mannelli L, Ghekardini C, Giorgi C, Innocenti M, Rugi F, Spepi A, Udisti R, and Valtancoli B. A novel manganese complex effective as superoxide anion scavenger and therapeutic agent against cell and tissue oxidative injury. *J Med Chem* 52: 7273–7283, 2009.
104. Faraggi M, Peretz P, and Weinraub D. Chemical properties of water-soluble porphyrins: 4. the reduction of a "picket-fence-like" iron(III) complex with superoxide oxygen couple. *Int J Radiat Biol* 49: 951–968, 1986.
105. Faulkner KM, Liochev SI, and Fridovich I. Stable Mn(III) porphyrins mimic superoxide dismutase in vitro and substitute for it *in vivo*. *J Biol Chem* 269: 23471–23476, 1994.

106. Ferrer-Sueta G, and Radi R. Chemical biology of peroxynitrite: kinetics, diffusion, and radicals. *ACS Chem Biol* 4: 161–177; 2009.
107. Ferrer-Sueta G, Batinić-Haberle I, Spasojević I, Fridovich I, and Radi R. Catalytic scavenging of peroxynitrite by isomeric Mn(III) *N*-methylpyridylporphyrins in the presence of reductants. *Chem Res Toxicol* 12: 442–449, 1999.
108. Ferrer-Sueta G, Hannibal L, Batinić-Haberle I, and Radi R. Reduction of manganese porphyrins by flavoenzymes and submitochondrial particles and the catalytic redox cycle of peroxynitrite. *Free Radic Biol Med* 41: 503–512, 2006.
109. Ferrer-Sueta G, Quijano C, Alvarez B, and Radi R. Reactions of manganese porphyrins and manganese-superoxide dismutase with peroxynitrite. *Methods Enzymol* 349: 23–37, 2002.
110. Ferrer-Sueta G, Vitturi D, Batinić-Haberle I, Fridovich I, Goldstein S, Czapski G, and Radi, R. Reactions of manganese porphyrins with peroxynitrite and carbonate radical anion. *J Biol Chem* 278: 27432–27438; 2003.
111. Figueroa-Romero C, Sadidi M, and Feldman EL. Mechanism of disease: the oxidative stress theory of diabetic neuropathy. *Rev Endocr Metab Disord* 9: 301–314, 2008.
112. Finsterer J. Is atherosclerosis a mitochondrial disorder? *Vasa* 36: 229–240, 2008.
113. Fiorillo C, Becatti M, Pensalfini a, Cecchi C, Lanzilao L, Donzelli G, Nassi N, Giannini L, Borchi E, and Nassi P. Curcumin protects cardiac cells against ischemia-reperfusion injury: effects on oxidative stress, NF-κB, and JNK pathways. *Free Radic Biol Med* 45: 839–846, 2008.
114. Fisher AEO, Hague TA, Clarke CL, and Naughton DP. Catalytic superoxide scavenging by metal complexes of the calcium chelator EGTA and contrast agent EHPG. *Biochem Biophys Chem Commun* 323: 163–167, 2004.
115. Fisher AEO and Naughton DP. Metal ion chelating peptides with superoxide dismutase activity. *Biomed Pharmacother* 59: 158–162, 2005.
116. Floyd RA, Kopke RD, Choi CH, Foster SB, Doblas S, and Towner RA. Nitrones as therapeutics. *Free Radic Biol Med* 45: 1361–1374, 2008.
117. Floyd RA. Nitrones as therapeutics in age-related diseases. *Aging Cell* 5: 51–57; 2006.
118. Frank C, Sink C, Mynatt L, Rogers R, and Rappazzo A. Surviving the "valley of death": a comparative analysis, *Technol Transfer* Spring-Summer: 61–69, 1996.
119. Fridovich I. An overview of oxyradicals in medical biology. *Adv Mol Cell Biol* 25: 1–14, 1998.
120. Fridovich I. Oxygen toxicity: a radical explanation. *J Exp Biol* 201: 1203–1209, 1998.
121. Fried LE and Arbiser JL. Honokiol, a multifunctional antiangiogenic and antitumor agent. *Antiox Redox Signal* 11: 1139–1148, 2009.
122. Fukui H and Moraes CT. The mitochondrial impairment, oxidative stress and neurodegeneration connection: reality or just an attractive hypothesis. *Trends Neurosci* 31: 251–256, 2007.
123. Gauter-Fleckenstein B, Fleckenstein K, Owzar K, Jian C, Batinić-Haberle I, and Vujasković Z. Comparison of two Mn porphyrin-based mimics of superoxide-dismutase (SOD) in pulmonary radioprotection. *Free Radic Biol Med* 44: 982–989, 2008.
124. Gauter-Fleckenstein B, Fleckenstein K, Owzar K, Jiang C, Rebouças JS, Batinić-Haberle I, and Vujasković Z. Early and late administration of antioxidant mimic MnTE-2-PyP^{5+} in mitigation and treatment of radiation-induced lung damage. *Free Radic Biol Med*, 2010 (doi: 10.1016/j .freeradbiomed.2010.01.020).
125. Gauuan PJF, Trova MP, Gregor-Boros L, Bocckino SB, Crapo JD, and Day BJ. Superoxide dismutase mimetics: structure-activity relationship study of MnTBAP analogues. *Bioorg Med Chem* 10: 3013–3021, 2002.
126. Genovese T, Mazzon E, Esposito E, Di Paola R, Murthy K, Neville L, Bramanti P, and Cuzzocrea S. Effects of a metalloporphyrinic peroxynitrite decomposition catalyst, ww-85, in a mouse model of spinal cord injury. *Free Radic Res* 43: 631–645, 2009.
127. Gershman Z, Goldberg I, and Gross Z. DNA binding and catalytic properties of positively charged corroles. *Angew Chem Int Ed* 46: 4320–4324, 2007.
128. Getzoff ED, Tainer JA, Weiner PK, Kollman PA, Richardson JS, and Richardson DC, Electrostatic recognition between superoxide and copper, zinc superoxide dismutase. *Nature* 306: 287–290, 1983.
129. Gharbi N, Pressac M, Hadchoule M, Szwarc h, Wilson SR, and Moussa F. [60]Fullerene is a powerful antioxidant in vivo with no acute or subacute toxicity. *Nano Lett* 5: 2578–2585, 2005.
130. Giblin GMP, Boc PC, Campbell IB, Nacock AP, Roomans S, Mills GI, Molloy C, Tranter GE, Walker AL, Doctrow SR, Huffman K, and Malfroy B. 6,6′-Bis(2-hydroxyphenyl)-2,2′-bipyridine manganese(III) complexes: a novel series of superoxide dismutase and catalase mimetics. *Bioorg Med Chem Lett* 11: 1367–1370, 2001.
131. Giles SS, Batinić-Haberle I, Perfect JR, and Cox GM. *Cryptococcus neoformans* mitochondrial superoxide dismutase: an essential link between antioxidant function and high temperature growth. *Eukariot Cell* 4: 46–54, 2005.
132. Gloire G and Piette J. Redox regulation of nuclear post-translational; modifications during NF-κB activation. *Antioxid Redox Signal* 11: 2209–2222, 2009.
133. Golden TR and Patel M. Catalytic antioxidants and neurodegeneration. *Antioxid Redox Signal* 11: 555–569, 2009.
134. Goldstein S and Samuni A. Kinetics and mechanism of peroxyl radical reactions with nitroxides. *J Phys Chem A* 111: 1066–1072, 2007.
135. Goldstein S, Czapski G, and Heller A. Osmium tetraoxide, used in the treatment of arthritic joints, is a fast mimic of superoxide dismutase. *Free Radic Biol Med* 38: 839–45, 2005.
136. Goldstein S, Fridovich I, and Czapski G. Kinetic properties of Cu, Zn-superoxide dismutase as a function of metal content: order restored. *Free Radic Biol Med* 41: 937–941, 2006.
137. Goldstein S, Mereney G, Russo A, and Samuni A. The role of oxoammonium cation in the SOD-like activity of cyclic nitroxides. *J Am Chem Soc* 125: 789–795, 2003.
138. Goldstein S, Samuni A, and Merenyi G. Kinetics of the reaction between nitroxide and thiyl radicals: nitroxides as antioxidants in the presence of thiols. *J Phys Chem A* 112: 8600–8605, 2008.
139. Goldstein S, Samuni A, and Merenyi G. Reactions of nitric oxide, peroxynitrite and carbonate radicals with nitroxides and their corresponding oxoammonium cations. *Chem Res Toxicol* 17: 250–257, 2004.
140. Goldstein S, Samuni A, Hideg K, and Merenyi G. Structure-activity relationship of cyclic nitroxides as SOD mimics and scavengers of nitrogen dioxide and carbonate radicals. *J Phys Chem A* 110: 3679–3685, 2006.
141. Gonzalez PK, Zhuang J, Doctrow SR, Malfroy B, Benson PF, Menconi MJ, and Fink MP. EUK-8 a synthetic super-

oxide dismutase and catalase mimetic ameliorates acute lung injury in endotoxemic swine. *J Pharmacol Exp Ther* 275: 798–806, 2002.
142. Gridley DS, Makinde AY, Luo X, Rizvi A, Crapo JD, Dewhirst MW, Moeller BJ, Pearlstein RD, and Slater JM. Radiation and a metalloporphyrin radioprotectant in a mouse prostate tumor model. *Anticancer Res* 27: 3101–3109, 2007.
143. Gross Z, Galili N, and Saltsman I. The first direct synthesis of corroles from pyrrole. *Angew Chem Int Ed* 38: 1427–1429, 1999.
144. Haber A, Mahammed A, Fuhrman B, Volkova N, Coleman R, Hayek T, Aviram M, and Gross Z. Amphiphilic/bipolar metallocorroles that catalyze the decomposition of reactive oxygen and nitrogen species, rescue lipoproteins from oxidative damage, and attenuate atherosclerosis. *Angew Chem Int Ed* 47: 7896–7900, 2008.
145. Halliwell B and Gutteridge JMC. *Free Radical Biology and Medicine* 4th ed. Oxford: Oxford University Press, 2007.
146. Halliwell B. Are polyphenols antioxidants or pro-oxidants? What do we learn from cell culture and in vivo studies. *Arch Biochem Biophys* 476: 107–112, 2008.
147. Hahn SM, DeLuca AM, Coffin D, Krishna CM, and Mitchell JB. *In vivo* radioprotection and effects on blood pressure of the stable free radical nitroxides. *Int J Radiat Oncol Biol Phys* 42: 839–842, 1998.
148. Hashemy SI, Ungerstedt JS, Avval FZ, and Holmgren A. Motexafin gadolinium, a tumor-selective drug targeting thioredoxin reductase and ribonucleotide reductase, *J Biol Chem* 281: 10691–10697, 2006.
149. Heckert EG, Karakoti AS, Seal S, and Self WT. The role of cerium redox state in the SOD mimetic activity of nanoceria. *Biomaterials* 29: 2705–2709, 2008.
150. Heckert EG, Seal S, and Self WT. Fenton-like reaction catalyzed by rare earth inner transition metal cerium. *Environ Sci Technol* 42: 5014–5019, 2008.
151. Hidalfo C and Donoso P. Crosstalk between calcium and redox signaling: from molecular mechanisms to health implications. *Antioxid Redox Signal* 10: 1275–1312, 2008.
152. Holley AK, Dhar SK, Xu Y, and St Clair DK. Manganese superoxide dismutase: beyond life and death. *Amino Acids*, 2010 (in press).
153. Hoshino T, Okamoto, M, Takei S, Sakazaki Y, Iwanaga T, and Aizawa H. Redox regulated mechanisms in asthma. *Antioxid Redox Signal* 10: 769–783, 2008.
154. Hoshino Y and Mishima M. Redox-based therapeutics for lung disease. *Antioxid Redox Signal* 10: 701–704, 2008.
155. Hoye AT, Davoren JR, and Wipf P. Targeting mitochondria. *Acc Chem Res* 41: 87–97, 2008.
156. Hyodo F, Soule BP, Matsumoto K-I, Matusmoto S, Cook JA, Hyodo E, Sowers A, Krishna MC, and Mitchell JB. Assessment of tissue redox status using metabolic responsive contrast agents and magnetic resonance imaging. *J Pharm Pharmacol* 60: 1049–1060, 2008.
157. Ilan Y, Rabani J, Fridovich I, and Pasternack RF. Superoxide dismuting activity of iron porphyrin. *Inorg Nucl Chem Lett* 17: 93–96, 1981.
158. Jackson IL, Chen L, Batinić-Haberle I, and Vujasković Z. Superoxide dismutase mimetic reduces hypoxia-induced $O_2^{\cdot-}$, TGF-β, and VEGF production by macrophages. *Free Radic Res* 41: 8–14, 2007.
159. Jackson IL, Gaunter-Fleckenstein BM, Batinić-Haberle I, Poulton S, Zhao Y, Dewhirst MW, and Vujasković, Z. Hyperthermia enhances the anti-angiogenic effect of metalloporphyrin mimetic of superoxide dismutase. 24th Annual Meeting of the European Society for Hyperthermic Oncology, Prague, Czech Republic, 2007.
160. Jan GP, Bischa D, and Bottle SE. Synthesis and properties of novel porphyrin spin probes containing isoindoline nitroxides. *Free Radic Biol Med* 43: 111–116, 2007.
161. Jaramillo MC, Frye JB, Crapo JD, Briehl MM, and Tome ME. Increased manganese superoxide dismutase expression or treatment with manganese porphyrin potentiates dexamethasone-induced apoptosis in lymphoma cells. *Cancer Res* 69: 5450–5457, 2009, DOI: 10.1158/0008-5472.CAN-08–4031.
162. Jensen AW, Wilson SR, and Schuster DI. Biological applications of fullerenes. *Bioorg Med Chem* 4: 767–779, 1996.
163. Jiang J, Kurnikov I, Belikova NA, Xiao J, Zhao Q, Amoscato AA, Braslau R, Studer A, Fink MP, Greenberger JS, Wipf P, and Kagan VE. Structural requirements for optimized delivery, inhibition of oxidative stress and antiapoptotic activity of targeted nitroxides. *J Pharmacol Exp Ther* 32: 1050–1060, 2007.
164. Jung C, Rong Y, Doctrow S, Baudry M, Malfroy B, and Xu Z. Synthetic superoxide/dismutase/catalase mimetics reduce oxidative stress and prolong survival in a mouse amyotrophic lateral sclerosis model. *Neurosci Lett* 304: 157–160, 2001.
165. Kachadourian R, Batinić-Haberle I, and Fridovich I. Mn(III)Cl_4T-2-PyP^{5+} exhibits a high superoxide dismuting rate. *Free Radic Biol Med* 25: S17, 1998.
166. Kachadourian R, Batinić-Haberle I, and Fridovich I. Syntheses and SOD-like activities of partially (1–4) β-chlorinated derivatives of manganese(III) meso-tetrakis (*N*-methylpyridinium-2-yl)porphyrin, *Inorg Chem* 38: 391–396, 1999.
167. Kachadourian R, Johnson CA, Min E, Spasojević I, and Day BJ. Flavin-dependent antioxidant properties of a new series of meso-*N,N*′-dialkyl-imidazolium substituted manganese(III) porphyrins. *Biochem Pharmacol* 67: 77–85, 2004.
168. Kajita M, Hikosaka K, Iitsuka M. Kanayama A, Toshima N, and Miyamoto Y. Platinum nanoparticle is a useful scavenger of superoxide anion and hydrogen peroxide. *Free Radic Res* 41: 615–626, 2007.
169. Kang JL, Lee HS, Jung HJ, and Kim HJ. Iron tetrakis (*N*-methyl-4′-pyridyl) porphyrinato inhibits proliferative activity of thymocytes by blocking activation of p38 mitogen-activated protein kinase, nuclear factor-kappaB, and interleukin-2 secretion. *Toxicol Appl Pharmacol* 191: 147–155, 2003.
170. Kang JL, Lee HS, Pack IS, Leonard S, and Castranova V. Iron tetrakis (*N*-methyl-4′-pyridyl) porphyrinato (FeTM-PyP) is a potent scavenging antioxidant and an inhibitor of stimulant-induced NF-κB activation of raw 264.7 macrophages. *J Toxicol Environ Health A* 64: 291–310, 2001.
171. Keaney M, Matthijssens F, Sharpe M, Vanfleteren J, and Gems D. Superoxide dismutase mimetics elevate superoxide dismutase activity in vivo but do not retard aging in the nematode *Caenorhabditis elegans*. *Free Radic Biol Med* 37: 239–250, 2004.
172. Khaldi MZ, Elouil H, Guiot Y, Henquin JC, and Jonas JC. Antioxidants *N*-acetyl-L-cysteine and manganese(III) tetrakis (4-benzoic acid)porphyrin do not prevent β-cell disfunction in rat islets cultured in high glucose for 1 wk. *Am J Physiol Endocrinol Metab* 29:E137–E146, 2006.
173. Kim J, Takahashi M, Shimizu T, Shirasawa T, Kajita M, Kanayama A, and Miyamoto Y. Effects of a potent antioxidant, platinum nanoparticle, on the lifespan of *Caenorhabditis elegans*. *Mech Ageing Dev* 129: 322–331, 2008.

174. Klug-Roth D, Fridovich I, and Rabbani J. Pulse radiolytic investigations of superoxide catalyzed disproportionation: mechanism for bovine superoxide dismutase. *J Am Chem Soc* 95: 2786–2790, 1973.
175. Kohanski MA, Dwyer DJ, Hayete B, Lawrence CA, and Collins JJ. *Cell* 130: 797–810, 2007.
176. Konorev EA, Kotamraju S, Zhao H, Shasi H, Kalivendi S, Joseph J, and Kalyanaraman B. Paradoxical effects of metalloporphyrins on doxorubicin-induced apoptosis: scavenging of reactive species versus induction of heme oxygenase-1. *Free Radic Biol Med* 33: 988–997, 2002.
177. Korsvik C, Patil S, Seal S, and Self WT. Superoxide dismutase mimetic properties exhibited by vacancy engineered ceria nanoparticles. *Chem Commun* 1056–1058, 2007.
178. Kos I, Benov L, Spasojević I, Rebouças JS, and Batinić-Haberle I. High lipophilicity of *meta* Mn(III) *N*-alkylpyridylporphyrin-based SOD mimics compensates for their lower antioxidant potency and makes them equally effective as *ortho* analogues in protecting *E. coli*. *J Med Chem* 52: 7868–7872, 2009.
179. Kos I, Rebouças JS, DeFreitas-Silva G, Salvemini D, Vujasković Z, Dewhirst MW, Spasojević I, and Batinić-Haberle I. The effect of lipophilicity of porphyrin-based antioxidants: comparison of ortho and meta isomers of Mn(III) *N*-alkylpyridylporphyrins. *Free Radic Biol Med* 47: 72–78, 2009.
180. Kos I, Rebouças JS, Sheng H, Warner DS, Spasojević I, and Batinić-Haberle I. Oral availability of MnTE-2-PyP^{5+}, a potent antioxidant and cellular redox modulator. *Free Radic Biol Med* 45: S86, 2008.
181. Krusic PJ, Wasserman E, Keizer PN, Morton JR, and Preston KF. Radical reaction of C60. *Science* 254: 1183–1185, 1991.
182. Lahaye D, Muthukumaran K, Hung CH, Gryko D, Rebouças JS, Spasojević I, Batinić-Haberle I, and Lindsey JS. Design and synthesis of manganese porphyrins with tailored lipophilicity: investigation of redox properties and superoxide dismutase activity. *Bioorg Med Chem* 15: 7066–7086, 2007.
183. Lam MA, Pattison DI, Bottle SE, Keddie DJ, and Davies MJ. Nitric oxide and nitroxides can act as efficient scavengers of protein-derived free radicals. *Chem Res Toxicol* 21: 211–2119, 2008.
184. Lee J, Hunt JA, and Groves JT, Mechanisms of iron porphyrins reactions with peroxynitrite. *J Am Chem Soc* 120: 7493–7501, 1998.
185. Lee J, Hunt JA, and Groves JT. Manganese porphyrins as redox-coupled peroxynitrite reductases. *J Am Chem Soc* 120: 6053–6061, 1998.
186. Lee JH and Park JW. A manganese porphyrin complex is a novel radiation protector. *Free Radic Biol Med* 37: 272–283, 2004.
187. Lee JH, Lee YM, and Park JW. Regulation of ionizing radiation-induced apoptosis by a manganese porphyrin complex. *Biochem Biophys Res Commun* 334: 298–305, 2005.
188. Li F, Sonveaux PP, Rabbani ZN, Liu S, Yan B, Huang Q, Vujasković Z, Dewhirst MW, and Li C-H. Regulation of HIF-1α stability through S-nitrosylation. *Mol Cell* 26: 63–74, 2007.
189. Li QX, Luo QH, Li YZ, and Shen MC. A study on the mimics of Cu-Zn superoxide dismutase with high activity and stability: two copper(II) complexes of 1,4,7-triazacyclononane with benzimidazole groups. *Dalton Trans* 2329–2335, 2004.
190. Li S, Yan T, Yang J-Q, Oberley TD, and Oberley LW, The role of cellular glutathione peroxidase redox regulation in the suppression of tumor cell growth by manganese superoxide dismutase. *Cancer Res* 60: 3927–3939, 2000.
191. Liang HL, Hilton G, Mortensen J, Regner K, Johnson CP, and Nilakantan V. MnTMPyP, a cell-permeant SOD mimetic, reduces oxidative stress and apoptosis following renal ischemia-reperfusion. *Am J Physiol Renal Physiol* 296: F266–F276, 2008.
192. Liang L-P, Huasng J, Fulton R, Day BJ, and Patel M. An orally active catalytic metalloporphyrin protects against 1-methyl-4-phenyl-1,2,3,6-tetrahydropyridine neurotoxicity in vivo. *J Neurosci* 27: 4326–4333, 2007.
193. Lin Y-T, Hoang H, Hsieh SI, Rangel N, Foster AL, Sampayo JN, Lithgow GJ, and Srinivasan C. Manganous ion supplementation accelerates wild type development, enhances stress resistance, and rescues the life span of a short-lived *Caenorhabditis elegans* mutant. *Free Radic Biol Med* 40: 1185–1193, 2006.
194. Ling X and Liu D. Temporal and spatial profile of cell loss after spinal cord injury: reduction by a metalloporphyrin. *J Neurosci Res* 85: 2175–2185, 2007.
195. Liochev SI and Fridovich I. Superoxide from glucose oxidase or from nitroblue tetrazolium? *Arch Biochem Biophys* 318: 408–410, 1995.
196. Liu J-Y, Li X-F, Li Y-Z, Chang WB, and Huang A-J. Oxidation of styrene by various oxidants with different kinds of metalloporphyrins. *J Mol Catal A: Chem* 187: 163–167, 2002.
197. Mabley JG, Pacher P, Bai P, Wallace R, Goonesekera S, Virag L, Southan GJ, and Szabó C. Suppression of intestinal polyposis in *Apc*$^{min/+}$ mice by targeting the nitric oxide or poly(ADP-ribose) pathways. *Mutat Res* 548: 107–116, 2004.
198. Macarthur H, Westfall TC, Riley DP, Misko TP, and Salvemini D. Inactivation of catecholamines by superoxide gives new insights on the pathogenesis of septic shock. *Proc Natl Acad Sci U S A* 97: 9753–9758, 2000.
199. Mackensen GB, Patel M, Sheng H, Calvi CL, Batinić-Haberle I, Day BJ, Liang LP, Fridovich I, Crapo JD, Pearlstein RD, and Warner DS. Neuroprotection from delayed post-ischemic administration of a metalloporphyrin catalytic antioxidant in the rat. *J Neurosci* 21: 4582–4592, 2001.
200. Mahammed A and Gross Z. Iron and manganese corroles are potent catalysts for the decomposition of peroxynitrite. *Angew Chem Int Ed* 45: 6544–6547, 2006.
201. Makinde AY, Luo-Owen X, Rizvi A, Crapo JD, Pearlstein RD, Slater JM, and Gridley DS. Effect of a metalloporphyrin antioxidant (MnTE-2-PyP) on the response of a mouse prostate cancer model to radiation. *Anticancer Res* 29: 107–118, 2009.
202. Mancuso C, Bates TA, Butterfield DA, Calafato S, Cornelius C, De Lorenzo A, Dinkova Kostova AT, and Calabrese V. Natural antioxidants in Alzheimer's disease. *Expert Opin Invest Drugs* 16: 1921–1931, 2007.
203. Mao XW, Crapo JD, Mekonnen T, Lindsey N, Martinez P, Gridley DS, and Slater JM. Radioprotective effect of a metalloporphyrin compound in rat eye model. *Curr Eye Res* 34: 62–72, 2009.
204. Maroz A, Kelso GF, Smith RAJ, Ware DC, and Anderson RF. Pulse radiolysis investigation on the mechanism of the catalytic action of Mn(II)-pentaazamacrocycle compounds as superoxide dismutase mimetics. *J Phys Chem A* 112: 4929–4935, 2008.
205. Marti MA, Bari SE, Estrin DA, and Doctorovich F. Discrimination of nitroxyl and nitric oxide by water-soluble Mn(III) porphyrins. *J Am Chem Soc* 127: 4680–4684; 2005.

206. Martin RC, Liu Q, Wo JM, Ray Mb, and Li Y. Chemoprevention of acrinogenic progression to esophageal adenocarcinoma by the manganese superoxide dismutase supplementation. *Clin Cancer Res* 13: 5176–5182, 2007.
207. Masini E, Bani D, Vannacci A, Pierpaoli S, Mannaioni PF, Comhair SAA, Xu W, Muscoli C, Erzurum SC, and Salvemini D. Reduction of antigen-induced respiratory abnormalities an airway inflammation in sensitized guinea pigs by a superoxide dismutase mimetic. *Free Radic Biol Med* 39: 520–531, 2005.
208. Masini E, Cuzzocrea S, Mazzon E, Marzocca C, Mannaioni PF, and Salvemini D. Protective effects of M40403, a selective superoxide dismutase mimetic, in myocardial ischaemia and reperfusion injury in vivo. *Br J Pharmacol* 136: 905–917, 2002.
209. Matsukawa N, Yasuhara T, Hara K, Xu L, Maki M, Yu G, Kaneko Y, Ojika K, Hess DC, and Borlongan CV. Therapeutic targets and limits of minocycline neuroprotection in experimental ischemic stroke. *BMC Neurosci* 10: 126, 2009.
210. Matthijssens F, Back P, Braeckman BP, and Vanfleteren JR. Prooxidant activity of the superoxide dismutase (SOD)-mimetic EUK-8 in proliferating and growth-arrested *Escherichia coli* cells. *Free Radic Biol Med* 45: 708–715, 2008.
211. Maybauer DM, Maybauer MO, Szabó C, Westphal M, Traber LD, Enkhbaatar P, Murthy KG, Nakano Y, Salzman AL, Herndon DN, and Traber DL. Lung-protective effects of the metalloporphyrinic peroxynitrite decomposition catalyst WW-85 in interleukin-2 induced toxicity. *Biochem Biophys Res Commun* 377: 786–791, 2008.
212. McCord JM and Fridovich I. Superoxide dismutase: an enzymatic function for erythrocuprein (hemocuprein). *J Biol Chem* 244: 6049–6055, 1969.
213. McDonald MC, d'Emamnuele Di Villa Blanca R, Wayman NS, Pinto A, Sharpe MA, Cuzzocrea S, Chatterjee PK, and Thiemermann C. A superoxide dismutase mimetic with catalase activity (EUK-8) reduces the organ injury in endotoxic shock. *Eur J Pharmacol* 466: 181–189, 2003.
214. McKinnon RL, Lidington D, and Tyml K, Ascorbate inhibits reduced arterial conducted vasoconstriction in septic mouse cremaster muscle. *Microcirculation* 14: 697–707, 2007.
215. Mehta MP, Shapiro WR, Phan SC, Gervais R, Carrie C, Chabot P, Patchell RA, Glantz MJ, Recht L, Langer C, Sur RK, Roa WH, Mahe MA, Fortin A, Nieder C, Meyers CA, Smith JA, Miller RA, and Renschler MF. Motexafin gadolinium combined with prompt whole brain radiotherapy prolongs time to neurologic progression in non-small-cell lung cancer patients with brain metastases: results of a phase III trial. *Int J Radiat Oncol Biol Phys* 73: 1069–1076, 2009.
216. Melov S, Ravenscroft J, Malik S, Gill MS, Walker DW, Clayton PE, Wallace DC, Malfroy B, Doctrow SR, and Lithgow GJ. Extension of life-span with superoxide dismutase/catalase mimetics. *Science* 289: 1567–1569, 2000.
217. Metz JA, Smith D, Mick R, Lustig R, Mitchell J, Cherakuri M, Glatstein E, and Hahn SM. A phase I study of topical tempol for the prevention of alopecia induced by whole brain radiotherapy. *Clin Cancer Res* 10: 6411–6417, 2004.
218. Michel E, Nauser T, Sutter B, Bounds PL, and Koppenol WH. Kinetics properties of Cu, Zn-superoxide dismutase as a function of metal content. *Arch Biochem Biophys* 439: 234–240, 2005.
219. Miller RJ, James-Kracke M, Sun GY, and Sun AY. Oxidative and inflammatory pathways in Parkinson's disease. *Neurochem Res* 34: 55–65, 2009.
220. Mocellin S, Bronte V, and Nitti D. Nitric oxide, a double edged sword in cancer biology: searching for therapeutic opportunities. *Med Res Rev* 27: 317–352, 2007.
221. Moeller BJ, Batinić-Haberle I, Spasojević I, Rabbani ZN, Anscher MS, Vujasković Z, and Dewhirst MW. A manganese porphyrin superoxide dismutase mimetic enhances tumor radioresponsiveness. *Int J Radiat Oncol Biol Phys* 63: 545–552, 2005.
222. Moeller BJ, Cao Y, Li CY, and Dewhirst MW. Radiation activates HIF-1 to regulate vascular radiosensitivity in tumors: role of oxygenation, free radicals and stress granules. *Cancer Cell* 5: 429–441, 2004.
223. Moon KH, Hood BL, Mukhopadhyay P, Rajesh M, Abdelmegeed MA, Kwon YI, Conrads TP, Veenstra TD, Song BJ, and Pacher P. Oxidative inactivation of key mitochondrial proteins leads to dysfunction and injury in hepatic ischemia reperfusion. *Gastroenterology* 135: 1344–1357, 2008.
224. Moriscot C, Candel S, Sauret V, Kerr-Conte J, Richard MJ, Favrot MC, and Benhamou PY. MnTMPyP, a metalloporphyrin-based superoxide dismutase/catalase mimetic, protects INS-1 cells and human pancreatic islets from an in vitro oxidative challenge. *Diabetes Metab* 33: 44–53, 2007.
225. Munroe W, Kingsley C, Durazo A, Gralla EB, Imlay JA, Srinivasan C, and Valentine JS, Only one of a wide assortment of manganese-containing SOD mimicking compounds rescues the slow aerobic growth phenotype of both *Escherichia coli* and *Saccharomyces cerevisiae* strains lacking superoxide dismutase enzymes. *J Inorg Biochem* 101: 1875–1882, 2007.
226. Murphy CK, Fey EG, Watkins BA, Wong V, Rothstein D, and Sonis ST. Efficacy of superoxide dismutase mimetic M40403 in attenuating radiation-induced oral mucositis in hamsters. *Clin Cancer Res* 14: 4292–4297, 2008.
227. Murphy MP and Smith RAJ. Targeting antioxidants to mitochondria by conjugation to lipophilic cations. *Annu Rev Pharmacol Toxicol* 47: 629–656, 2007.
228. Murphy MP. Targeting lipophilic cations to mitochondria. *Biochim Biophys Acta* 177**:** 1028–1031, 2008.
229. Muscoli C, Cuzzocrea S, Ndengele MM, Mollace V, Porreca F, Fabrizi F, Esposito E, Masini M, Matuschak GM, and Salvemini, D. Therapeutic manipulation of peroxynitrite attenuates the development of opiate-induced antinociceptive tolerance. *J Clin Invest* 117: 1–11; 2007.
230. Muscoli C, Cuzzocrea S, Riley DP, Zweier JL, Thiemermann C, Wang Z-Q, and Salvemini D. On the selectivity of superoxide dismutase mimetics and its importance in pharmacological studies. *Br J Pharmacol* 140: 445–460, 2003.
231. Naidu BV, Farivar AS, Woolley SM, Fraga C, Salzman AL, Szabó C, Groves JT, and Mulligan MS. Enhanced peroxynitrite decomposition protects against experimental obliterative bronchiolitis. *Exp Mol Pathol* 75: 12–17, 2003.
232. Naidu BV, Fraga C, Salzman AL, Szabó C, Verrier ED, and Mulligan MS. Critical role of reactive nitrogen species in lung ischemia-reperfusion injury. *J Heart Lung Transplant* 22: 784–793, 2003.
233. Ndengele MM, Muscoli C, Wang Q-Z, Doyle TM, Matuschak GM, and Salvemini D. Superoxide potentiates NF-κB activation and modulates endotoxin-induced cytokine production in alveolar macrophages. *Shock* 23: 186–193, 2005.
234. Nepomuceno MF, Tabak M, and Vercesi AE. Opposite effects of Mn(III) and Fe(III) forms of meso-tetrakis(4-*N*-methyl pyridiniumyl) porphyrins on isolated rat liver mitochondria. *J Bioenerg Biomembr* 34: 41–47, 2002.

235. Nilsson J, Bengtsson E, Fredrikson GN, and Bjorkbacka H. Inflammation and immunity in diabetic vascular complications. *Curr Opin Lipidol* 19: 519–524, 2008.
236. Noberis A and Navarro A. Brain mitochondrial dysfunction in aging. *IUBMB Life* 60: 308–314, 2008.
237. Oberley LW, Leuthauser SW, Pasternack RF, Oberley TD, Schutt L, and Sorenson JR. Anticancer activity of metal compounds with superoxide dismutase activity. *Agents Actions* 15: 535–538, 1984.
238. Obrosova IG, Mabley JG, Zsengellér Z, Charniauskaya T, Abatan OI, Groves JT, and Szabó C. Role for nitrosative stress in diabetic neuropathy: evidence from studies with peroxynitrite decomposition catalyst. *FASEB J* 19: 401–403, 2005.
239. Ohse T, Nagaoka S, Arakawa Y, Kawakami H, and Nakamura K. Cell death by reactive oxygen species generated from water-soluble cationic metalloporphyrins as superoxide dismutase mimics. *J Inorg Biochem* 85: 201–208, 2001.
240. Okado-Matsumoto A and Fridovich I. Subcellular distribution of superoxide dismutases (SOD) in rat liver. *J Biol Chem* 276: 38388–38393, 2001.
241. Okado-Matsumoto A, Batinić-Haberle I, and Fridovich I. Complementation of SOD deficient *Escherichia coli* by manganese porphyrin mimics of superoxide dismutase, *Free Radic Biol Med* 37: 401–410, 2004.
242. Okun Z, Kupershmidt, L, Amit T, Mandel S, Bar-Am O, Youdim MBH, and Gross Z. Manganese corroles prevent intracellular nitration and subsequent death of insulin-producing cells. *ACS Chem Biol* 4: 910–914, 2009.
243. Olcott A, Tocco G, Tian J, Zekzer D, Fukuto J, Ignarro L, and Kaufman DL. A salen-manganese catalytic free radical scavenger inhibits type 1 diabetes and islet allograft rejection. *Diabetes* 53: 2574–2580, 2004.
244. Orell RW. AEOL-10150 Aeolus. *Expert Opin Invest Drugs* 7: 70–80, 2006.
245. Park W and Lim D. Effect of oligo(ethylene glycol) group on the antioxidant activity of manganese salen complexes. *Bioorg Med Chem Lett* 19: 614–617, 2009.
246. Pasternack RF and Halliwell B. Superoxide dismutase activities of an iron porphyrin and other iron complexes. *J Am Chem Soc* 101: 1026–1031, 1979.
247. Pasternack RF and Skowronek WR Jr. Catalysis of the disproportionation of superoxide by metalloporphyrins. *J Inorg Biochem* 11: 261–267, 1979.
248. Pasternack RF, Banth A, Pasternack JM and Johnson CS. Catalysis of the disproportionation of superoxide by metalloporphyrins, III. *J Inorg Biochem* 15: 261–267, 1981.
249. Pasternack RF, Gibbs EJ, and Villafranca AC. Interactions of porphyrins with nucleic acids. *Biochemistry* 22: 2406–2414, 1983.
250. Pasternack RF, Gibbs EJ, and Villafranca AC. Interactions of porphyrins with nucleic acids. *Biochemistry* 22: 5409–5417, 1983.
251. Patel M. Metalloporphyrins improve survival of Sod2-deficient neurons. *Aging Cell* 2: 219–224, 2003.
252. Peretz P, Solomon D, Weinraub D, and Faraggi M. Chemical properties of water-soluble porphyrins, 3: the reaction of superoxide radicals with some metalloporphyrins. *Int J Radiat Biol* 42: 449–456, 1982.
253. Pérez MJ and Cederbaum AI. Antioxidant and pro-oxidant effects of a manganese porphyrin complex against CYP2E1-dependent toxicity. *Free Radic Biol Med* 33:111–127, 2002.
254. Piganelli JD, Flores SC, Cruz C, Koepp J, Young R, Bradley B, Kachadourian R, Batinić-Haberle I, and Haskins K. A metalloporphyrin superoxide dismutase mimetic (SOD mimetic) inhibits autoimune diabetes. *Diabetes* 51: 347–355, 2002.
255. Pollard JM, Rebouças JS, Durazo A, Kos I, Fike F, Panni M, Gralla EB, Valentine JS, Batinić-Haberle, I, and Gatti RA. Radioprotective effects of manganese-containing superoxide dismutase mimics on ataxia telangiectasia cells. *Free Radic Biol Med* 47: 250–260, 2009.
256. Quick KL, Ali SS, Arch R, Xiong C, Wozniak D, and Dugan LL. A carboxyfullerene SOD mimetic improves cognition and extends the lifespan of mice. *Neurobiol Aging* 289: 117–128, 2008.
257. Rabbani Z, Batinić-Haberle I, Anscher MS, Huang J, Day BJ, Alexander E, Dewhirst MW, and Vujasković Z. Long term administration of a small molecular weight catalytic metalloporphyrin antioxidant AEOL10150 protects lungs from radiation-induced injury. *Int J Radic Oncol Biol Phys* 67: 573–580, 2007.
258. Rabbani Z, Salahuddin FK, Yarmolenko P, Batinić-Haberle I, Trasher BA, Gauter-Fleckenstein B, Dewhirst MW, Anscher MS, and Vujasković Z. Low molecular weight catalytic metalloporphyrin antioxidant AEOL10150 (5 mg/kg) protects rat lungs from fractionated chronic radiation-induced injury. *Free Radic Res* 41: 1273–1282, 2007.
259. Rabbani ZN, Spasojević I, Zhang X, Moeller BJ, Haberle S, Vasquez-Vivar J, Dewhirst MW, Vujasković Z, and Batinić-Haberle I. Antiangiogenic action of redox-modulating Mn(III) meso-tetrakis(*N*-ethylpyridinium-2-yl)porphyrin, MnTE-2-PyP^{5+}, via suppression of oxidative stress in a mouse model of breast tumor. *Free Radic Biol Med* 47: 992–1004, 2009.
260. Rahman I and Adcock IM. Oxidative stress and redox regulation of lung inflammation in COPD. *Eur Respir J* 28: 219–242, 2006.
261. Rebouças JS, de Carvalho MEMD, Idemori YM. Perhalogenated 2-pyridylporphyrin complexes: synthesis, self-coordinating aggregation properties, and catalytic studies. *J Porphyrins Phthalocyanines* 6: 50–57, 2002.
262. Rebouças JS, DeFreitas-Silva G, Idemori YM, Spasojević I, Benov L, and Batinić-Haberle I. Impact of electrostatics in redox modulation of oxidative stress by Mn porphyrins: protection of SOD-deficient *Escherichia coli* via alternative mechanism where Mn porphyrin acts as a Mn carrier. *Free Radic Biol Med* 45: 201–210, 2008.
263. Rebouças JS, Kos I, Vujasković Z, and Batinić-Haberle I. Determination of residual manganese in Mn porphyrin-based superoxide dismutase (SOD) and peroxynitrite reductase mimics. *J Pharm Biomed Anal* 50: 1088–1091, 2009.
264. Rebouças JS, Spasojević I, and Batinić-Haberle I. Pure manganese(III) 5,10,15,20-tetrakis(4-benzoic acid)porphyrin (MnTBAP) is not a superoxide dismutase mimic in aqueous systems: a case of structure-activity relationship as a watchdog mechanism in experimental therapeutics and biology. *J Inorg Biol Chem* 13: 289–302, 2008.
265. Rebouças JS, Spasojević I, and Batinić-Haberle I. Quality of Mn-porphyrin-based SOD mimics and peroxynitrite scavengers for preclinical mechanistic/therapeutic purposes. *J Pharm Biomed Anal* 48: 1046–1049, 2008.
266. Rebouças JS, Spasojević I, Tjahjono DH, Richaud A, Méndez F, Benov L, and Batinić-Haberle I. Redox modulation of oxidative stress by Mn porphyrin-based therapeutics: the effect of charge distribution. *Dalton Trans* 1233–1242, 2008.

267. Reddi AR, Jensen LT, Naranuntarat A, Rosenfeld L, Leung E, Shah R, and Culotta VC. The overlapping roles of manganese and Cu/ZnSOD in oxidative stress protection. *Free Radic Biol Med* 46: 154–162, 2009.
268. Rees MD, Bottle SE, Fairfull-Smith KE, Malle E, Whitelock JM, and Davies MJ. Inhibition of myeloperoxidase-mediated hypochlorous acid production by nitroxides. *Biochem J* 421: 79–86, 2009.
269. Riley DP, Lennon PJ, Neumann WL, and Weiss RH. Toward the rational design of superoxide dismutase mimics: mechanistic studies for the elucidation of substituent effects on the catalytic activity of macrocyclic manganese(II) complexes. *J Am Chem Soc* 119: 6522–6528, 1997.
270. Robak J and Gryglewski RJ. Bioactivity of flavonoids. *Pol J Pharmacol* 48: 555–564, 1996.
271. Roberston L and Hartley R. Synthesis of *N*-arylpyridinium salts bearing a nitron spin trap as potential mitochondria-targeted antioxidants. *Tetrahedron* 65: 5284–5292, 2009.
272. Rosenthal RA, Huffman KD, Fisette LW, Damphousse CA, Callaway WB, Malfroy B, and Doctrow SR. Orally available Mn porphyrins with superoxide dismutase and catalase activity. *J Biol Inorg Chem* 14: 979–991, 2009.
273. Rubbo H and Radi R. Protein and lipid nitration: role in redox signaling and injury. *Biochim Biophys Acta* 1780: 1318–1324, 2008.
274. Saba H, Batinić-Haberle I, Munusamy S, Mitchell T, Lichti C, Megyesi J, and MacMillan-Crow LA. Manganese porphyrin reduces renal injury and mitochondrial damage during ischemia/reperfusion, *Free Radic Biol Med* 42: 1571–1578, 2007.
275. Saltsman I, Botoshansky M, and Gross Z, Facile synthesis of ortho-pyridyl-substituted corroles and molecular structures of analogous porphyrins. *Tetrahedron Lett* 49: 4163–4166, 2008.
276. Salvemini D, Doyle TM, and Cuzzocrea S. Superoxide, peroxynitrite and oxidative/nitrative stress in inflammation. *Biochem Soc Trans* 34: 965–970, 2006.
277. Salvemini D, Wang Z-Q, Zweier JL, Samouilov A, Macarthur H, Misko TOP, Currie MG, Cuzzocrea S, Sikorski JA, and Riley DP. A nonpeptidyl mimic of superoxide dismutase with therapeutic activity in rats. *Science* 286: 304–306, 1999.
278. Samlowski WE, Peterson R, Cuzzocrea S, Macarthur H, Burton D, McGregor JR, and Salvemini D. A nonpeptidyl mimic of superoxide dismutase, M40403, inhibits dose-limiting hypotension associated with interleukin-2 and increases its antitumor effects. *Nat Med* 9: 750–755, 2009.
279. Sanchez RJ, Srinivasan C, Munroe WH, Wallace MA, Martins J, Kao TY, Le K, Gralla EB, and Valentine JS. Exogenous manganous ion at millimolar levels rescues all known dioxygen-sensitive phenotypes of yeast lacking CuZnSOD. *J Biol Inorg Chem* 10: 913–923, 2005.
280. Satoh M and Takayanagi I. Pharmacological studies on fullerene (C_{60}), a novel carbon allotrope, and its derivatives. *J Pharmacol Sci* 100: 513–518, 2006.
281. Schubert R, Erker L, Barlow C, Yakushiji H, Larson D, Russo A, Mitchell JB, and Wynshaw-Boris A. Cancer chemoprevention by the antioxidant tempol in *Atm*-mice. *Hum Mol Genet* 13: 1793–1802, 2004.
282. Sessler JL and Miller RA. Texaphyrins: new drugs with diverse clinical applications in radiation and photodynamic therapy. *Biochem Pharmacol* 59: 733–739, 2000.
283. Sharma SS and Gupta S. Neuroprotective effect of MnTMPyP, a superoxide dismutase/catalase mimetic in global cerebral ischemia is mediated through reduction of oxidative stress and DNA fragmentation. *Eur J Pharmacol* 561: 72–79, 2007.
284. Sharpe MA, Ollosson R, Stewart VC, and Clark JB. Oxidation of nitric oxide by oxomanganese-salen complexes: a new mechanism for cellular protection by superoxide dismutase/catalase mimetics. *Biochem J.* 366: 97–107, 2002.
285. Shen J, Ijaimi NE, Chkounda M, Gros CP, Barbe J-M, Shao J, Guilard R, and Kadish KM. Solvent, anion and structural effects on the redox potentials and UV-visible spectral properties of mononuclear manganese corroles. *Inorg Chem* 47: 7717–7727, 2008.
286. Sheng H, Enghild J, Bowler R, Patel M, Calvi CL, Batinić-Haberle I, Day BJ, Pearlstein RD, Crapo JD, and Warner DS. Effects of metalloporphyrin catalytic antioxidants in experimental brain ischemia. *Free Radic Biol Med* 33: 947–961, 2002.
287. Sheng H, Spasojević I, Warner DS, and Batinić-Haberle I. Mouse spinal cord compression injury is ameliorated by intrathecal manganese(III) porphyrin. *Neurosci Lett* 366: 220–225, 2004.
288. Sheng H, Yang W, Fukuda S, Tse HM, Paschen W, Johnson K, Batinić-Haberle I, Crapo JD, Pearlstein RD, Piganelli J, and Warner DS. Long-term neuroprotection from a potent redox-modulating metalloporphyrin in the rat. *Free Radic Biol Med* 47: 917–923, 2009.
289. Shimanovich R, Hannah S, Lynch V, Gerasimchuk N, Mody TD, Magda D, Sessler J, and Groves JT. Mn(II)-texaphyrin as a catalyst for the decomposition of peroxynitrite. *J Am Chem Soc* 123: 3613–3614, 2001.
290. Shoham A, Hadziahmetovic M, Dunaief JL, Mydlarski MB, and Schipper HM. Oxidative stress in diseases of human cornea. *Free Radic Biol Med* 45: 1047–1055, 2008.
291. Shukla S and Gupta S. Suppression of constitutive and tumor necrosis factor α-induced nuclear factor (NF-κB activation and induction of apoptosis by apigenin in human prostate carcinoma PC-3 cells: correlation with down-regulation of NF-κB–responsive genes. *Clin Cancer Res* 10: 3169–3178, 2004.
292. Silva D. Suppression of cancer invasiveness by dietary compounds. *Mini Rev Med Chem* 8: 677–688, 2008.
293. Solomon D, Peretz P, and Faraggi M. Chemical properties of water-soluble porphyrins, 1: the reaction of iron(IIII) tetrakis(4-*N*-methylpyridyl)porphyrin with superoxide radical dioxygen couple. *J Phys Chem* 86: 1842–1849, 1982.
294. Sompol P, Ittarat W, Tangpong J, Chen Y, Doubinskaia I, Batinić-Haberle I, Mohammad Abdul H, Butterfield A, and St Clair DK. Alzheimer's disease: an insight into the mechanisms of oxidative stress-mediated mitochondrial injury. *Neuroscience* 153: 120–130, 2008.
295. Soukhova-O'Hara GK. Ortines RV, Gu Y, Nozdrachev AD, Prabhu SD, and Gozal D. Postnatal intermittent hypoxia and developmental programming of hypertension in spontaneously hypertensive rats. *Hypertension* 52: 156–162, 2008.
296. Soule BP, Hyodo F, Matsumoto K, Simone NL, Cook JA, Krishna MC, and Mitchell JB. The chemistry and biology of nitroxide compounds. *Free Radic Biol Med* 42: 1632–1650, 2007.
297. Soule BP, Hyodo F, Matsumoto, K-I, Simone NL, Cook JA, Krishna MC, and Mitchell JB. Therapeutic and clinical applications of nitroxide compounds. *Antioxid Redox Signal* 9: 1731–1743, 2007.
298. Souza JM, Peluffo G, and Radi R. Protein tyrosine nitration: functional alteration or just a biomarker? *Free Radic Biol Med* 45: 357–366, 2008.

299. Spasojević I and Batinić-Haberle I. Manganese(III) complexes with porphyrins and related compounds as catalytic scavengers of superoxide. *Inorg Chim Acta* 317: 230–242, 2001.
300. Spasojević I, Batinić-Haberle I, and Fridovich I. Nitrosylation of manganese(II) tetrakis(*N*-ethylpyridinium-2-yl)porphyrin, *Nitric Oxide* 4: 526–533, 2000.
301. Spasojević I, Batinić-Haberle I, Rebouças JS, Idemori YM, and Fridovich I. Electrostatic contribution in the catalysis of $O_2^{\cdot -}$ dismutation by superoxide dismutase mimics. *J Biol Chem* 278: 6831–6837, 2003.
302. Spasojević I, Batinić-Haberle I, Stevens RD, Hambright P, Thorpe AN, Grodkowski J, Neta P, and Fridovich I. Manganese(III) biliverdin IX dimethylester. a powerful catalytic scavenger of superoxide employing the Mn(III)/Mn(IV) redox couple *Inorg Chem* 40: 726–739, 2001.
303. Spasojević I, Chen Y, Noel TJ, Fan P, Zhang L, Rebouças JS, St Clair DK, and Batinić-Haberle I. Pharmacokinetics of the potent redox modulating manganese porphyrin, MnTE-2-PyP^{5+} in plasma and major organs of B6C3F1 mice. *Free Radic Biol Med* 45: 943–949, 2008.
304. Spasojević I, Colvin OM, Warshany KR, and Batinić-Haberle I. New approach to the activation of anti-cancer pro-drug by metalloporphyrin-based cytochrome P450 mimics in all-aqueous biologically relevant system, *J Inorg Biochem* 100: 1897–1902, 2006.
305. Spasojevic I, Sheng H, Warner DS, and Batinic-Haberle I. Metalloporphyrins are versatile and powerful therapeutics: biomimetics of SOD, peroxyredoxin, and cyt P450. 2nd World Conference on Magic Bullets (Ehrlich II), Nurnberg, 2008.
306. Spasojević I, Yumin C, Noel T, Yu I, Pole MP, Zhang L, Zhao Y, St Clair DK, and Batinić-Haberle I. Mn porphyrin-based SOD mimic, MnTE-2-PyP^{5+} targets mouse heart mitochondria. *Free Radic Biol Med* 42: 1193–1200, 2007.
307. Srinivasan V, Doctrow S, Singh VK, and Whitnall MH. Evaluation of EUK-189, a synthetic superoxide dismutase/catalase mimetic as radiation countermeasure. *Immunopharmacol Immunotoxicol* 30: 271–290, 2008.
308. Stavrovskaya IG and Kristal BS. The powerhouse takes control of the cell: is the mitochondrial permeability transition a viable therapeutic target against neuronal dysfunction and death? *Free Radic Biol Med* 38: 687–697, 2005.
309. Stefanutti G, Pierro A, Smith VV, Klein NJ, and Eaton S. Peroxynitrite decomposition catalyst FeTMPyP provides partial protection against intestinal ischemia and reperfusion injury in infant rats. *Pediatr Res* 62: 43–48, 2007.
310. Stern MK, Jensen MP, Kramer K. Peroxynitrite decomposition catalysts. *J Am Chem Soc* 118: 8735–8736, 1996.
311. Strimpakos AS and Sharma RA. Curcumin: preventive and therapeutic properties in laboratory studies and clinical trials. *Antioxid Redox Signal* 10: 511–545, 2008.
312. Sun H-L, Liu Y-N, Huang Y-T, Pan S-L, Huang D-J, Guh J-H, Lee F-Y, and Kuo S-C. YC-1 inhibits HIF-1 expression in prostate cancer cells: contribution of Akt/NF-kB signaling to HIF-1α accumulation during hypoxia. *Oncogene* 26: 3941–3951, 2007.
313. Szabó C, Mabley JG, Moeller SM, Shimanovich R, Pacher P, Virag L, Soriano VG, Van Duzer JH, Williams W, Salzman AL, and Groves JT. Part I: Pathogenetic role of peroxynitrite in the development of diabetes and diabetic vascular complications: studies with FP15, a novel potent peroxynitrite decomposition catalyst. *Mol Med* 8: 571–580, 2002.
314. Tauskela JS, Brunette E, Kiedrowski L, Lortie K, Hewitt M, and Morley P. Unconventional neuroprotection against Ca^{2+}-dependent insults by metalloporphyrin catalytic antioxidants. *J Neurochem* 98: 1234–1342, 2006.
315. Tauskela JS, Brunette E, O'Reilly N, Mealing G, Comas T, Gendron, TF, Monette R, and Morley P. An alternative Ca^{2+}-dependent mechanism of neuroprotection by metalloporphyrin class of superoxide dismutase mimetics. *FASEB J* 19: 1734–1736, 2005.
316. Tawfik HE, Cena J, Schulz R, and Kaufman S. Role of oxidative stress in multiparity-induced endothelial disfunction. *Am J Physiol Heart Circ Physiol* 295: H1736–H1742, 2008.
317. Toyokuni S. Molecular mechanisms of oxidative stress-induced carcinogenesis: from epidemiology to oxygenomics. *IUBMB Life* 60: 441–447, 2008.
318. Trnka J, Blaikie FH, Logan A, Smith RAJ, and Murphy MP. Antioxidant properties of MitoTEMPOL and its hydroxylamine. *Free Radic Res* 43: 4–12, 2009.
319. Trnka J, Blaikie FH, Smith RA, and Murphy MP. A mitochondria-targeted nitroxide is reduced to its hydroxylamine by ubiquinol in mitochondria. *Free Radic Biol Med* 44: 1406–1419, 2008.
320. Trostchansky A, Ferrer-Sueta G, Batthyány C, Botti H, Batinić-Haberle I, Radi R, and Rubbo H. Peroxynitrite flux-mediated LDL oxidation is inhibited by manganese porphyrins in the presence of uric acid. *Free Radic Biol Med* 35: 1293–1300, 2003.
321. Trova MP, Gauuan PJF, Pechulis AD, Bubb SM, Bocckino SB, Crapo JD, and Day BJ. Superoxide dismutase mimetics, part 2: synthesis and structure-activity relationship of glyoxylate- and glyoxamide-derived metalloporphyrins. *Bioorg Med Chem* 11: 2695–2707, 2003.
322. Tse H, Milton MJ, and Piganelli JD. Mechanistic analysis of the immunomodulatory effects of a catalytic antioxidant on antigen-presenting cells: implication for their use in targeting oxidation/reduction reactions in innate immunity. *Free Radic Biol Med* 36: 233–247, 2004.
323. Ungvari Z, Parrado-Fernandez C, Csiszar A, and de Cabo R. Mechanisms underlying caloric restriction and lifespan regulation: implications for vascular aging. *Circ Res* 102: 519–528, 2008.
324. Van Empel VPM, Bertrand AT, Van Oort RJ, Van der Nagel R, Engelen M, Van Rijen HV, Doevendans PA, Crijns HJ, Ackerman SL, Sluiter W, and De Windt LJ. EUK-8, a superoxide dismutase and catalase mimetic, reduces cardiac oxidative stress and ameliorates pressure overload-induced heart failure in the harlequin mouse mutant. *J Am Coll Cardiol* 48: 824–832, 2006.
325. Vance CK and Miller AF. A simple proposal that can explain the inactivity of metal-substituted superoxide dismutases. *J Am Chem Soc* 120: 461–467, 1998.
326. Viani GA, Mantya GB, Fonseca EC, De Fendi LI, Afonso SL, and Stefano EJ. Whole brain radiotherapy with radiosensitizer for brain metastases. *J Exp Clin Cancer Res* 28: 47, 2009.
327. Vincet A, Babu S, Heckert E, Dowding J, Hirst SM, Inerbaev TM, Self WT, Reily CM, Masunov AE, Rahman TS, and Seal S. Protonated nanoparticle surface governing ligand tethering and cellular targeting. *ACS Nano* 3: 1203–1211, 2009.
328. Vujasković Z, Batinić-Haberle I, Rabbani ZN, Feng Q-F, Kang SK, Spasojević I, Samulski TV, Fridovich I, Dewhirst MW, and Anscher MS. A small molecular weight catalytic metalloporphyrin antioxidant with superoxide dismutase (SOD) mimetic properties protects lungs from radiation-induced injury. *Free Radic Biol Med* 33: 857–863, 2002.

329. Wang Z-Q, Porecca F, Cuzzocrea S, Galen K, Lightfoot R, Masini E, Muscoli E, Mollace V, Ndengele M, Ischirpoulos H, and Salvemini D. A newly identified role for superoxide in inflammatory pain. *J Pharmacol Exp Ther* 309: 869–878, 2004.
330. Wang JF. Defects of mitochondrial electron transport chain in bipolar disorder: implications for mood-stabilizing treatment. *Can J Psychiatry* 52: 753–762, 2007.
331. Watanabe T, Owada S, Kobayashi HP, Kawakami H, Nagaoka S, Murakami E, Ishiuchi A, Enomoto T, Jinnouchi Y, Sakurai J, Tobe N, Koizumi S, Shimamura T, Asakura T, Nakano H, and Otsubo T. Protective effects of MnTM2Py4P and Mn-salen against small bowel ischemia/reperfusion injury in rats an in vivo and ex vivo electron paramagnetic resonance technique with a spin probe. *Transplant Proc* 39: 3002–3006, 2007.
332. Weinraub D, Peretz P, and Faraggi M. Chemical properties of water-soluble porphyrins, 1. Equilibria between some ligands and iron(III) tetrakis(4-*N*-methylpyridyl)porphyrin. *J Phys Chem* 86: 1839–1842, 1982.
333. Werinraub D, Levy P, and Faraggi M. Chemical properties of water-soluble porphyrins, 5. Reactions of some manganese (III) porphyrins with the superoxide and other reducing radicals. *Int J Radiat Biol* 50: 649–658, 1986.
334. Wilcox CS and Pearlman A. Chemistry and antihypertensive effects of tempol and other nitroxides. *Pharmacol Rev* 60: 418–469; 2009.
335. Winterbourn CC. Reconciling the chemistry and biology of reactive species. *Nat Chem Biol* 4: 278–286, 2008.
336. Winterbourn CC and Hampton MB. Thiol chemistry and specificity in redox signaling. *Free Radic Biol Med* 45: 549–561, 2008.
337. Wise-Faberowski L, Warner DS, Spasojević I, and Batinić-Haberle I. The effect of lipophilicity of Mn (III) *ortho N*-alkylpyridyl- and di*ortho N, N'*-imidazolylporphyrins in two *in-vitro* models of oxygen and glucose deprivation-induced neuronal death. *Free Radic Res* 43: 329–339, 2009.
338. Wolak M and van Eldik R. Mechanistic studies on peroxide activation by a water-soluble iron(III)–porphyrin: implications for O-O bond activation in aqueous and nonaqueous solvents. *Chem Eur J* 13: 4873–4883, 2007, and references therein.
339. Wolf G, Hannken T, Schroedr R, Zahner G, Ziyadeh FN, and Stahl RAK. Antioxidant treatment induces transcription and expression of transforming growth factor β in cultured renal proximal tubular cells. *FEBS Lett* 488: 154–159, 2001.
340. Wu AS, Kiaei M, and Aguirre N, Crow JP, Calingasan NY, Browne SE, and Beal MF. Iron porphyrin treatment extends survival in transgenic animal model of amyotrophic lateral sclerosis. *J Neurochem* 85: 142–150, 2003.
341. Wu T-J, Khoo NH, Zhou F, Day BJ, and Parks DA. Decreased hepatic ischemia-reperfusion injury by manganese-porphyrin complexes. *Free Radic Res* 41: 127–134, 2007.
342. Wu Z, Zhang J, and Zhao B. Superoxide anion regulates the mitochondrial free Ca^{2+} through uncoupling proteins. *Antioxid Redox Signal* 11: 1805–1818, 2009.
343. Xu Y, Liu B, Zweier JL, and He G. Formation of hydrogen peroxide and reduction of peroxynitrite via dismutation of superoxide at reperfusion enhances myocardial blood flow and oxygen consumption in postischemic mouse heart. *J Pharmacol Exp Ther* 327: 402–410, 2008.
344. Yadava N and Nicholls DG. Spare respiratory capacity rather than oxidative stress regulates glutamate excitotoxicity after partial respiratory inhibition of mitochondrial complex I with rotenone. *J Neurosci* 27: 7310–7317, 2007.
345. Yan H, Parsons DW, Jin G, McLendon R, Rasheed BA, Yuan W, Kos I, Batinić-Haberle I, Jones S, Riggins GJ, Friedman H, Friedman A, Reardon D, Herndon J, Kinzler KW, Velculescu VE, Vogelstein B, and Bigner DD. IDH1 and IDH2 mutations in gliomas. *N Engl J Med* 360: 765–773, 2009.
346. Ye X, Fels D, Dedeugd C, Dewhirst MW, Leong K, and Batinic-Haberle I. The *in vitro* cytotoxic effects of Mn(III) alkylpyridylporphyrin/ascorbate system on four tumor cell lines, *Free Radic Biol Med* 47: S136, 2009.
347. Yin J-J, Lao F, Fu PP, Wamer WG, Zhao Y, Wang PC, Qiu Y, Sun B, Xing G, Dong J, Liang X-J, and Chen C. The scavenging of reactive oxygen species and potential for the cell protection by functionalized fullerene materials. *Biomaterials* 3: 611–621, 2009.
348. Yu L, Ji X, Derrick M, Drobyshevsky A, Liu T, Batinic-Haberle I, and Tan S. Testing new porphyrins in in vivo model system: effect of Mn porphyrins in animal model of cerebral palsy (abstract). Sixth International Conference on Porphyrins and Phthalocyanines. New Mexico, 2010.
349. Yudoh K, Shishido K, Murayama H, Yano M, Matsubayashi K, Takada H, Nakamura H, Masuko K, Kato T, and Nishioka K. Water-soluble C60 fullerene prevents degradation of articular cartilage in osteoarthritis via down-regulation of chondrocyte catabolic activity and inhibition of cartilage degeneration during disease development. *Arthritis Rheum* 56: 3307–3318, 2007.
350. Zhao Y, Chaiswing L, Oberley TD, Batinić-Haberle I, St Clair W, Epstein CJ, and St Clair D. A mechanism-based antioxidant approach for the reduction of skin carcinogenesis, *Cancer Res* 65: 1401–1405, 2005.

Address correspondence to:
Ines Batinić-Haberle, Ph.D.
Department of Radiation Oncology–Cancer Biology
Duke University Medical Center
Research Drive
281b/285 MSRB I, Box 3455
Durham, NC 27710

E-mail: ibatinic@duke.edu

Date of first submission to ARS Central, September 3, 2009; date of final revised submission, January 17, 2010; date of acceptance, January 22, 2010.

Abbreviations Used

ACN = acetonitrile
AEOL11207 = Mn(III) 5,15-bis(methylcarboxylato)-10,20-bis(trifluoromethyl)porphyrin
AEOL11209 = Mn(III) 5,15-bis(4-carboxylatophenyl)-10,20-bis(formyl)porphyrin
AP-1 = activator protein-1
CAT-1 = 4-trimethylammonium-tempo iodide
$CO_3^{\cdot -}$ = carbonate radical
$Cu^{II}Br_8TM\text{-}4\text{-}PyP^{4+}$ = Cu(II) β-octabromo-*meso*-tetrakis(*N*-methylpyridinium-4-yl)porphyrin
$CuTM\text{-}4\text{-}PyP^{4+}$ = Cu(II) *meso*-tetrakis (*N*-methylpyridinium-4-yl) porphyrin

Abbreviations Used (cont.)

$E_{1/2}$ = half-wave reduction potential
EBAME = bis-(5-aminosalicylic acid) methyl ester
EDTA = ethylenediaminetetraacetic acid
EGTA = ethylenebis(oxyethylenenitrilo) tetraaceticacid
EHPG = ethylenebis(hydroxyphenylglycine)
FeTM-4-PyP^{5+} = Fe(III) *meso*-tetrakis(N-methylpyridinum-4-yl) porphyrin; the axial ligation is not indicated but at pH~7 monohydroxo species is present in solution
HIF-1α = hypoxia inducible factor-1
ICV = intracerebroventricularly
MCAO = middle cerebral artery occlusion
MnBr$_8$TM-3-PyP^{4+} = Mn(II) β-octabromo-*meso*-tetrakis(*N*-methylpyridinium-3-yl)porphyrin
[MnBV^{2-}]$_2$ = Mn(III) biliverdin IX
[MnBVDME]$_2$ = Mn(II) biliverdin IX dimethylester
[MnBVDT^{2-}]$_2$ = Mn(III) biliverdin IX ditaurate
Mn^{II}Br$_8$TM-4-PyP^{4+} = Mn(II) β-octabromo-*meso*-tetrakis (*N*-methylpyridinium-4-yl) porphyrin
Mn(III) salen = EUK-8
Mn^{III}Br$_8$TCPP^{3-} = Mn(III) β-octabromo-*meso*-tetrakis(4-carboxylatophenyl) porphyrin (also Mn^{III}Br$_8$TBAP^{3-})
Mn^{III}Br$_8$TSPP^{3-} = Mn(III) β-octabromo-*meso*-tetrakis(4-sulfonatophenyl) porphyrin
Mn^{III}TCPP^{3-} = Mn(III) *meso*-tetrakis (4-carboxylatophenyl)porphyrin (also Mn^{III}TBAP^{3-}, also abbreviated as MnTBAP), AEOL10201
Mn^{III}TSPP^{3-} = Mn(III) *meso*-tetrakis (4-sulfonatophenyl)porphyrin
[MnMBVDME]$_2$ = Mn(III) mesobiliverdin IX dimethylester
MnP = Mn porphyrin
MnT-2-PyP^{+} = Mn(III) *meso*-tetrakis(2-pyridyl) porphyrin
MnTalkyl-2,3,4-PyP^{5+} = Mn(III) *meso*-tetrakis (*N*-alkylyridinium-2 or 3 or 4-yl) porphyrin, alkyl being methyl (M, AEOL10112), ethyl (E, AEOL10113), *n*-propyl (nPr), *n*-butyl (nBu), *n*-hexyl (nHex), *n*-heptyl (nHep), *n*-octyl (nOct); 2 and 3 relate to *ortho* and *meta* isomers, respectively
MnTDE(or M or nPr)-2-ImP^{5+} = Mn(III) tetrakis[*N,N'*-diethyl (or dimethyl or di-*n*-propyl) imidazolium-2-yl)porphyrin; diethyl analogue is AEOL10150
MnTDM-4-PzP^{5+} = Mn(III) *meso*-tetrakis(*N,N'*-dimethylpyrazolium-4-yl)porphyrin
MnTDMOE-2-ImP^{5+} = Mn(III) tetrakis[*N,N'*-di(2-methoxethyl)imidazolium-2-yl) porphyrin
MnTrM-2-corrole^{3+} = Mn(III) *meso*-tris(*N*-methylpyridinium-2-yl)corrole
MnTTEG-2-PyP^{5+} = Mn (III) 5,10,15,20-tetrakis(*N*-(1-(2-(2(-2-methoxyethoxy)ethoxy) ethyl)pyridinium-2-yl) porphyrin
NBT = nitrobluetetrazolium
NF-κB = nuclear factor κB
NHE = normal hydrogen electrode
$^{\cdot}$NO = nitric oxide
$O_2^{\cdot-}$ = superoxide
PN = peroxynitrite
P_{OW} = partition coefficient between *n*-octanol and water
R_f = thin-layer chromatographic retention factor that presents the ratio between the solvent and compound path in 10:10:80 = satKNO$_3$(aq):H$_2$O:acetonitrile
RNS = reactive nitrogen species
ROS = reactive oxygen species
Salen = *N,N'*-bis-(salicylideneamino) ethane
SOD = superoxide dismutase
Tempo = 2,2,6,6,-tetramethylpiperidine-1-oxyl
Tempol = 4-OH-2,2,6,6,-tetramethylpiperidine-1-oxyl
TF = transcription factor
TLC = thin-layer chromatography
TPA = 12-*O*-tetradecanoylphorbol-13-acetate
X = xanthine
XO = xanthine oxidase

This article has been cited by:

1. Ines Batinic-Haberle , Julio S. Reboucas , Ivan Spasojevic . 2011. Response to Rosenthal et al.Response to Rosenthal et al.. *Antioxidants & Redox Signaling* **14**:6, 1174-1176. [Citation] [Full Text] [PDF] [PDF Plus]
2. Rosalind A. Rosenthal , Susan R. Doctrow , Wyeth B. Callaway . 2011. Superoxide Dismutase MimicsSuperoxide Dismutase Mimics. *Antioxidants & Redox Signaling* **14**:6, 1173-1173. [Citation] [Full Text] [PDF] [PDF Plus]
3. Nicolò Mazzucco, Stefano Zanconato, Davide Lucrezia, Emanuele Argese, Irene Poli, Giovanni Minervini. 2011. Design and dynamic simulation of minimal metallo-proteins. *Journal of Molecular Modeling* . [CrossRef]
4. Valentina Oliveri, Antonino Puglisi, Graziella Vecchio. 2011. New conjugates of β-cyclodextrin with manganese(iii) salophen and porphyrin complexes as antioxidant systems. *Dalton Transactions* . [CrossRef]
5. E. J. Moon, P. Sonveaux, P. E. Porporato, P. Danhier, B. Gallez, I. Batinic-Haberle, Y.-C. Nien, T. Schroeder, M. W. Dewhirst. 2010. NADPH oxidase-mediated reactive oxygen species production activates hypoxia-inducible factor-1 (HIF-1) via the ERK pathway after hyperthermia treatment. *Proceedings of the National Academy of Sciences* **107**:47, 20477-20482. [CrossRef]
6. Bensu Karahalil, Elvin Kesimci, Esra Emerce, Tulin Gumus, Orhan Kanbak. 2010. The impact of OGG1, MTH1 and MnSOD gene polymorphisms on 8-hydroxy-2′-deoxyguanosine and cellular superoxide dismutase activity in myocardial ischemia–reperfusion. *Molecular Biology Reports* . [CrossRef]
7. Junqiang Tian , Donna M. Peehl , Susan J. Knox . 2010. Metalloporphyrin Synergizes with Ascorbic Acid to Inhibit Cancer Cell Growth Through Fenton ChemistryMetalloporphyrin Synergizes with Ascorbic Acid to Inhibit Cancer Cell Growth Through Fenton Chemistry. *Cancer Biotherapy & Radiopharmaceuticals* **25**:4, 439-448. [Abstract] [Full Text] [PDF] [PDF Plus] [Supplementary material]
8. Ana Budimir, József Kalmár, István Fábián, Gábor Lente, István Bányai, Ines Batinić-Haberle, Mladen Biruš. 2010. Water exchange rates of water-soluble manganese(iii) porphyrins of therapeutical potential. *Dalton Transactions* **39**:18, 4405. [CrossRef]
9. Tin Weitner, Ana Budimir, Ivan Kos, Ines Batinić-Haberle, Mladen Biruš. 2010. Acid–base and electrochemical properties of manganese meso(ortho- and meta-N-ethylpyridyl)porphyrins: potentiometric, spectrophotometric and spectroelectrochemical study of protolytic and redox equilibria. *Dalton Transactions* **39**:48, 11568. [CrossRef]